5-1-2013

Using information processing techniques to forecast, schedule, and deliver sustainable energy to electric vehicles

Praneeth Pulusani

Using Information Processing Techniques to Forecast, Schedule, and Deliver Sustainable Energy to Electric Vehicles

by

Praneeth R Pulusani

A Thesis Submitted in Partial Fulfillment of the Requirements for the Degree of Master of Science in Computer Engineering

Supervised by

Dr. Andres Kwasinski
Department of Computer Engineering
Kate Gleason College of Engineering
Rochester Institute of Technology
Rochester, New York
May 2013

Approved by:

Dr. Andres Kwasinski, Assistant Professor
Thesis Advisor, Department of Computer Engineering

Dr. Shanchieh Yang , Associate Professor
Committee Member, Department of Computer Engineering

Dr. Thomas Trabold, Associate Professor
Committee Member, Golisano Institute for Sustainability

Thesis Release Permission Form

Rochester Institute of Technology
Kate Gleason College of Engineering

Title:

Using Information Processing Techniques to Forecast, Schedule, and Deliver Sustainable Energy to Electric Vehicles

I, Praneeth R Pulusani, hereby grant permission to the Wallace Memorial Library to reproduce my thesis in whole or part.

Praneeth R Pulusani

Date

The most memorable adventures are the ones in which you nudge Grim Reaper and return home, chuckling.

Abstract

Using Information Processing Techniques to Forecast, Schedule, and Deliver Sustainable Energy to Electric Vehicles

Praneeth R Pulusani

Supervising Professor: Dr. Andres Kwasinski

As the number of electric vehicles on the road increases, current power grid infrastructure will not be able to handle the additional load. Some approaches in the area of Smart Grid research attempt to mitigate this, but those approaches alone will not be sufficient. Those approaches and traditional solution of increased power production can result in an insufficient and imbalanced power grid. It can lead to transformer blowouts, blackouts and blown fuses, etc. The proposed solution will supplement the "Smart Grid" to create a more sustainable power grid. To solve or mitigate the magnitude of the problem, measures can be taken that depend on weather forecast models. For instance, wind and solar forecasts can be used to create first order Markov chain models that will help predict the availability of additional power at certain times. These models will be used in conjunction with the information processing layer and bidirectional signal processing components of electric vehicle charging systems, to schedule the amount of energy transferred per time interval at various times.

The research was divided into three distinct components: (1) Renewable Energy Supply Forecast Model, (2) Energy Demand Forecast from PEVs, and (3) Renewable Energy Resource Estimation. For the first component, power data from a local wind turbine, and weather forecast data from NOAA were used to develop a wind energy forecast model, using a first order Markov chain model as the foundation. In the second component, additional macro energy demand from PEVs in the Greater Rochester Area was forecasted by simulating concurrent driving routes. In the third component, historical

data from renewable energy sources was analyzed to estimate the renewable resources needed to offset the energy demand from PEVs. The results from these models and components can be used in the smart grid applications for scheduling and delivering energy. Several solutions are discussed to mitigate the problem of overloading transformers, lack of energy supply, and higher utility costs.

Contents

. . . . . **iii**

Abstract . . . . . **iv**

1 Introduction **1**
1.1 Background 1
1.2 Historical Review 6
1.2.1 Impact of EVs on the grid 6
1.2.2 Markov chain model 8
1.3 Thesis Contribution 10

2 Renewable Energy Supply Forecast Model **13**
2.1 Overview 13
2.2 Wind energy forecast model based on first order Markov chain 15
2.3 Steady state probabilities 17
2.4 Forecasting electric power from steady state probabilities . . 18
2.5 Results 18
2.5.1 Markov chain model configuration 21
2.5.2 Numerical computation of steady state vectors . . . 22
2.5.3 Evaluating the accuracy of the Energy Forecast Model 23

3 Energy Demand Forecast from PEVs **25**
3.1 Overview 25
3.2 Estimating number of PEVs on the road in 2020 26

3.3 Estimating hourly traffic profile for Greater Rochester Area . 29
3.4 Energy profile of a Plug-in Electric Vehicle 32
3.4.1 Estimating energy consumption of a PEV in a route . 34
3.5 Forecasting the macro energy demand from Plug-in Electric Vehicles 35
3.5.1 Generating Origins and Destinations 38
3.5.2 Generating Routes 39
3.5.3 Simulating Macro Energy demand 39
3.6 Results 39

4 Renewable Energy Resource Estimation 42
4.1 Overview 42
4.2 Offshore Wind Energy in Greater Rochester Area 42
4.3 Wind and Solar complementarity 43
4.4 Assumptions 45
4.5 Results 47
4.5.1 Configurations for resource evaluation 47
4.5.2 Analysis 51

5 Conclusion 53

6 Discussion and future work 54
6.1 Indirect coupling of battery banks and the grid 54
6.2 Smart or decentralized charging algorithm 54
6.3 Benefits for consumer, utility companies and the environment 55
6.4 Future Work 55

Bibliography 57

A Energy Supply Forecast Model Matrices 64

B Energy Demand Forecast Figures **65**

C Code **91**

List of Tables

3.1 Electric vehicle sales projection 28
3.2 Estimated hourly traffic profile for Greater Rochester Area . 31
3.3 Chevy Volt Power Profile 35

4.1 Time delayed release of energy from battery banks 51

List of Figures

1.1 Variability in renewable electricity generation 4
1.2 Typical residential home load profile in Southern California with superimposed PHEV charging load [1] 6
1.3 Fuhrlander FL-250 Wind Turbine Power Profile [2] 9
1.4 Envisioned System Integration of Energy Supply and Demand Forecast 10

2.1 Wind Energy Forecast Methodology 16
2.2 Mathematical view of the Energy Forecast Model 17
2.3 Wind Energy Forecast - Sample Algorithm Run 20
2.4 CDF of results at different resolutions 22
2.5 Cumulative Distribution Function for the prediction error . . 24

3.1 Area of Interest: Greater Rochester 25
3.2 Household Vehicle Age Distribution [3] 27
3.3 Plug-in EV Sales Growth Assumption 28
3.4 Rochester Urban Area [4] 29
3.5 Estimated hourly traffic profiles for Greater Rochester Area . 30
3.6 Chevy Volt Power Profile 34
3.7 A sample route 36
3.8 2000 Sample Routes 37
3.9 Energy Demand from PEVs at various times of the day . . . 40

4.1 Average Wind Speed near Rochester [5] 43
4.2 Rochester,NY wind speeds 44

4.3 Rochester,NY Daylight hours and Solar flux [6] 44
4.4 Energy Demand at Each Hour 45
4.5 Three day wind+solar energy output 47
4.6 Energy Supply - Depletion, cumulative 3 day tracking 48
4.7 Energy Supply - Depletion, variable number of installations . 49
4.8 Time Delayed Release of Energy Supply 49

Chapter 1

Introduction

1.1 Background

Day after day, increasing number of electric vehicles enter into our neighborhoods and into our power grid. The power grid we currently have is outdated and may not be able to fulfill the additional energy energy needs of electric vehicles, especially at peak times. Previous research shows that having an electric car doubles the average power consumption of a home [7]. Furthermore, the local grid and the transformers will not be able to handle multiple additional electric vehicles effectively [8]. If more PEVs are added to the grid than it can handle, the grid will become unstable, and further problems such as premature transformer aging, voltage drop and tripping in the low voltage distribution can arise [9]. Additional issues are present when charging time is considered. For instance, a ten minute quick charge is equivalent to the instantaneous energy demand of 140 average small homes. An energy demand of this scale cannot be satisfied by the current distribution grids in the U.S. [8].

Meeting the peak demand is one of the biggest concerns that electric companies have. If they can take 10 percent demand off the peak hours, significant benefits can be reaped in terms of consumer utility prices and the need to invest in building new expensive assets [10]. Using smart grid technologies effectively can solve the problem at a fraction of the cost and resources. We envision a convenient charging model in the future, where consumers will be able to charge quickly, wherever and whenever, similar to our present gas refueling model. For a convenient charging infrastructure

to work, the charging stations will need to have batteries at the local site, to store reserve energy, and provide it at high power, or in large volume at a later time. In addition, another significant reason to have local energy storage systems is to decouple critical infrastructure [11]. For instance, if there is a large scale power outage, it is extremely important for the transportation infrastructure, which will contain many PEVs in the future, to continue working. This research aims at providing a solution using existing models to forecast energy supply and demand and to provide that information to the smart grid applications. This energy forecast model and signal processing techniques will be able to keep the electrical grid more balanced, sustainable and functioning, and will help maintain the optimal charge in the charging stations' batteries.

One of the many advocates for pushing sustainable transportation is the U.S. Department of Energy. The "EV Everywhere Grand Challenge", sponsored by USDOE, is striving to help the U.S. produce Plug-in electric vehicles that are as affordable as conventional vehicles with internal combustion engines, by the year 2022. It is very reasonable to assume the demand is growing as shown by sales charts [12], and the immense amount of progress can be realized as PEVs are making through having won many competitions. For instance, the Chevy Volt has topped Consumer Reports owner satisfaction survey twice, Nissan Leaf has earned the 2011 World Car of the Year, Tesla Model S acclaimed the 2013 Motor Trend Car of the Year, and Ford C-MAX achieved the 2012 Green Car Vision award. While PEVs are getting high ratings and sales are increasing, a problem that is not addressed is the need to improve the charging infrastructure. Nonetheless, grid integration for the charging infrastructure is identified as necessary and the U.S. Department of Energy hopes to make it happen. Some of the changes include the following [13]. Utility rates will be dynamic and consumers will be able to charge PEVs based on best utility rates. Groundwork will be laid for bi-directional power flow through Vehicle-to-Grid technologies, which will improve the grid stability. Lastly, wind and solar systems will be installed for variable distributed generation, and PEVs can be controlled to overlap charging time with renewable electricity generation for favorable

utility rates [13].

Plug-in Electric Vehicles come in two main varieties - Plug-in Hybrid Electric Vehicles and Battery Electric Vehicles. PHEVs have an internal combustion engine as well as an electric motor. The well known Chevy Volt has a 16.5 kWh battery, with an estimated range of 38 miles. Its charging time is up to 16 hours on a standard 120 V electric outlet, and approximately 4 hours on a 240 V charging dock [14]. Similarly, the Toyota Prius Plug-in has a 4.4 kWh battery, with an estimated range of 11 miles. It charges in 3 hours from a standard 120 V outlet, and half of that from a 240 V outlet [15]. To compare BEVs with PHEVs, two of the eight passenger BEVs recognized by the U.S. Department of Energy, Nissan Leaf and Tesla Model S, were chosen [16]. Nissan Leaf has a 24kWh battery and its charging times are approximately 30 minutes (0-80%) with a DC50kW Quick charger, and less than 8 hours (0-100%) with a Home-use AC240V charging dock [17]. Similarly, the Tesla Model S comes with two sizes of battery packs - 60 kWh and 85 kWh, with estimated ranges of 232 mi and 301 mi, respectively. For the 85 kWh battery to charge to full capacity, it takes approximately 52.5 hours with a 120 V - 12 A charger, 9.5 hours with a 240 V - 20 A charger, 5 hours with a 240 V - 80 A charger, and 30 minutes (0-50% only) with a Tesla 90 kW Supercharger [18].

In this research, to meet the needs of PEVs in the future, we focus on renewable energy. Renewable sources are preferred over fossil fuel-based conventional sources for many reasons. Some of the well known reasons include energy security and independence, sustainability, lower long term energy costs and mitigation of climate change. Energy security and independence are important for the functioning of a modern economy. Sustainability, reduced environmental impact and prevention of climate change are important to ensure the survival of future generations. Long term energy cost savings are simply added benefits.

While renewable energy appear free, apart from the initial investment and maintenance, it comes with various challenges and issues. A few of

the hurdles with wind and solar power are variability, large footprint, noise, perceived aesthetics and upfront investment. For instance, at present, an average solar panel (GE - GEPV200) with an efficiency of 14% takes 5 m^2 of solar panels for a maximum output of 2 kW [19]. The variability of renewable sources are illustrated in Figure 1.1. The data is from two specific days; however, it illustrates the general trends. Wind energy generation does not have a specific shape but solar energy generation has a bell shaped trend, with the smoothness and amplitude varying across the days and seasons.

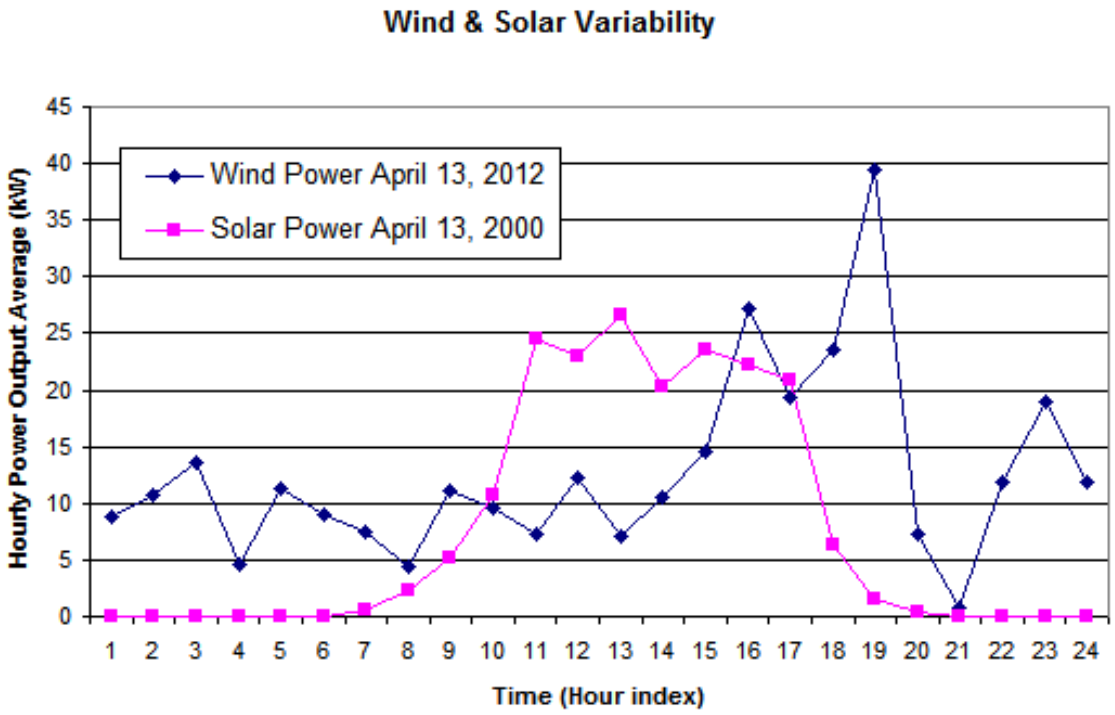

Figure 1.1: Variability in renewable electricity generation
Wind energy is generally more unpredictable than solar energy. The amplitude of the solar energy generation varies but the coarse bell shape is persistent.

The volatility or the variability in wind and solar energy sources, can be addressed by Pumped-Storage Hydroelectric systems, large and distributed installations of battery banks, and compressed air energy systems. Of the large scale storage systems, Pumped-Storage Hydroelectricity is the most efficient, at the moment. The efficiency is known to be in the range of

70-85% [20]. At present, in the U.S., the total power generation capacity of Pumped Storage systems is about 25 GW [20], with average facility capacity of 1 GW [20]. In this pumped-storage system, two reservoirs are naturally or artificially built in close proximity but at different elevations. During off peak hours, excess energy generated is used to pump water from the reservoir at lower level into the reservoir at the higher level. During peak demand or when there isn't enough supply of wind or solar energy, the water from the upper reservoir is let through the turbines, into the lower reservoir at varying volumes, generating the needed electricity. It may not be feasible in locations without access to a large water resource. In areas without access to the needed natural resources, a large distributed energy storage system comprising of batteries can be used. For instance, a trailer load of batteries will be necessary to store about 1 MWh of energy [20], which may be sufficient for a charging station. Nonetheless, there is significant research taking place in the domain of batteries. Compressed Air Energy Systems are not as feasible because they require natural cave formations underground and they have a low efficiency of about 66% [20].

As of January 2013, the installed capacity of Wind and Solar systems in the U.S. are 98.56 GW and 4.44 GW [21]. In addition, they are 5.17% and 0.38% of the total energy generation capacity respectively [21]. Globally, as of 2011, the installed energy generating capacities for wind and solar were 239 GW and 73 GW. On a more local scale, New York is known to have 1-4% of its electricity come from non-hydroelectric renewable energy. Nonetheless, the number of installations and amount of generation are projected to grow significantly and rapidly [22].

1.2 Historical Review

1.2.1 Impact of EVs on the grid

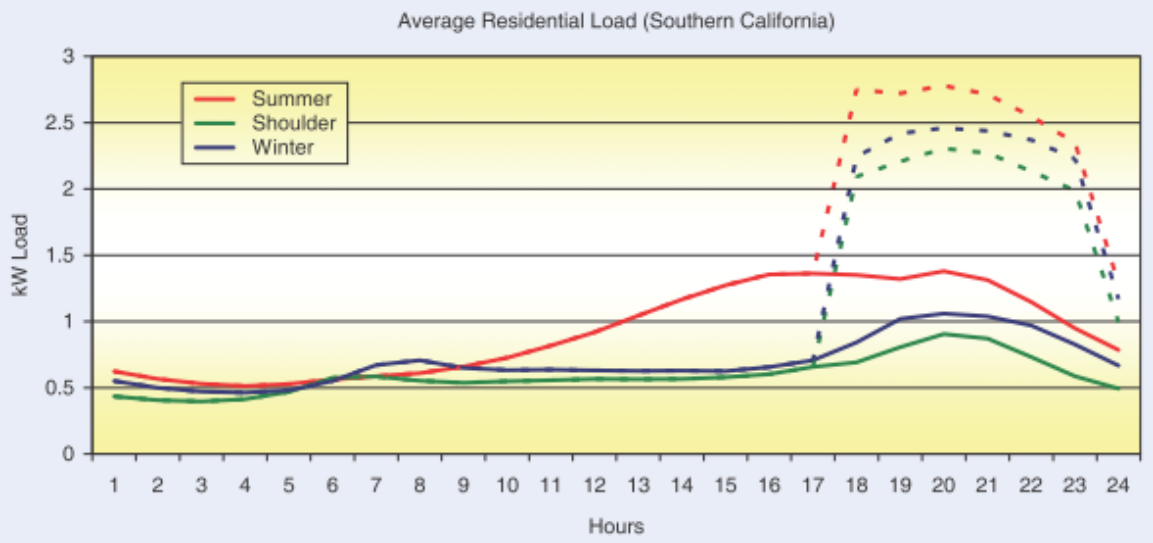

Figure 1.2: Typical residential home load profile in Southern California with superimposed PHEV charging load [1]
During a PEV's charging time with a 1.4 kW charger, an average household electric load is doubled. It was also noted that, fast chargers, at 6.6 kW or higher, will significantly alter the load pattern of the consumer.

Since EVs have a high energy capacity, their mass deployment will have a significant impact on the power grid. As previously mentioned in Chapter 1.1, charging an EV overnight requires the same amount of power as that of an average small home and charging an EV with a 10 minute quick charge creates an equivalent impact of 140 homes [8]. In addition, EV penetration in the distribution power system was simulated with German conditions. It is estimated that electric vehicles will account for 4% of annual electricity consumption in 2020, and also that they will account for 8% of peak power demand [23]. Also, charging of PEVs with AC Level 2 charging stations were observed in simulation to significantly wear out transformers, compared to a AC Level 1 charging stations [9]. Nonetheless, there are many studies [24, 25, 1, 9, 26, 27, 28, 29] proposing various opportunistic charging schemes, but those methods are not self-sufficient. Some of the proposed

methods include utilization of off-peak and idle-generation for EV charging, demand response or retail ratemaking, and demand-side management. Demand response was explained as influencing the moment of charging in response to pricing signals [27]. Retail ratemaking, explained by [25], seems to be synonymous with demand response. In both policies, the pricing of electricity was suggested to be used, to encourage charging of the EVs when the grid is not constrained. Demand-side management was explained as an active management of electricity demand, to prevent overloading of the grid [27]. An example implementation of demand side management was simulated, assuming a small scale PHEV penetration [30]. It indicated that even a small scale PHEV penetration into a residential distribution network will create new significant peaks in the distribution transformer, resulting in decrease in transformer operating efficiency and overloading of the transformers. Simulating demand side management using automated metering interface and predetermined load information, it was observed that the electricity demand peaks can be removed. In this small scale penetration simulation, PHEVs' charging supply was controlled to charge only when the measured load is less than predetermined peak load. One caveat was that large scale demand was not simulated. Similarly, it was mentioned that utilizing off peak and idle generation charging scheme works with the current demand and low number of EVs [29]. However, as EV adoption rates increase, managing the charging patterns may become increasingly difficult and there could be significant increase in utility requirements and costs. With smart grid applications, energy cost savings could be delivered to consumers, along with the benefits of reduced green house gas emissions and less environmental impact [29].

On the other hand, having additional EVs on the grid along with Vehicle-to-grid can provide utility and cost benefits to both consumers and utilities. EVs can act as a distributed energy storage source supporting the grid during electricity demand swings [29]. In addition, consumer behavior could be altered by providing incentives to encouraged dynamic charging [29].

Also, the effects on the grid depend on many factors such as power level,

timing and duration of the EV's connection to the grid, and the user behavior, etc. For instance, [25] mentioned that a joint study by Electric Power Research Institute and Natural Resources Defense Council assumed 74% of PEV charging will take place off peak and the resulting estimated net increase in peak power demand for state of New York was 900 MW. Adoption of EVs is believed to create a transformative impact on the electric grid and each individual EV is estimated to create additional load on an electric grid of the same order of magnitude as that of an average home [7]. The problems anticipated through addition of these EV loads to the grid include power quality problems such as momentary voltage drops. Uncoordinated charging of EVs on large scale may result in poor electric energy distribution. Thus, integrating charging of PEVs into the smart grid via data and signal processing is deemed necessary [7].

1.2.2 Markov chain model

The two main processes that determine the electric power that can be obtained from a wind turbine are the wind speed and the conversion at the turbine of the kinetic energy in the wind speed into electric energy. Because of its importance in weather and climate prediction, there exists a large body of research aimed at modeling wind. The work in [31] statistically confirmed the use of the first order Markov chain model to characterize the wind speed into different states (0 - 2 mph, 2 - 4 mph, etc) and, further, applied the model to the accurate synthetic generation of wind speed. Another recent work addressing the modeling of wind speed is [32], where a method to forecast wind speed on an hourly basis is presented that uses a two-step methodology based on a Bayesian combination algorithm, and three neural network models.

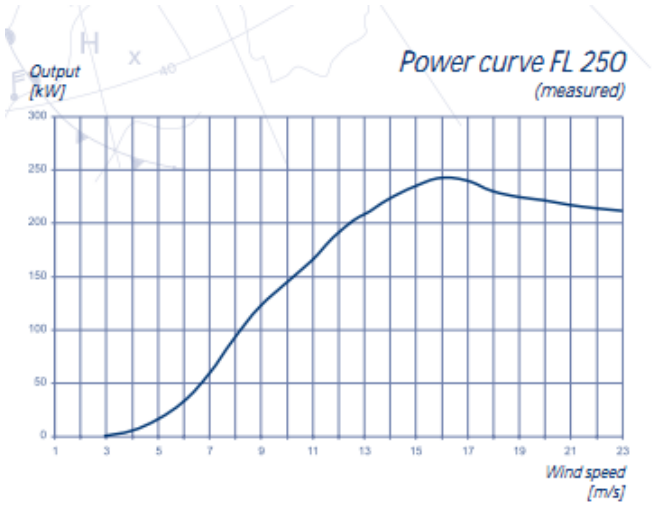

Figure 1.3: Fuhrlander FL-250 Wind Turbine Power Profile [2]

Our work is concerned with the prediction of electric power output as opposed to the forecasted wind output state. It was discussed in [33] that the electric power output can also be represented with a first order Markov chain model. This is because the electric power output is related to wind speed through a non-linear function characterizing the wind turbine (e.g. Figure 1.3). The work in [33] studied this function and modeled the conversion of wind speed to electric power for different types of wind turbines. These results had been applied in the literature to generate synthetic time series of electric power from wind turbines. In particular, the work in [34] combined the first order Markov chain model for wind speed and wind turbines models to generate synthetic data of wind power generation. A similar approach, based on the first order Markov chain model was used in [35] to generate the synthetic electric power data with the intermittent characteristic typical of using renewable sources (wind and others). The utilization of a basic first order discrete Markov chain model results in fixed state transition probability matrices. However, if the wind speed data is generated synthetically or randomly, the Bayesian Inference of Transition Matrix methodology described in [36] produces better results, when verified using a 95% credible interval. A 95% credible interval was described as the interval between the 2.5% and 97.5% percentiles of the posterior distribution of a random variable. The basic Markov model only considers the aleatory uncertainty (also

known as statistical uncertainty), whereas the Bayesian method considers the aleatory uncertainty from the random number generation as well as the epistemic uncertainty (also known as systematic uncertainty) of estimated transition probabilities. This method is intended for applications of wind farm reliability analysis, but some of its principles may be applied to wind energy forecasts and smart grid applications.

1.3 Thesis Contribution

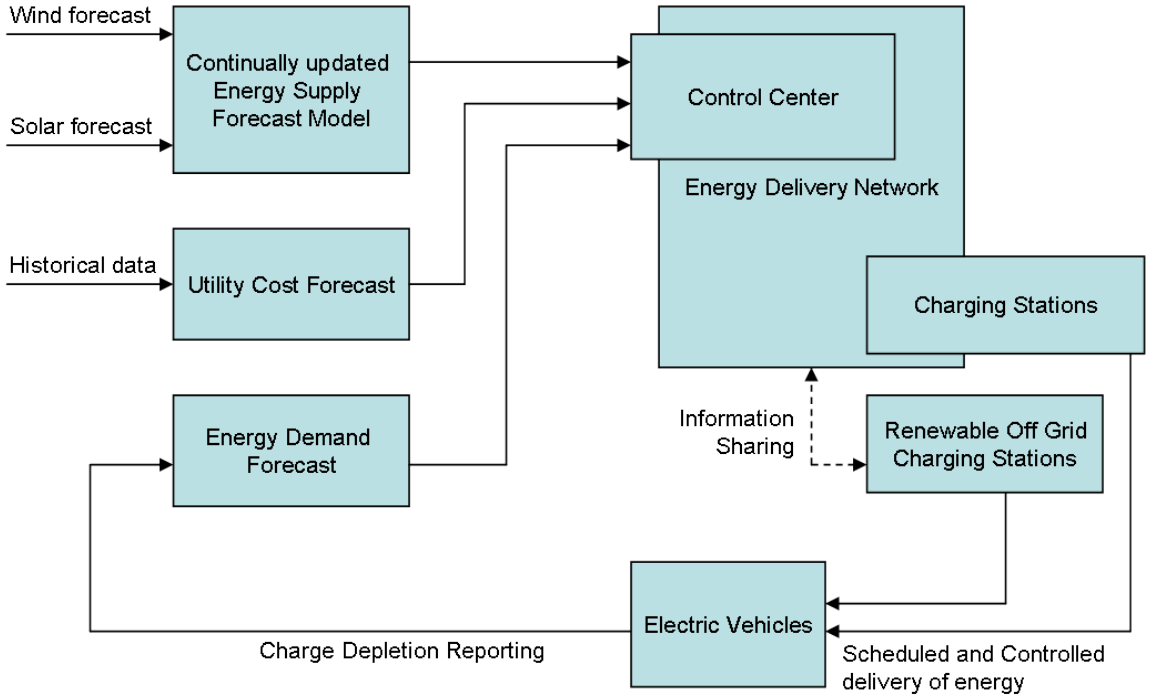

Figure 1.4: Envisioned System Integration of Energy Supply and Demand Forecast

As previously mentioned in Section 1.1 (Background), we envision a convenient charging model in the future, in which consumers will be able to charge quickly, wherever and whenever, similar to out present gas refueling model. As discussed in Section 1.2.1 (Impact of EVs on the grid), there are many proposed opportunistic schemes for a smart grid; However, we believe that these schemes are not sufficient. Our primary motivation is to contribute components to smart grid applications, so that we are one step

closer to having an ideal smart grid that can handle the influx of electric vehicles as well as support the convenient charging model. The specific components that we contribute are the next three chapters of this thesis. The way that these components fit into the smart grid realm is loosely illustrated by the envisioned system integration shown in Figure 1.4. Their purposes are concisely explained in this section.

The first component, the Energy Supply Forecast Model can be visualized as a continually updated data provider for the energy delivery network that supplies renewable energy forecast data. It is based off of a first order Markov Chain model and NOAA weather forecast, and the model is further explained in detail, in its own chapter (Chapter 2). An example scenario is in which this model is useful is as follows. The "Control center" can mandate prices such that the utility prices are inversely proportional to the availability of renewable energy supply. This will incentivize PEV owners to charge at least peak times, improving overall grid stability. Equally as important is that the off grid local charging stations based on renewable sources of energy [7] can use the forecast, to determine the amount of charge needed to maintain the batteries at a charging station. If the forecast is not very favorable, the charging stations can charge their battery bank from the conventional grid during non peak times. This process will help with prevent sudden voltage drops on the conventional grid, as the charging stations will be able to provide electricity to PEVs at high power, during peak times, without affecting the conventional grid. This model is shown as the top left block labeled "Continually updated Energy Supply Forecast Model". To note, only the wind forecast model was developed. The solar forecast model could not be developed due to delays in installation of the resources, at the Golisano Institute for Sustainability.

The second component is an offline model to forecast energy demand caused by PEVs in the future. At some point in the future, the model can be further developed so that it provides live demand forecast to the grid operators and the operators can plan routing dynamics of the energy flow, but it will require some form of information sharing from the PEVs. At that time,

this component will represent the “Energy Demand Forecast” and “Charge Depletion Reporting” in Figure 1.4. At present, the model reports charge depletion with offline information, and also provides a way to visually observe the energy demand from different regions of an area, at different times of the day, in the year 2020. The model estimates the number of PEVs and hourly traffic on the road, and the energy a PEV consumes in different route profiles, to forecast the energy demand from PEVs, in different regions of the chosen area. Utility companies can use the data to improve the transformers in the regions with higher anticipated demand prior to improving regions with lesser anticipated demand. The energy demand forecast is also useful to the smart grid operators, who can dynamically route energy to the regions in high demand. Lastly, it will help determine how many charging stations to put in various regions, and at what capacity, in terms of power output and energy storage.

The third component loosely falls into both, the “Control Center” in Figure 1.4, and outside of the whole system integration. It suggests a way to use minimal number of renewable resources and also proposes to store energy during non peak hours, and release it during peak hours, proportional to the anticipated demand at that hour. The control center can perform the anticipated demand calculations for various regions of the grid and provide optimal hourly energy release timing information to the corresponding charging stations. This will help reduce peak demand, which the current grid may not be able to support, if it is beyond additional 8% [23].

Chapter 2

Renewable Energy Supply Forecast Model

2.1 Overview

Smart Grid-related techniques address the issues arising from climate change and the dependence on the use of unsustainable energy sources and other resources. One of these techniques is the increased use of electric energy obtained from renewable sources, such as solar radiation or wind. Yet, the effective use of renewable source of energy presents the challenge that they are typically intermittent with varied degrees of randomness.

The intermittent and random characteristics of renewable sources limit their applicability. For applications where the renewable generation is integrated into regional or national grids, the variability in power generation can be absorbed with power generation from traditional non-renewable sources. Also, the availability of power over a large region from many sources tends to absorb some of the intermittency and randomness into values close to an average. In addition, to manage this type of application it suffices to have estimates of the power generation with resolutions ranging from weeks to days. At the same time, there is a significant push for other electric grid architectures and applications that will require estimates of power output with an hourly resolution for their better management. One example of a new architecture is the paradigm of a "microgrid", [37], which is based on the use of distributed power generation systems placed close to their loads (e.g. a neighborhood, an industrial park, etc.). One example of an application, that shares our motivation, is the deployment of fast charging stations for electric vehicles, which are primarily powered from renewable sources, [7].

Due to the presence of a large variability factor in renewable energy, we have a need to forecast the energy output to effectively make use of fast charging stations powered from renewable sources. In this Chapter, we present a novel method for the prediction of electric power that can be obtained on an hourly basis from a wind turbine. The method is based on modeling the time evolution of the wind electric power output as a Markov chain and uses as input parameter the wind speed forecasted a day in advance. The novelty of the method is based on producing estimates of wind electric power output with a much finer resolution, on an hourly basis, than other prediction methods. The proposed method provides also finer resolution in the estimate of power output, as other works have focused on obtaining predictions in the order of Mega Watts, applicable for large wind power generation and regional distribution systems. The method is also novel in using short-term weather forecast instead of long-term climate forecast. Also, the method goes beyond the prediction of wind speed, as it also incorporates the dynamics of the turbine that converts wind speed into electric power. The method was implemented and evaluated using forecast data from the US National Oceanic and Atmospheric Administration (NOAA) and generation data from a 250 kW wind turbine operated in Harbec, a plastic molding factory in the vicinity of Rochester, New York. NOAA was chosen for weather forecasts as it provided wind forecasts at the desired hourly resolution. The wind power output data was used from Harbec, as they provided open access to their wind turbine data with a resolution of 10 minutes.

Absence of Solar Energy Forecast Model

Initially, forecast models for both solar and wind sources energy were planned to be developed. The data for a Solar Panel installation was anticipated to be acquired from Golisano Institute for Sustainability at RIT. However, due to the delay in installation and setup of the solar panel equipment at the institute, a solar energy forecast model could not be incorporated or developed in time.

2.2 Wind energy forecast model based on first order Markov chain

Following [33] and [34], it was assumed that the wind power stochastic process follows a first order Markov chain model. In this model, the electric power from wind is partitioned into equal length intervals. Each of these intervals corresponds to a state of the Markov chain. When considering the weather-related variability of wind speed over time intervals in the order of one hour or less, the state transition probabilities and the state probabilities in the Markov chain change based on the wind conditions. For example, for intervals when the wind speed is small, it is to expect that the probability of states corresponding to low generated electric power will be large, the probability of states corresponding to high generated electric power will be small and the state transition probabilities to high wind power states will be small. Conversely, for intervals when the wind speed is large, it is to expect that the probability of states corresponding to low generated electric power will be small, the probability of states corresponding to high generated electric power will be large and the state transition probabilities to high wind power states will be large. In the proposed prediction method, the forecasted wind speed is divided into a discrete number of intervals, each covering a range of wind speeds. It is assumed that for each interval of forecasted wind speed there is a different set of statistics, i.e. state transition and state probabilities, characterizing the Markov chain.

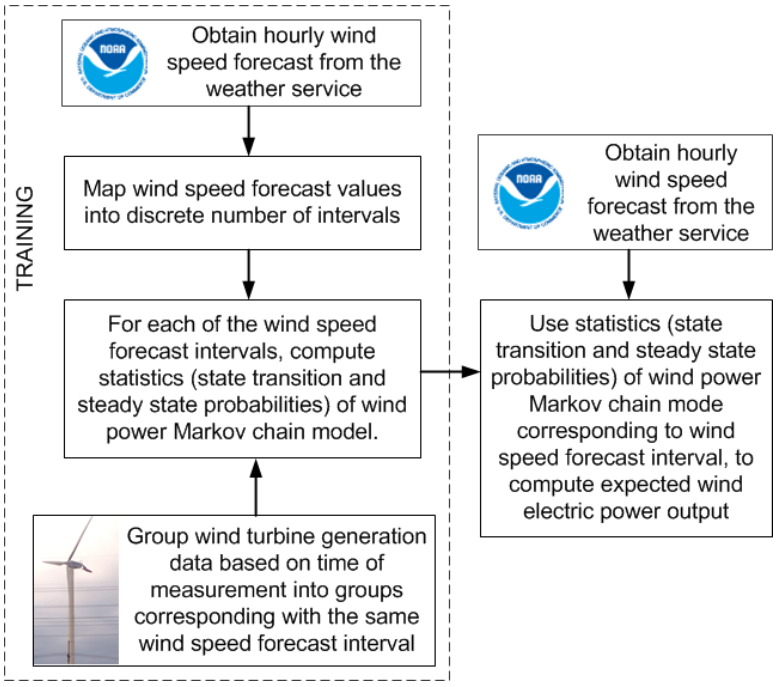

Figure 2.1: Wind Energy Forecast Methodology

With these considerations in mind, the prediction method is outlined in Figure 2.1. The method utilizes training data measuring the electric power output from a wind turbine measured at ten minutes intervals. The data is separated and classified into groups. The data in each group corresponds to time periods for which the forecasted wind speed is the same. For example, if it is decided on a forecasted wind speed resolution of 2 mph, one group of data will contain all the wind turbine output data for measuring times with forecasted wind speed between 0 and 1.99 mph, a second group will contain all the wind turbine output data for times with forecasted wind speed between 2 and 3.99 mph, etc. The data in each group is used to estimate the state transition probabilities for the Markov chain associated with the group and, by extension, the forecasted wind speed that defined the data group. As customary with Markov chains, the state transition probabilities are jointly represented in a state transition matrix, which we denote as $\mathbf{P}^{(g)}$, and where g is the index to the group corresponding with a range of forecasted wind speeds. In the proposed method, the elements of the state transition matrix,

$p_{ij}^{(g)}$, are estimated from the maximum likelihood estimate

$$p_{ij}^{(g)} = \frac{n_{ij}^{(g)}}{\sum_{k=1}^{N} n_{ik}^{(g)}}, \tag{2.1}$$

where $n_{ij}^{(g)}$ is the count of transitions from wind power state i to state j encountered in the data for the group g, and N is the number of states in the Markov chain. A visualization of this technique is shown in Figure 2.2.

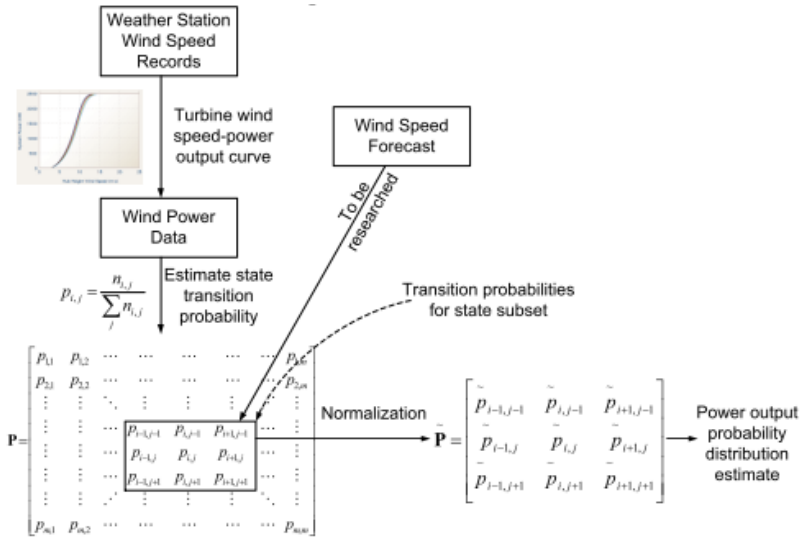

Figure 2.2: Mathematical view of the Energy Forecast Model

2.3 Steady state probabilities

After the state transition matrices are computed, it is necessary to compute the steady state probabilities, as the collection of steady state vectors for different wind groups provides a lookup mechanism to forecast energy output. From each of the state transition matrices, it is possible to compute the steady state probabilities for the states in the wind power Markov chain by

solving the system of equations, [38],

$$\begin{aligned} \pi^{(g)} &= \pi^{(g)}\mathbf{P}^{(g)}, \\ \sum_{i=0}^{N-1} \pi_i^{(g)} &= 1, \end{aligned} \tag{2.2}$$

where $\pi^{(g)}$ is the vector of steady state probabilities (stationary state pmf) for the wind power Markov chain associated with forecasted wind speed in the gth. range of values and with elements $\pi_i^{(g)}$, $i = 0, 1, \ldots, N-1$.

2.4 Forecasting electric power from steady state probabilities

Once the collection of steady state vectors for various wind speed ranges are established, the prediction of electric power output is calculated by using as input, the forecasted wind speed at an hour of interest for the next day. The forecasted wind speed is used to select the corresponding wind power Markov chain statistics or the corresponding steady state vector. The following equation was used to predict electric power

$$\hat{W} = \sum_{k=0}^{N-1} W_k \pi_k^{(g)}, \tag{2.3}$$

where $\hat{W}$ is the forecasted power output, W_k is the mid-point value of the range of wind power values associated with state k, g is the index of the wind speed range the input wind speed falls in.

2.5 Results

The proposed prediction method was evaluated using electric power generation data from a Fuhrlander FL 250 wind turbine located in a plastic molding

factory in the vicinity of Rochester, New York, and with a maximum generation capacity of 250 kW. The time resolution of this data is 10 minutes. The turbine is used in a microgrid application to power the plastic molding factory. The forecast data was obtained daily from the standard information provided by the USA National Oceanic and Atmospheric Administration (NOAA) [39]. The time resolution of the forecast data is 1 hour. Wind forecast data for the city of Rochester, NY was recorded for the months of April and May 2012. Similarly, the wind turbine power output data was also captured for the same timeframe. Part of the data, the first 75%, or April 14 to May 15, was used as training data to build the model. Then, the rest of the data, 25%, or May 16 to May 21, was used to test the validity of the technique. The discrete algorithm can be seen in Figure 2.1. The process of the algorithm illustrates this procedure in a sample run of the algorithm shown in Figure 2.3. The configuration or results from each individual steps of the technique are further explained in the following subsections.

```
Power state resolution: 60kw
Power state transitions in the Wind State 0 (0.0 - 25.0mph )
        S0      S1      S2      S3      S4
S0      3648    111     2       0       0
S1      112     283     41      1       0
S2      1       42      50      2       0
S3      0       0       3       8       0
S4      0       0       0       0       0

Markov Probability Matrix for the Hit Matrix above
        S0      S1      S2      S3      S4
S0      .970    .030    .001    x       x
S1      .256    .648    .094    .002    x
S2      .011    .442    .526    .021    x
S3      x       x       .273    .727    x
S4      x       x       x       x       x
------------------------------------------------------------

Power state transitions in the Wind State 1 (25.0 - 50.0mph )
        S0      S1      S2      S3      S4
S0      37      7       1       0       0
S1      8       32      5       0       0
S2      0       7       15      2       0
S3      0       0       2       0       0
S4      0       0       0       0       0

Markov Probability Matrix for the Hit Matrix above
        S0      S1      S2      S3      S4
S0      .822    .156    .022    x       x
S1      .178    .711    .111    x       x
S2      x       .292    .625    .083    x
S3      x       x       1.000   x       x
S4      x       x       x       x       x
------------------------------------------------------------

Steady State probablilites for wind resolution: 25mph
WindSt\PowerSt  S0      S1      S2      S3      S4
0.0-25.0mph     .873    .101    .023    .003    .000
25.0-50.0mph    .401    .401    .183    .015    .000
------------x---------
```

Figure 2.3: Wind Energy Forecast - Sample Algorithm Run

A sample run of the algorithm as described in Figure 2.1, is shown here. In the sample, the extremely low resolutions (Power state resolution: 60 kW and wind group Resolution: 25 mph) were chosen only for ease of illustration, as they produce a smaller output, displayable here.

2.5.1 Markov chain model configuration

The theoretical maximum output of the FL-250 Wind Turbine is 250 kW, but 300 kW has more factors and lets us divide it evenly with more integers for experimentation. So, the power range was selected to be 0 - 300 kW. For wind speed range, the maximum wind speed observed in the data set was 30 mph. However, on the possibility that a new data set might have a wind speed higher than 30 mph, a reasonable assumption was made that the wind speeds in a new data set may not be above 50 mph. Therefore, the wind speed range was selected to be 0 - 50 mph. Following the first order Markov chain technique explained in section 2.2, the power states for the Markov state transition matrix were made to have a resolution or intervals of 1kW and the forecastable wind speeds were divided into groups with the resolution of 2 mph. Various combinations of power state resolution and wind group resolution were experimented with, but resolutions 1 kW and 2 mph yielded the best results and therefore selected for reporting. These resolutions were considered most favorable as determined by the CDF analysis. The CDF analysis at different resolutions can be seen in Figure 2.4. The analysis is further explained in Section 2.5.3.

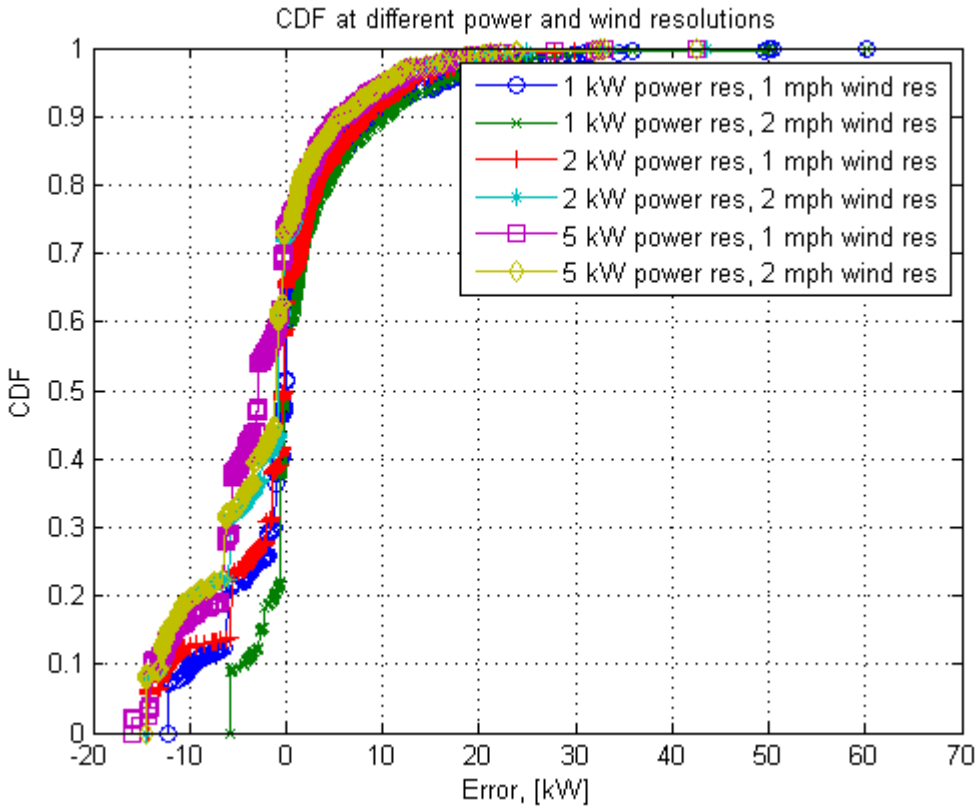

Figure 2.4: CDF of results at different resolutions

With 1 kW resolution for power states, there were 300 power states in the Markov chain; since the resolution was picked to be 2 mph, there were 25 groups or first order Markov transition matrices matrices. From these transition-count matrices, the probability matrices for each wind group were generated by applying Equation 2.1 ($p_{ij}^{(g)} = \frac{n_{ij}^{(g)}}{\sum_{k=1}^{N} n_{ik}^{(g)}}$). Once the probability matrices were calculated, steady state vectors for each wind group were computed.

2.5.2 Numerical computation of steady state vectors

Algorithmically, $\pi^{(g)}$ is the state probability vector after a number of transitions approaching infinity: $\pi^{(g)} = [\mathbf{P}^{(g)}]^k \pi_0^{(g)}$ for $k \to \infty$ and $\pi_0^{(g)}$ being a vector of initial stationary state pmf. The computation can be solved by

raising $\mathbf{P}^{(g)}$ to a power k sufficiently large [40]. It was computed numerically instead of solving system of equations as the computation time with a current CPU was very insignificant, and $k = 1000$ was used to achieve a minimum 4 decimal precision. The precision of 4 decimals was desired as we did not want to risk zeroing of the low frequency transitions. The precision was verified by using the values $k = 1000$ and $k = 1001$ and verifying that the results were same upto 4 decimal places. Once a steady state vector was generated for each wind group, the collection of them together represents the steady state state lookup matrix, each row representing the steady state probabilities for the corresponding wind group. In essence, there were 25 rows, representing 25 wind groups of 2 mph, and there were 300 columns representing 300 power states of 1kW each and this set of lookup vectors was used to predict the electric power.

2.5.3 Evaluating the accuracy of the Energy Forecast Model

Weather or wind forecast data from May 16, 2012 to May 21, 2012 was used in the energy forecast model to get power forecast for each hour of the next day. Given an input wind speed, the power forecast was obtained by looking up the corresponding steady state vector in the steady state vector collection and using Equation 2.3 ($\hat{W} = \sum_{k=0}^{N-1} W_k \pi_k^{(g)}$) to get an estimated power in kW. The accuracy of the prediction was evaluated using the Cumulative Distribution Function to measure prediction error; prediction error was defined as the difference between average measured power output of the turbine for the hour and the predicted power output for the same time frame. The error analysis for some of the resolution choices are shown in Figure 2.4. The power state and wind speed resolutions of 1 kW and 2 mph yielded the best results, as that combination had least amount of error. The resolution combination was analyzed individually, and the result can be observed more clearly in Figure 2.5. It shows that 80% of the predictions were within $\pm$5 kW of error and 40% of the predictions were within $\pm$1 kW of error. The error was considered reasonable as the charging stations will need to maintain charge in the order of several hundred kWh to support fast charging of multiple PEVs.

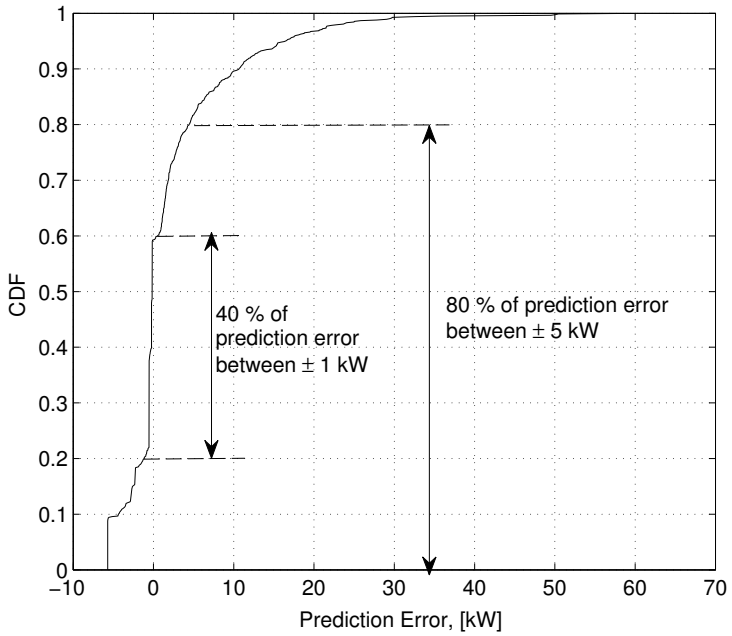

Figure 2.5: Cumulative Distribution Function for the prediction error

For errors larger in magnitude than 1 kW, we observe that there is an approximately 20 % probability for over-prediction and 40 % probability for under-prediction. The difference is due to the inaccuracies in the complete estimation system, such as those from NOAA's wind speed forecast. Nevertheless, a case of under-prediction is preferable to over-prediction, since this will result in a surplus, rather than a deficit, of available renewable energy from wind.

Chapter 3

Energy Demand Forecast from PEVs

3.1 Overview

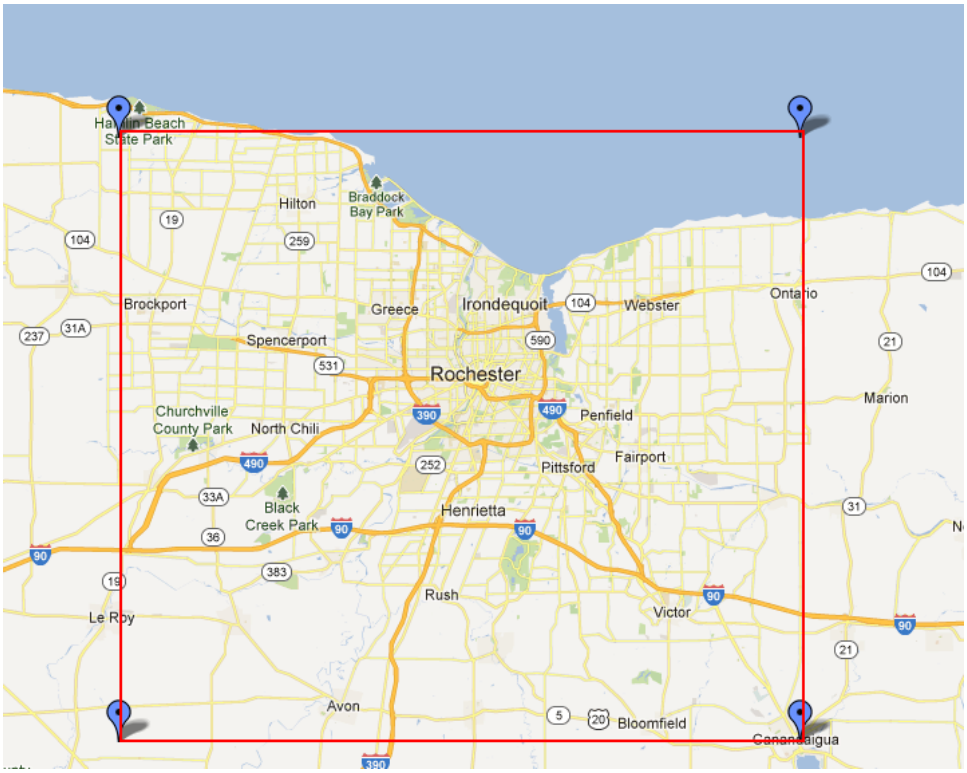

Figure 3.1: Area of Interest: Greater Rochester

The area considered for this research is bounded within latitudes of 42.885021 and 43.337165, and longitudes of -77.976837 and -77.277832, as shown in Figure 3.1. At present, the market share of electric vehicles is very low (less

than 0.1% [12]), especially when car sales from last 20+ years are considered; such low number of PEVs do not pose a significant load on the grid. However, their market share is growing rapidly and we need to understand the scale of demand they will put on the grid in the future, so that the necessary steps can be taken to ensure that our grid will be ready to handle the load. This component of the research aims at providing the methodology to anticipate energy demand that will be created by PEVs in 2020, at various times of the day, in different regions of an area of interest. This information is envisioned to be useful to the local renewable charging stations can use Energy Demand forecast along with information from Energy Supply Forecast model to anticipate net energy supply, and use the conventional grid to charge their battery banks from the conventional grid to the needed capacity. Also, they can plan their day ahead, to release the stored energy, proportionally to the anticipated electricity demand, so that the peak demand on conventional grid is mitigated. The energy demand forecast is also useful to the smart grid operators, who can dynamically route energy to the regions in high demand. It can be used along side some of the proposed solutions from Historical Review, such as demand-side management (active management of electricity demand) [27] and ratemaking [25]. To achieve a reasonable estimation of the anticipated demand, we need to estimate the number of PEVs in service, how much traffic there will be at different times of the day, how much energy a PEV consumes in different route profiles, etc. Each of the estimations are discussed in the following sections individually. The area of interest considered in this case study is the Greater Rochester Area of New York.

3.2 Estimating number of PEVs on the road in 2020

In the area considered, the data from census tracts was used to estimate the population of 858,844 [41]. The number of cars per 1000 in New York state is estimated to be around 570 [42]. Using this information and the population, the number of cars in the area of interest is estimated to be 500,000. Within those cars, the cars of age 9 years or younger is approximately 61% [3], as shown in Figure 3.2, equaling about 300,000 cars.

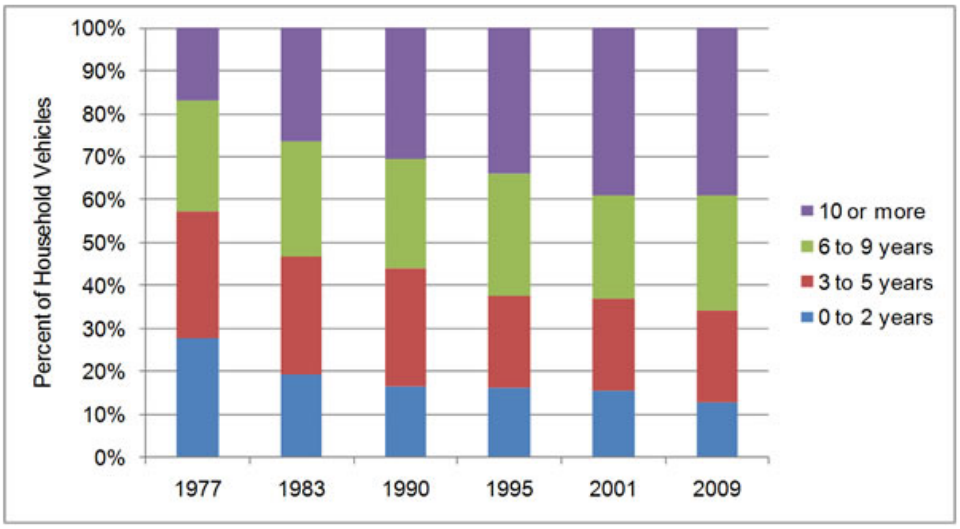

Figure 3.2: Household Vehicle Age Distribution [3]

According to Goldman Sachs, PEVs sales contribute about 4% of all vehicle sales in 2020 and it is estimated to be 3.7 million vehicles [43]. In addition, Pike research suggests that US will occupy about 26% of the global PEV market [44]. Inferring from the two sources, 26% of the 4% global PEV sales equals 0.95 million PEVs. The annual US PEV market-share in 2020 is estimated to be around 7% considering an average of 13 million vehicles sold in a year. Table 3.1 displays actual PEV sales for last 3 few years and the projected estimated sales upto 2020. The sales data was acquired from Electric Drive Transportation Association [12]. The growth in PEV sales could follow a linear, exponential or logarithmic model and it would mainly depend on the technological advances, policy changes etc. For simplicity, linear growth was assumed, to estimate the market share of PEVs in the year 2020. The assumed growth model seemed reasonable, as the growth of PHEVs, similar class of vehicles, was also modeled linearly [45]. The assumed model for PEVs can be seen in Figure 3.3.

Table 3.1: Electric vehicle sales projection

Year	PEVs	Total Vehicles	% Market share	Notes
2010	345	965731	0.036	Dec only
2011	17735	12734356	0.139	
2012	52835	14439684	0.366	
2013	17413	3674935	0.474	Jan - Mar
2014	191700	13500000	1.420	Estimated
2015	319950	13500000	2.370	Estimated
2016	448200	13500000	3.320	Estimated
2017	575100	13500000	4.260	Estimated
2018	703350	13500000	5.210	Estimated
2019	831600	13500000	6.160	Estimated
2020	959850	13500000	7.110	Estimated
	Avg % market share 2012-2020		3.41	

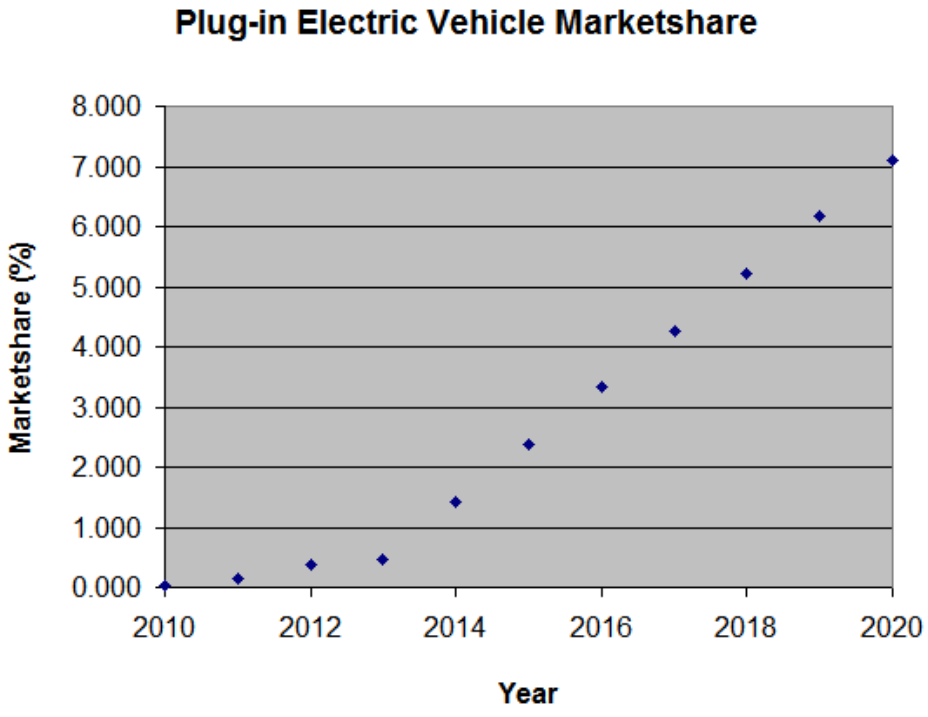

Figure 3.3: Plug-in EV Sales Growth Assumption

Using this estimation, the sales percentages from 2012 to 2020 were averaged and the percentage of PEVs is estimated to be about 3.4% of the cars 9 years or younger in 2020. Using the information from car age distribution chart [3], the number of PEVs in the Greater Rochester Area is estimated to be around 10,000 cars. With almost every car manufacturer introducing a PEV in the coming years, this seems to be a very reasonable assumption [46].

3.3 Estimating hourly traffic profile for Greater Rochester Area

Figure 3.4: Rochester Urban Area [4]

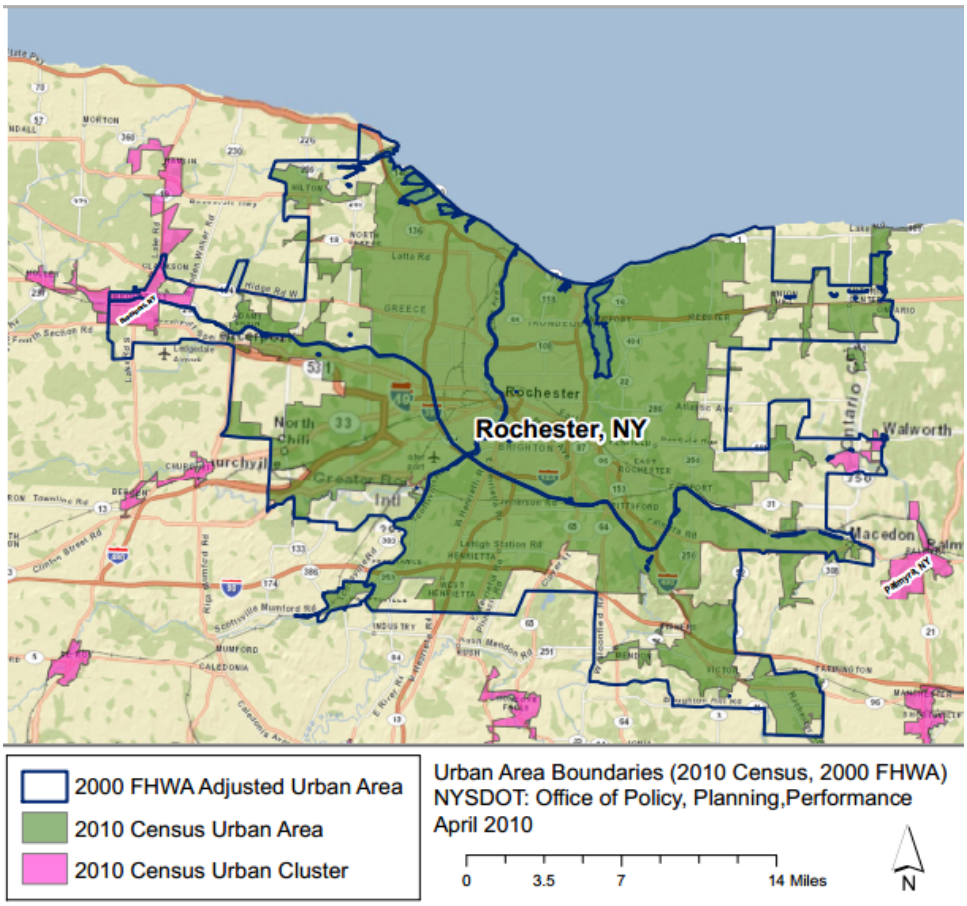

To estimate the number of vehicles on the road by the hour of a day,

statistics from Illinois traffic profile were considered [47]. As the area of interest, shown in Fig 3.1 significantly overlaps the urban area, shown in Fig 3.4 as considered by the Census bureau [4], the traffic patterns of a Illinois Downstate urban area were used.

Figure 3.5: Estimated hourly traffic profiles for Greater Rochester Area

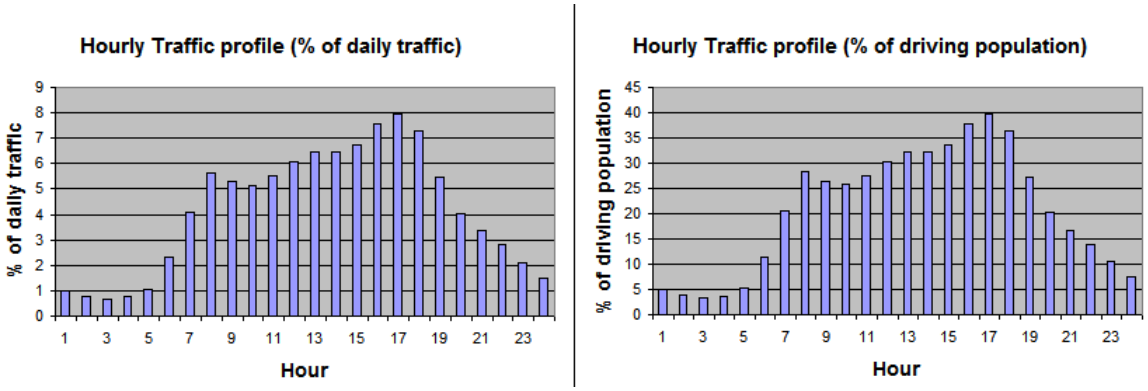

The Illinois DOT provided percent daily traffic statistics for interstate and non-interstate. However, the percent of daily traffic, or in common words, the busyness of the roads at different hours, on both interstate and non-interstate was perceived to be approximately the same. Since the Greater Rochester Area contains both interstate and non-interstate roads, the statistics at each hour were averaged as shown in Table 3.2, to get a single set of statistics for the entire area. However, no data or methodology could be found, to correlate the percent of daily traffic with the percentage of all cars in the area being on the road during the corresponding hour. Due to the lack of statistics, a reasonable assumption had to be made. Considering that a significant workforce leaves work at between 4PM - 5PM, and along with the residual traffic on the road, a peak traffic of 7.95% between 4PM - 5PM was correlated to be 40% of the driving population, a significant minority. The estimated percent daily traffic profile based on ILDOT statistics and correlated percent of driving population at each hour are displayed in Figure 3.5. The percent of driving population on the road at each hour was estimated using this relationship $\hat{N}_h = \frac{\hat{P}_{dp}}{100} * \hat{M}$, where $\hat{N}_h$ is the estimated

number of PEVs on the road at hour index h, $\hat{P_{dp}}$ is the percent of driving population at hour index h, and $\hat{M}$ is the estimated total number of PEVs in the area (10,000 in this case study).

Table 3.2: Estimated hourly traffic profile for Greater Rochester Area

Hour	Downstate Urban (Non-Hwy) % daily traffic	Downstate Urban (Hwy) % daily traffic	Avg of Hwy and Non-Hwy	% of driving population on road	Number of cars on road
0	0.8	1.2	1	5	500
1	0.6	1	0.8	4	400
2	0.4	0.9	0.65	3.25	325
3	0.5	1	0.75	3.75	375
4	0.8	1.3	1.05	5.25	525
5	1.8	2.8	2.3	11.5	1150
6	3.7	4.5	4.1	20.5	2050
7	5.4	5.9	5.65	28.25	2825
8	5.3	5.3	5.3	26.5	2650
9	5.3	5	5.15	25.75	2575
10	5.7	5.3	5.5	27.5	2750
11	6.6	5.5	6.05	30.25	3025
12	7	5.9	6.45	32.25	3225
13	6.8	6.1	6.45	32.25	3225
14	7.1	6.4	6.75	33.75	3375
15	7.8	7.3	7.55	37.75	3775
16	8.1	7.8	7.95	39.75	3975
17	7.3	7.3	7.3	36.5	3650
18	5.5	5.4	5.45	27.25	2725
19	4.1	4	4.05	20.25	2025
20	3.4	3.3	3.35	16.75	1675
21	2.8	2.8	2.8	14	1400
22	2	2.2	2.1	10.5	1050
23	1.2	1.8	1.5	7.5	750
Total	100	100	100		

*Assuming peak 7.95% of daily traffic at 4-5pm = 40% of driving population

3.4 Energy profile of a Plug-in Electric Vehicle

The energy needed by a vehicle to travel a certain distance is expressed with this relationship [48]:

$$E_t = \int_0^t \frac{V}{1000}(Mgf_r + \frac{1}{2}\rho_a C_D A_f V^2 + M\delta\frac{dV}{dt} + Mgi)$$

where
- M is the mass of the vehicle in kg
- V is the speed of the vehicle in m/s
- g = 9,81 m/s^2 is the gravity constant
- ρ_a = 1,205 Kg/m^3 is the air density
- C_D is the aerodynamic drag coefficient
- A_f is the front area of the vehicle in m^2
- δ is the rotational inertia factor
- $\frac{dV}{dt}$ the acceleration in m/s^2
- i is the spatial gradient of the road, equal to 0 for the standard city cycle.

Another source [49] expressed the energy required by a vehicle to travel certain distance as follows:

$$Energy = Power * Time = [\frac{1}{2}C_d\rho_{air}A_{car}v^3]/E_e * [\frac{d}{v}]$$

where
- C_d is the aerodynamic drag coefficient
- ρ_{air} is the air density
- A_{car} is the front area of the vehicle
- v is the velocity of the vehicle
- E_e is the engine efficiency
- d is the distance traveled

While an analytical method can be used, both relationships provided results, in magnitudes different than the range estimates provided by a manufacturer (Chevrolet), possibly due to our inaccurate assumptions of unavailable parameter information. However, since we had access to a 2013 Chevy Volt and it is the most popular PEV in United States at present, we considered the use of experimental data obtained from it. Kilowatt usage was recorded while the vehicle was traveling different speeds and the experiment provided more reasonable results. For example, it can be observed from Figure 3.6, that at 50 mph, the vehicle uses close to 16 kWh of charge to travel 50 mi. This data seemed reasonably close to the official range of 38 mi, by USDOE [16] and was chosen to model the charge depletion profile of a PEV. In addition, the energy lost in acceleration was approximated to equal to energy gained through regenerative braking. Therefore, the energy transfers were ignored and the power model obtained through experimental data along with the relationship

$$Energy = Power \times Time$$

were used to calculate the energy required by a PEV to travel a certain distance, at a certain speed, in a certain time.

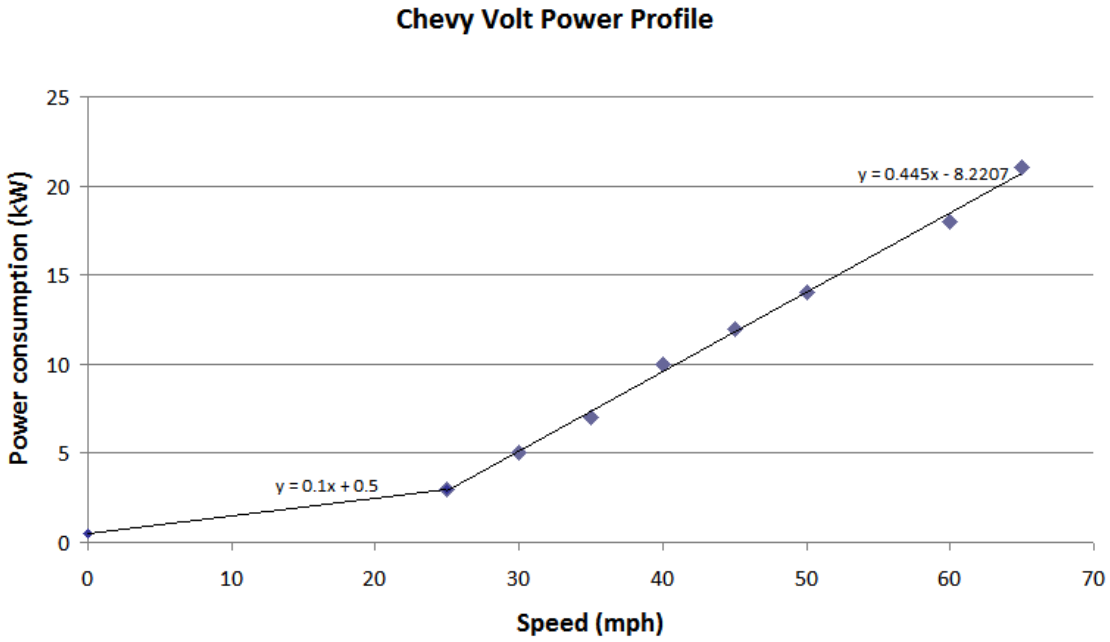

Figure 3.6: Chevy Volt Power Profile

The power profile of the 2013 Chevy Volt used is shown in Figure 3.6, and the corresponding data is presented in table 3.3. From this data, the relationship between speed of the vehicle and the power consumed by the vehicle is modeled by this relationship

$$p(s) = \begin{cases} 0.1s + 0.5, & s < 25 \\ 0.45s - 8.22, & s \geq 25 \end{cases} \tag{3.1}$$

where $p(s)$ is the instantaneous Power consumption in kW and s is the speed of the vehicle in mph.

3.4.1 Estimating energy consumption of a PEV in a route

When a route is considered, there are many sections in it, and each section has a varying speed limit. Considering the speed in each section while calculating energy consumption was deemed to be more accurate, as it accounts for different power consumption and different speeds. If the average speed based on total route distance and route time is considered, the variability in

Table 3.3: Chevy Volt Power Profile

Speed (mph)	Power consumption (kW)	Measurement location
0	0.5	RIT campus
25	3	RIT campus
30	5	RIT campus
35	7	Scottsville Road
40	10	Scottsville Road
45	12	Scottsville Road
50	14	Scottsville Road
60	18	390N
65	21	390N

power consumption rate along the route is lost. Therefore, the energy consumed was calculated for each section and summed to get the total energy depletion for the route. It is expressed by the following relationship:

$$\begin{aligned} E_l &= P(s_l) \times D_l \\ E_r &= \sum E_l \end{aligned} \tag{3.2}$$

where
E_r is energy consumed during the route
E_l is energy consumed during a leg of the route
$P(s_l)$ is the average power consumption during the route, given by equation (3.1)
D_l is the time duration of the section

3.5 Forecasting the macro energy demand from Plug-in Electric Vehicles

A number of routes take place in the greater Rochester area, at each hour, by the plug-in electric vehicles. The specific number at each hour is estimated as described in Section 3.3 (Estimating hourly traffic profile for Greater Rochester Area).

Figure 3.7: A sample route
The dots indicate waypoints of the route, and the colors indicate the cumulative amount of energy depleted at that waypoint.

The energy consumption for each of the routes is modeled as described in Section 3.4.1 (Estimating energy consumption of a PEV in a route). For visualization, a sample route is shown in Figure 3.7. The color of the waypoint represents the kWh depletion/energy consumption as time and distance increase. Figure 3.8 shows 2000 routes that were analyzed.

To see the macro energy demand visually, we need to divide the area of interest into smaller regions. Therefore, Greater Rochester Area was divided into smaller "tracts." In this thesis, a tract refers to a census tract or a geographic area, and not a path as one may commonly interpret. The area of interest was divided into tracts, instead of any other form of division, due to the availability of shape and population information. A key decision made here was that the depletion of the PEV's energy is imposed on the grid within the hour, when the route ends. This assumption reflects our vision that consumers will want a convenient charging model similar to our present gas refueling model. To estimate the macro energy demand caused by PEVs, we simulate driving routes across the Greater Rochester Area, at each hour of the day. Each route has a origin, some way points and a destination, as shown in Figure 3.7. After the routes are simulated, the energy consumption or "kWh depletion" of each tract is calculated by summing the "kWh depletion" from all the routes that end in that tract. This calculation is represented in Equation 3.3 as $E_t = \sum E_{r_t}$. The kWh depletion in the all tracts considered together lets us estimate the PEV energy demand in the Greater Rochester Area. The energy demand of each tract and the Greater

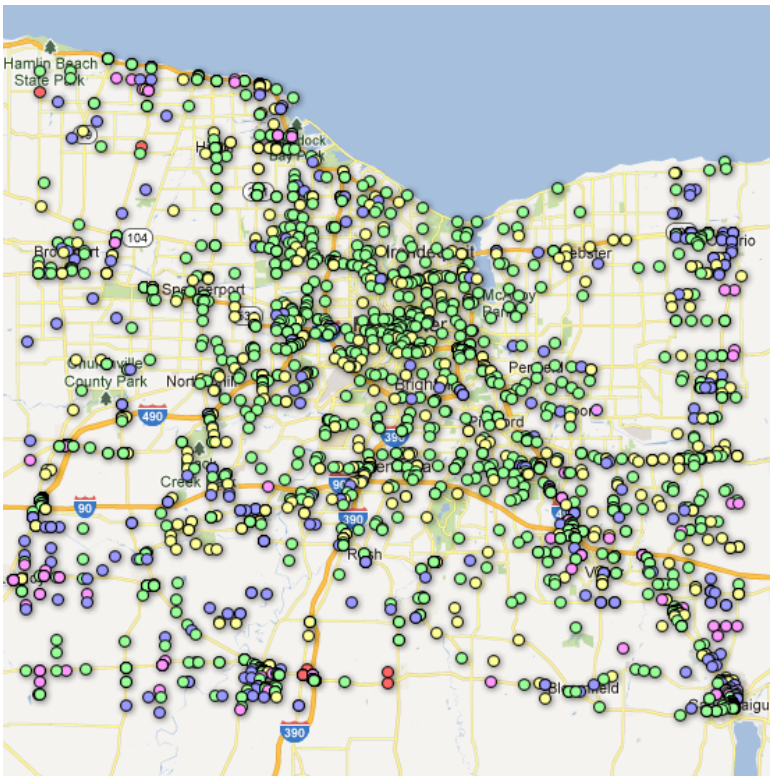

Figure 3.8: 2000 Sample Routes
The dots indicate waypoints of various routes, and the colors indicate the cumulative amount of energy depleted at that waypoint.

Rochester area are described by this relationship:

$$\begin{aligned} E_t &= \sum E_{r_t} \\ E_{gr} &= \sum E_t \end{aligned} \tag{3.3}$$

where E_{r_t} is the energy consumption of a route in a tract, in a particular hour, E_t is the energy depletion/consumption in that tract, in that particular hour, and E_{gr} is the total energy demand in Greater Rochester Area in the same hour.

3.5.1 Generating Origins and Destinations

As previously described in Section 3.5, the Greater Rochester Area was divided into census tracts, using New York State census tract shape information [41]. At the same time, 20,000 uniformly distributed geographic coordinates within the bounds of the area of interest (Figure 3.1) were generated using a random distribution function, reasonably hoping to have at least one location fall under each census tract. Once a set of coordinates that belong to each tract was established, a weighted random function with the weight being population density was used to generate the origins and destinations. In this population density distributed function, the probability of a tract being selected is proportional to the 2010 Census population of the tract. Once a tract is selected, uniform random distribution function was used to select one of the geographic coordinates belonging to the tract. The population weighted origin and destination selection process is represented mathematically as follows:

$$\begin{aligned} &\sum_{k=1}^{N_T} R_{T_k} = 1 \\ &R_{T_k} = \frac{P_{T_k}}{P_{GROC}} \\ &R_{T_{k+1}} = R_{T_k} + \frac{P_{T_k}}{P_{GROC}} \\ &k_T = U_R[0, 1.00] \\ &l_{k_T} = U_R[1, N_{l_{K_T}}] \end{aligned} \tag{3.4}$$

where
N_T is the number of tracts in Greater Rochester Area
R_{T_k} is the population percent of tract k in Greater Rochester Area
P_{T_k} is the population of tract k
P_{GROC} is the population of Greater Rochester Area
U_R is a uniform distribution random function
k_T is the selected tract from Greater Rochester Area
$N_{l_{K_T}}$ is the number of available locations in tract k

l_{k_T} is the selected location in tract K

3.5.2 Generating Routes

Google Directions API was used to get the route info between origins and destinations. The route profile includes, sections of the trip, each section representing the road between two turns, including the start and end of the route. Each section information includes the distance covered by the section and the estimated time it takes to complete the section. Information from the individual sections was used to better estimate the energy consumption in a route, as explained in detail in Section 3.4.1 (Estimating energy consumption of a PEV in a route).

3.5.3 Simulating Macro Energy demand

Using the number of the routes at each hour estimated in Section 3.3 (Estimating hourly traffic profile for Greater Rochester Area), power demand was estimated for each tract for each hour of the day. For each origin and destination combination, while the routes are generated, the cumulative charge depletion was calculated. The charge depletion for each leg of the route was computed by using Equation 3.1. Similarly, the cumulative charge depletion was computed by using Equation 3.2. For every tract in the area of interest, all the cumulative charge depletions were summed (Equation 3.3) to represent the tract's energy demand from PEVs at that hour. Similarly, the demand from all the tracts summed together gives us an anticipated Energy Demand caused by PEVs in the greater Rochester Area, in the year 2020.

3.6 Results

Anticipated macro energy demand at various hours of the day in 2020, of the Greater Rochester Area, is visualized in Figure 3.9. Only a few samples were selected from the simulation procedure described in 3.5.3. The

Figure 3.9: Energy Demand from PEVs at various times of the day

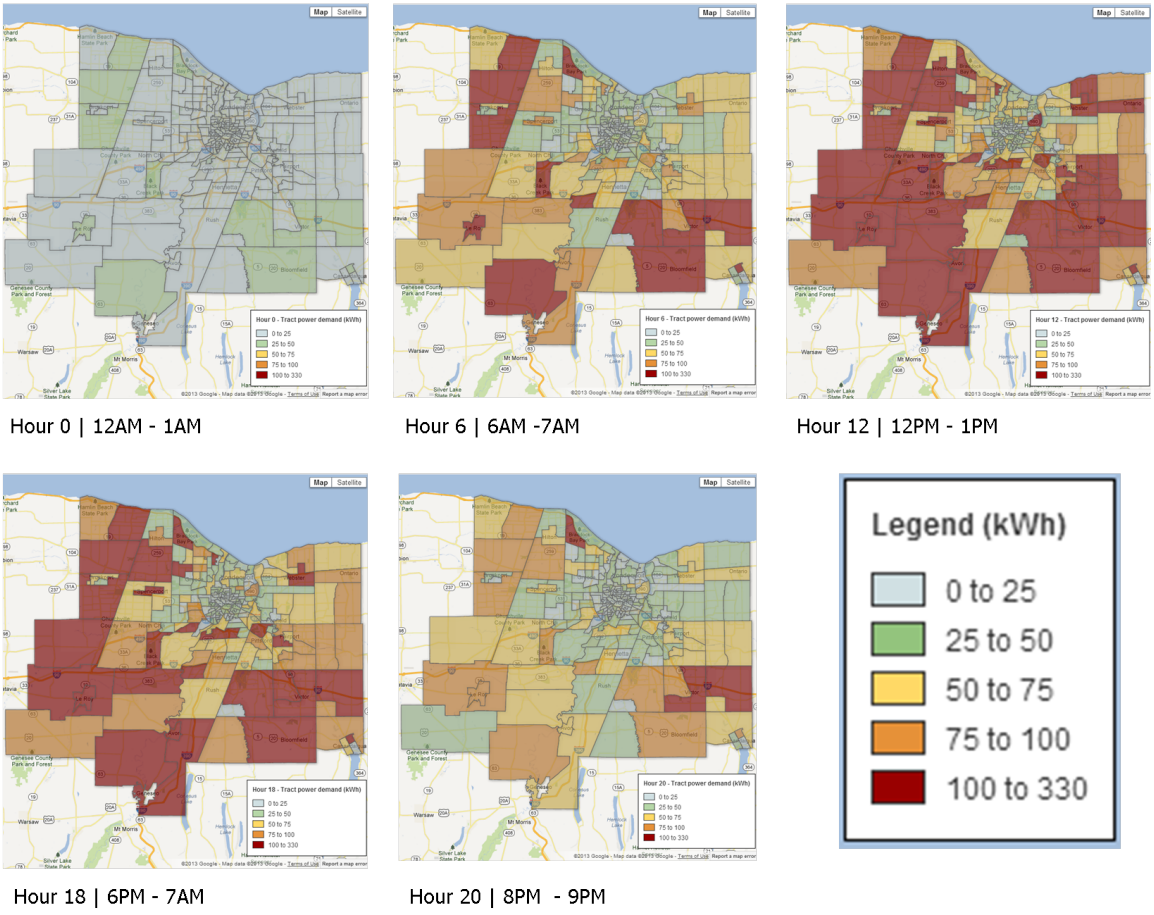

visualizations for the rest of the results are located in appendix B. The energy demand was categorized into 5 intervals, 0-25 kWh, 25-50 kWh, 50-75 kWh, 75-100 kWh and 100 kWh+. It shows the variation in energy demand during a day at varying levels in different tracts of the area. Finer resolutions for energy demand intervals can be chosen, but considering the uncertainty in PEV sales and traffic on a particular day, the granularity of the legend was believed to be sufficient. The raw data is available on the CD-ROM for reclassification.

While observing the macro energy demand results, it hints the possibility that the larger tracts have larger energy demand simply because there could be more number of people in that tract compared to a much smaller

tract; however, there is another reasonable possibility. The people with either origin or destination or both in larger tracts generally have to drive farther distances than the people with both origin and destination in smaller tracts based on the technique presented in Section 3.5. For instance, an example to clarify this plausibility is that, considering a workplace to be the origin and corresponding home to be the destination there is higher probability that the distance between home and work place in two small tracts is smaller (because most of the small tracts are in center of the city) than the distance between a home in a large tract and the corresponding workplace in a small tract (because most of the large tracts are away from the center, away from the small tracts), than the converse. The demand forecast can be normalized to eliminate the population factor, but it was deemed unnecessary because the energy demand per capita is not of importance to the charging stations. The absolute energy demand is the parameter of importance to the local charging stations, as it lets them anticipate demand and schedule the charging of their battery banks. In addition, these results are also useful to the smart grid operators, who can dynamically route energy to the regions in high demand, as well as alleviate some demand by utilizing the demand forecast to set ratemaking prices [25].

Chapter 4

Renewable Energy Resource Estimation

4.1 Overview

Renewable energy is deemed necessary for many reasons. As previously mentioned, some of the well known ones include energy security and independence, sustainability, lower long term energy costs and prevention or mitigation of climate change. As the energy demand from PEVs was forecasted for 2020, in the previous Chapter, it was desired to estimate the amount and type of renewable sources that would be needed to offset or mitigate the demand caused by PEVs. In this research, wind and solar renewable sources of energy were considered as they are widely available and commonly deployed, and experimental data for an installation of each was available.

4.2 Offshore Wind Energy in Greater Rochester Area

One of the factors to consider for wind energy is the wind speeds in the area. As shown in Figure 4.1, the shores of Greater Rochester Area seem to have access to average wind speeds of 7-9 m/s [5]. With these speeds, a GE 1.6-82.5 Wind Turbine theoretically generates between 1.2-1.4MW and a GE 1.5-77 Wind Turbine generates between 1-1.2MW of power [50]. In addition, there are a wide range of wind turbines available ranging up to 7.5MW. However, in this research, only wind speeds over the land was considered due to the availability of experimental data.

Figure 4.1: Average Wind Speed near Rochester [5]

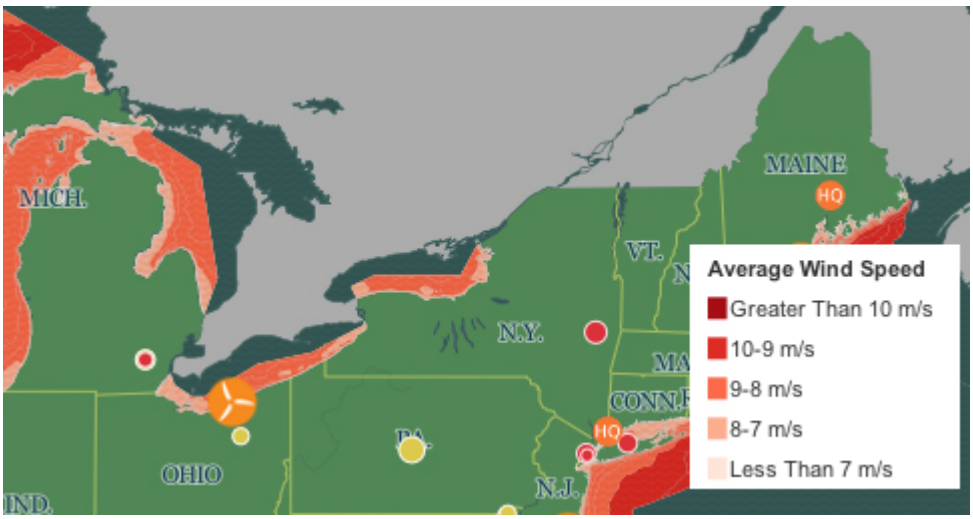

4.3 Wind and Solar complementarity

An intuitive thought to consider is that stormy days are windy and cloudy while days with clear skies are calmer. Therefore, having both solar and wind power generation systems can complement each other to provide a more consistent amount of supplemental renewable energy to the grid. In addition, the characteristic can be applied through out the year. On average, days in winter are more windy than the days in summer, and days in summer have more sun due to the earth's angle towards the sun. Using these principles, a practical implementation was developed by Southewst Windpower. One of their products, the Skystream Hybrid 6 wind and solar system, aims to supply consistent renewable energy throughout the year [51].

Figure 4.2: Rochester,NY wind speeds

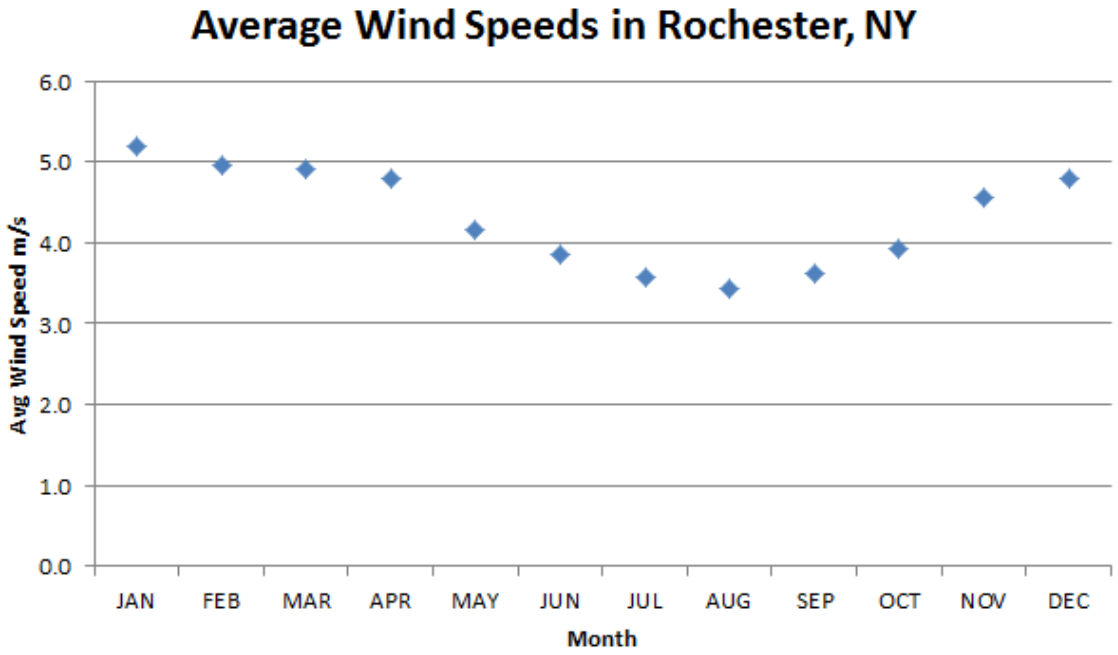

Using information from National Climate Data Center, NOAA [52], the average wind speeds in Rochester, NY across the year were plotted as shown in Figure 4.2, to realize the lower wind speeds during the summer months.

Figure 4.3: Rochester,NY Daylight hours and Solar flux [6]

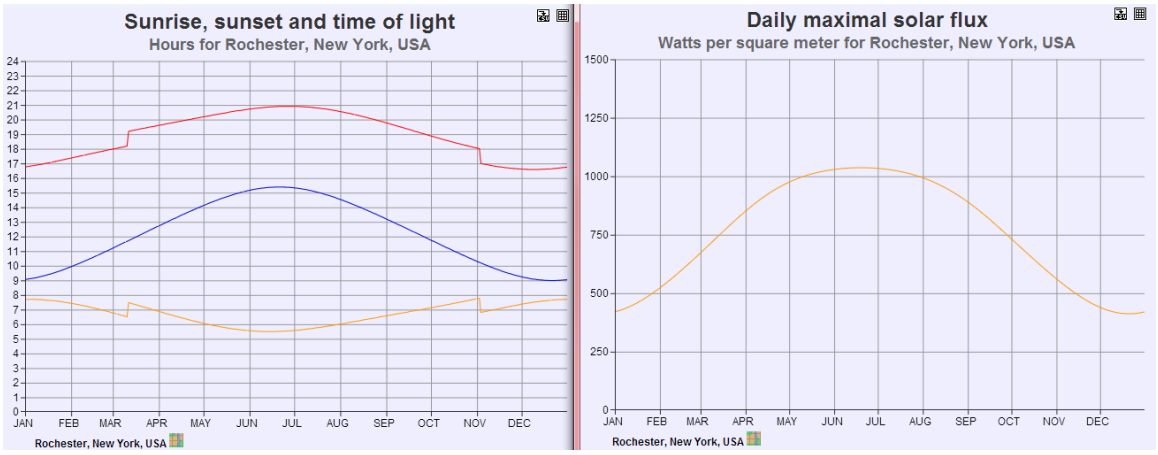

Similarly, the average daylight and the solar flux graphs were obtained from [6], shown in Figure 4.3 to observe the inverse relationship to the wind speeds. It essentially shows that, since there is higher solar energy in summer months when the wind speeds are lower on average, both renewable sources of energy can potentially be used to complement each other to deliver electricity more consistently throughout the year.

4.4 Assumptions

The 2020 anticipated or assumed PEV energy demand, estimated from analysis in Chapter 3, that is desired to be met or mitigated, is illustrated by Figure 4.4. In Figure 4.4a, each tract's energy profile of the day is displayed in a stacked layout. The peak energy demand of all the 217 tracts considered in this research, amounts to more than 10 MWh at the peak hours of 4 PM and 5 PM. In Figure 4.4b, the same data is displayed as an accumulation over the day.

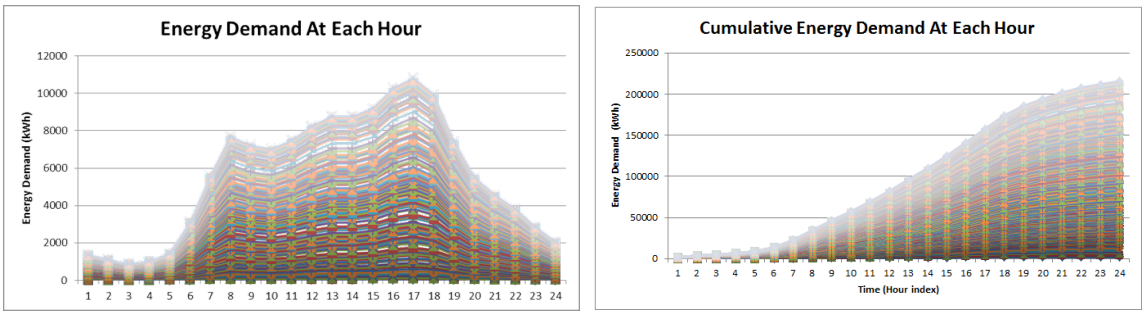

(a) Hourly

(b) Hourly Cumulative

Figure 4.4: Energy Demand at Each Hour
Each colored line in the above filmstrip represents a tract's anticipated energy demand, in the year 2020. The energy demand values of the tracts are stacked on each other, to observe the energy demand of the entire Greater Rochester Area.

A 250 kW Wind Turbine and a 60kW Photovoltaic Array with efficiency of 14% were considered as the base units for estimation of renewable resources, as historical data was available for this equipment. The Wind Turbine data, as previously mentioned in Chapter 2, was from a local plastic molding factory. The Solar Energy data was obtained from an experiment

at Baylor University [53]. The experimental solar data contained annual maximum instantaneous power output of 153 watts per photovoltaic cell. To approximate and envision a future solar panel installation, the roof area (3630 sq ft ,W: 33 ft, L: 110 ft) of a nearby gas station (Hess at 222 Jefferson Road, Rochester, NY) was considered. Using a solar panel power estimator[19], it was estimated that 3000 sq ft or 375 panels of a generic Polycrystalline solar panel model will generate approximately a maximum of 62.6 kW. Therefore, we scaled the 153 watts maximum from the experimental data, approximately by a factor of 392, to a 60 kW maximum output of an envisioned future solar panel installation. In addition, underpredicting the energy supply was favored over overpredicting it. For instance, larger, taller and newer wind turbines than the one considered may provide more energy with better reliability. Similarly, the solar panels will probably become more efficient over the next few years as the current public policy favors grants towards renewable energy research especially solar [54].

Wind and solar energy data from three overlapping days were used to get a coarse estimation of the available renewable energy supply. The wind power data from April 13, 14 and 15 of year 2012, from Rochester, NY and the solar power data from April 13, 14 and 15 of year 2012 from Waco, TX were used as they were the only available experimental data. The combined power output is shown in Figure 4.5.

Figure 4.5: Three day wind+solar energy output

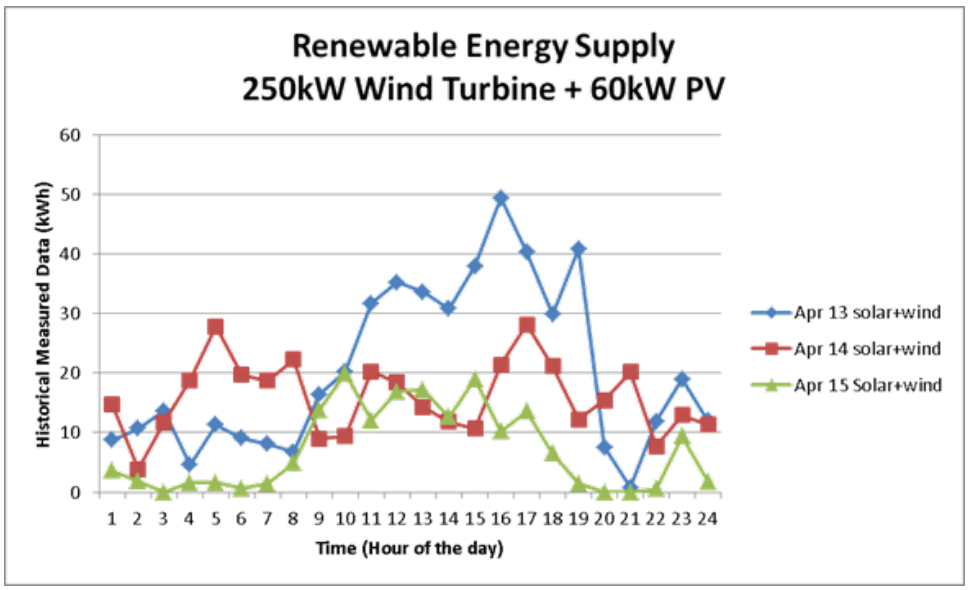

The volatility of these resources can be seen, as the average hourly energy generated for the three days were 20.4kWh, 15.9kWh and 7.1kWh.

4.5 Results

4.5.1 Configurations for resource evaluation

A few configurations of renewable resources were tested for three consecutive days - Fixed number of wind and solar installations per tract, variable number of wind and solar installations per tract based on the area of the tract, and time delayed release of energy from the battery banks.

Fixed number of installations per tract

In the first method, fixed number of two and three wind and solar hybrid installations per tract were evaluated. The results are shown in Figures 4.6a and 4.6b. It was observed that two of each installations per tract is insufficient, while three of each installations per tract may be excessive, and excess energy may be lost if excess supply accrued is magnitudes larger, as it is unreasonable to expect extremely large energy storage systems. However, in

many cases, excess demand may also be be sold or credited to the conventional grid in a policy commonly referred as net metering. As of 2010, net metering was offered in 43 states in the U.S. [55]. In addition, the results can be vastly different with wind and solar data from other days.

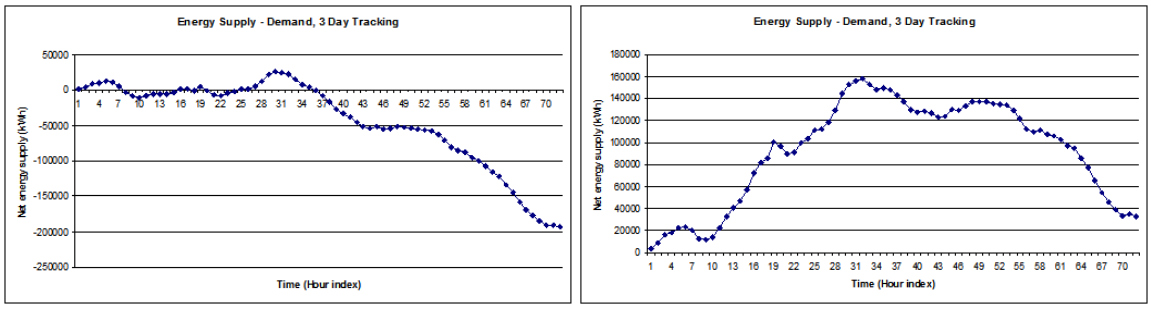

(a) 2 installations per tract

(b) 3 installations per tract

Figure 4.6: Energy Supply - Depletion, cumulative 3 day tracking
Two installations of Wind and Solar energy sources seems to fall short of the demand on low wind and sun days. Three installations per tract will require massive storage in terms of battery banks. However, if net metering [55] is available and a renewable charging station is connected to the conventional power grid, excess energy can be sold to the convention grid.

Variable number of installations per tract

An alternate approach to increase grid stability and efficiency is to try to mitigate the demand, instead of trying to meet the demand. In this approach, the number of installations in a tract was chosen based on the area of the tract. For tracts less than 10 sq mi, a single installation of wind turbine and a solar installation was chosen for evaluation and for tracts greater than 10 sq mi, two installations of wind and solar were assumed. The results for this approach are shown in Figure 4.7a.

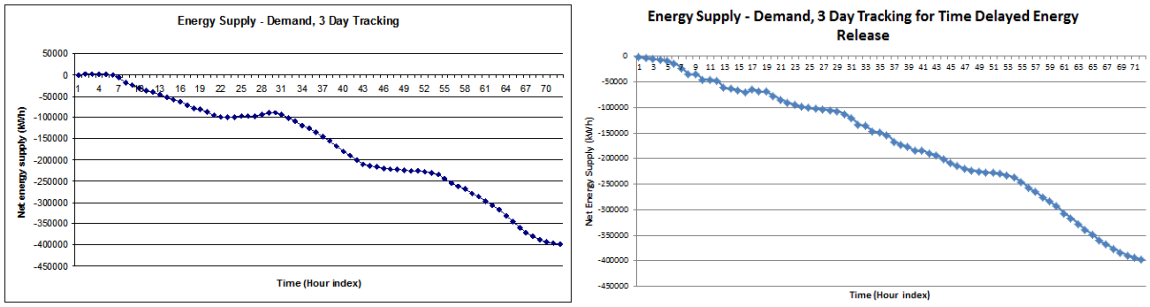

(a) Instantaneous Release of Energy

(b) Time Delayed Release of Energy

Figure 4.7: Energy Supply - Depletion, variable number of installations

In this configuration, 1 or 2 installations were considered based on the area of the tract. Figure 4.7a shows the cumulative net energy depletion that needs to be fullfilled by the conventional grid. The demand is observed to be non-linear, with surges at peak times. The net energy depletion shown in Figure 4.7b is same as the net energy depletion shown in Figure 4.7a. However, releasing the energy in varying amounts at different times of the day shows linear accumulation of the energy needed to be fulfilled by the conventional grid.

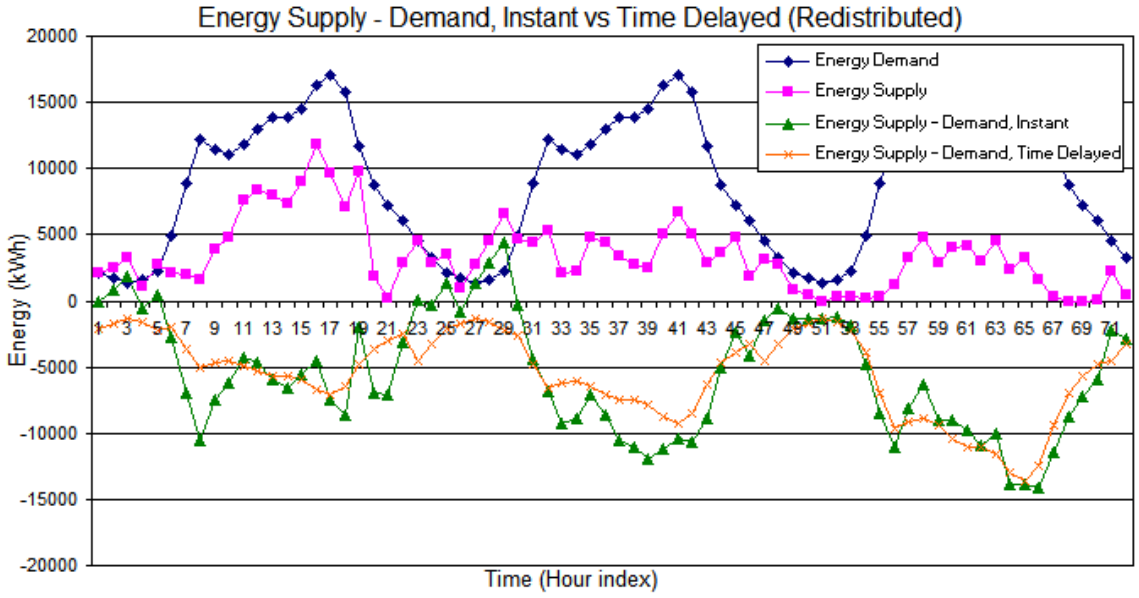

Figure 4.8: Time Delayed Release of Energy Supply

The net energy depletion shown here is same as the net energy depletion shown in 4.7b. However, it is shown at energy depletion at each hour, rather than a cumulative accumulation of net energy depletion.

Time delayed release of energy

An improvement to the method previously described is to store the renewable or supplemental energy in battery banks or pumped-storage systems and release the energy during particular periods of time to linearize the power demand over the course of the day. This ensures that the utilities see a flatter power demand throughout the day, which helps them generate conventional power more efficiently and avoid overloading of the distribution grid. The time delay release was modeled such the percent of renewable energy released in an hour is directly proportional to the percent of anticipated demand at the corresponding hour. The results can be seen in Figure 4.7b. The graph is intended to simply give an illustration of how a time delay release can mitigate peak power demand. The data representation is not completely accurate, as we distributed energy from the future. It was represented this way because, to estimate how much energy to release at the first hour, we don't have information of how much renewable energy was generated and stored during the previous 23 hours. The energy released at each hour of a day, in Illustration 4.7b, is expressed by this relationship:

$$R_k = \begin{cases} 0, & 6 > k > 22 \\ \frac{D_k}{\sum_{m=6}^{22} D_m} * \sum_{n=1}^{24} S_n, & 6 \leq k \leq 22 \\ Undefined, & 1 > k > 24 \end{cases}$$

where k is the hour index of the day, R_k is the proposed energy release during hour k, D_k is the anticipated energy demand during hour k, D_m is the anticipated energy demand during hour m, S_n is the renewable energy generated during hour n. The range for m was chosen by observing the high energy demand times in Figure 4.4a (Energy Demand at each hour). The duration between 12AM to 7AM and 10PM to 12AM were selected to have no renewable energy release, as those times had relatively low energy demand. The chosen energy release percentages are shown in Table 4.1.

Table 4.1: Time delayed release of energy from battery banks

Hour	% daily energy released
1	0
2	0
3	0
4	0
5	0
6	0.025
7	0.044
8	0.061
9	0.058
10	0.056
11	0.060
12	0.066
13	0.070
14	0.070
15	0.073
16	0.082
17	0.086
18	0.079
19	0.059
20	0.044
21	0.036
22	0.030
23	0
24	0

4.5.2 Analysis

Renewable energy resource estimation was performed based on the order of number of wind and solar hybrid installations per census tract of the Greater Rochester Area. To verify the effectiveness of the estimation, the net energy supply was tracked cumulatively for a set of random three consecutive days, for which solar and wind data was available.

Considering the anticipated demand is approximately 200 MWh per day,

as shown in Figure 4.4, the number of required wind and solar energy systems varied from two per tract on a optimal day to five systems per tract on a non-optimal day. The variation will be much higher when results across more days are considered. In a worst case scenario, on a day without any wind and complete cloud coverage, the renewable energy generated will be very insignificant. Consequently, the energy storage systems may not be able to supply the needed energy for long duration, without being replenished. Since such uncertainty seems unreasonable to completely depend on renewable resources (to meet energy from PEVs), an alternate and a more reasonable approach is evaluated. It is to simply use renewable resources to reduce the peak demand by offloading it onto non-peak times, instead of trying to meet the demand. For instance, as shown in Figure 4.7b, fewer renewable resources can be used to make the demand more constant or have linear cumulative growth across the day. Essentially, renewable energy generated during off peak hours will be stored and released during peak hours. The overall grid will be more efficient as the utility companies can generate more constant power output with a flatter demand across the day and the distribution grid will not be overloaded as the energy is stored locally.

Chapter 5

Conclusion

There are existing Markov based wind forecast models to estimate power output via probability and there are numerous solutions offering ways to make an electric grid smarter but there isn't any known study that bridges the gap between them to mitigate the additional load caused by the influx of the electric vehicles.

The model developed in chapter 2 can be used by the charging stations or a centralized control center to forecast renewable energy a day ahead, and guide or incentivize consumers to possibly charge ahead of time. If the forecasted renewable energy is too low, the battery banks at charging stations can also be charged via the conventional grid during off-peak hours to reduce the surge during upcoming peak hours.

The results from near future energy depletion caused by the PEVs and resource estimation, chapters 3 and 4, can be used to make long term budget plans to invest in the recommended resources. Using results from this research and solutions from other smart grid applications, the problem of imbalanced grid and insufficient power supply due to the influx of PEVs can be very reasonably solved.

Chapter 6

Discussion and future work

There are many other possibilities to mitigate the issue addressed by this research. Some of the other supplementary and/or complementary solutions and future work are discussed here.

6.1 Indirect coupling of battery banks and the grid

Keeping the charging stations indirectly coupled may provide significant benefits. For instance, if the wind and solar forecast for next day is too low, the battery bank at a charging station can be charged during off peak hours, to be well prepared to offset peak demand during peak hours. On the other hand, when multiple PEVs connect to the charging station at high amperage and voltage difference for quick charging, there will not be sudden voltage drops imposed on the conventional grid.

6.2 Smart or decentralized charging algorithm

Some PEVs, such as Tesla Model S, have a charge mode selection capability to select standard range or maximum range. Similarly, that feature can probably extended to let the user decide how much time the EV has to charge to desired capacity. As described in [7], the EV battery capacity, charging price, speed and deadlines can be used as part of a distributed algorithm for scheduling via signal processing. The EVs can be capable of computing a charging profile that intends to reduce the combined demand from all PEVS at a time. If the aggregated demand is too high, the utility or the control

center can set a higher utility price and guide the EVs voluntarily adapt to a different charging profile based on user constraints mentioned before.

6.3 Benefits for consumer, utility companies and the environment

Sustainable energy can be used along with electric vehicle signal processing capabilities to schedule the EVs to charge at a higher or faster rate when there is a higher energy forecast and less when there is a lesser energy forecast. This benefits the customer as the time to be charged can be picked to be when the utility rates are low. The utility companies benefit as they gain more control to balance the grid and could potentially use electricity from the EVs to support the grid during occasional surge in electricity demand (based on user configuration), etc [29].

6.4 Future Work

Similar to a Markov chain model, there seem to be atleast two other models that can be used for short term wind power forecasting. A reference was made by [36], that a Auto Regressive Moving Average model can also be used for wind power forecast. As mentioned in Chapter 1.2 (Historical Review), neural network models can also be used for wind power forecast. The same data and conditions can be tested with those models to observe if they yield more accurate results.

As previously noted in Section 2.1 (Overview section of Renewable Energy Supply Forecast Model), a solar forecast model could not be integrated into research due to delays in equipment installation. It will be beneficial to experiment with existing solar forecast models, to evaluate how accurately solar energy can be forecasted in hourly intervals for the next day, using standard hourly weather forecast as an input. In addition, when the Golisano Institute for Sustainability or any other entity provides access to data from a wind and solar energy hybrid system, where all resources are

present in the same location, the wind and solar complementarity analysis will yield more accurate results than the ones presented in this research.

Bibliography

[1] Ali Ipakchi and Farrokh Albuyeh, "Grid of the future," *Power and Energy Magazine, IEEE*, vol. 7, no. 2, pp. 52–62, 2009.

[2] Fuhrlander Aktiengesellschaft, "Fuhrlander FL 250," http://www.fuhrlander.com/images/fl250_de.pdf.

[3] "National household travel survey," http://www.fhwa.dot.gov/policyinformation/presentations/his_nhts2011.cfm.

[4] "Urban Area Boundaries," https://www.dot.ny.gov/divisions/policy-and-strategy/darb/dai-unit/ttss/repository/roc10.pdf.

[5] "Accelerating offshore wind development," http://energy.gov/articles/accelerating-offshore-wind-development.

[6] "Sunrise, sunset, daylight in a graph," http://ptaff.ca/soleil/?lang=en_CA.

[7] Andres Kwasinski and Alexis Kwasinski, "Signal Processing in the Electrification of Vehicular Transportation: Techniques for Electric and Plug-In Hybrid Electric Vehicles on the Smart Grid," *Signal Processing Magazine, IEEE*, vol. 29, no. 5, pp. 14 – 23, September 2012.

[8] Christopher Decker, "Electric Vehicle Charging and Routing Management via Multi-Infrastructure Data Fusion," M.S. thesis, Rochester Institute of Technology, October 2012.

[9] Alexander D Hilshey, Pooya Rezaei, Paul DH Hines, and Jeff Frolik, "Electric vehicle charging: Transformer impacts and smart, decentralized solutions," in *Power and Energy Society General Meeting*. IEEE, 2012, pp. 1–8.

[10] Thomas Magee, "Con Edison builds a smart distribution grid," *Electric Perspectives*, p. 82, June 2011.

[11] Alexis Kwasinski, "Local energy storage as a decoupling mechanism for interdependent infrastructures," in *Systems Conference (SysCon), 2011 IEEE International*. IEEE, 2011, pp. 435–441.

[12] "Electric drive vehicle sales figures," `http://www.electricdrive.org/index.php?ht=d/sp/i/20952/pid/20952`.

[13] "EV Everywhere Grand Challenge Blueprint," `http://www1.eere.energy.gov/.../pdfs/eveverywhere_blueprint.pdf`, Jan 2013.

[14] Chevrolet, "2013 volt models and specs," `http://www.chevrolet.com/volt-electric-car/features-specs/options.html`.

[15] Toyota, "Prius plug-in hybrid 2013," `http://www.toyota.com/prius-plug-in`.

[16] U.S. Department of Energy, "Electric vehicles: Compare side-by-side," http://www.fueleconomy.gov/feg/evsbs.shtml, May 2013.

[17] Sebastian Blanco, "Details on nissan leaf battery pack, including how recharging speed affects battery life," *Autoblog*, May 2010.

[18] Tesla Motors Inc, "Charge your model s," http://www.teslamotors.com/charging.

[19] Weather Underground Inc, "Solar calculator," http://www.wunderground.com/calculators/solar.html?MR=1.

[20] Christine Schoppe, "Wind and pumped-hydro power storage:determining optimal commitment policies with knowledge gradient non-parametric estimation," B.S. Thesis, Princeton University, 2010.

[21] "Office of Energy Projects Energy Infrastructure Update For January 2013," Tech. Rep., Federal Energy Resulatory Commission, January 2013.

[22] "Innovate, Manufacture, Complete: A Clean Energy Action Plan," Tech. Rep., The Pew Charitable Trusts, 2012.

[23] Martin Geske, M Stotzer, P Komarnicki, and Zbigniew A Styczynski, "Modeling and simulation of electric car penetration in the distribution power system - Case study," in *Modern Electric Power Systems (MEPS), 2010 Proceedings of the International Symposium*. IEEE, 2010, pp. 1–6.

[24] Shengnan Shao, Manisa Pipattanasomporn, and Saifur Rahman,

"Challenges of PHEV penetration to the residential distribution network," *2009 IEEE Power & Energy Society General Meeting*, pp. 1–8, July 2009.

[25] NY ISO, "Alternate route: Electrifying the transportation sector," *New York ISO, NY, Tech. Report, June*, June 2009.

[26] SW Hadley, "Impact of plug-in hybrid vehicles on the electric grid," Tech. Rep. ORNL/TM-2006/554, October 2006.

[27] Larry Dickerman and Jessica Harrison, "A new car, a new grid," *Power and Energy Magazine, IEEE*, vol. 8, no. 2, pp. 55–61, 2010.

[28] N DeForest, J Funk, A Lorimer, and B Ur, "Impact of Widespread Electric Vehicle Adoption on the Electrical Utility BusinessThreats and Opportunities," Tech. Rep. 2009.5.v.1.1, CET, University of California, Berkeley, 2009.

[29] National Energy Technology Laboratory, "Assessment of Future Vehicle Transportation Options and Their Impact on the Electric Grid," `http://www.netl.doe.gov/energy-analyses/pubs/repVehicle_ElecGridImpact.pdf`.

[30] Shengnan Shao, Manisa Pipattanasomporn, and Saifur Rahman, "Challenges of PHEV penetration to the residential distribution network," in *Power & Energy Society General Meeting, 2009. PES'09. IEEE*. IEEE, 2009, pp. 1–8.

[31] A. Shamshad, M.A. Bawadi, W.M.A. Wan Hussin, T.A. Majid, and S.A.M. Sanusi, "First and second order Markov chain models for synthetic generation of wind speed time series," *Energy*, vol. 30, no. 5, pp. 693 – 708, 2005.

[32] Gong Li, Jing Shi, and Junyi Zhou, "Bayesian adaptive combination of short-term wind speed forecasts from neural network models," *Renewable Energy*, vol. 36, no. 1, pp. 352 – 359, 2011.

[33] Mohit Singh, *Dynamic models for wind power plants*, Ph.D. thesis, University of Texas at Austin, Aug. 2011.

[34] George Papaefthymiou and Bernd Klockl, "MCMC for wind power simulation," *Energy Conversion, IEEE Transactions on*, vol. 23, no. 1, pp. 234–240, 2008.

[35] D.A. Halamay and T.K.A. Brekken, "A methodology for quantifying variability of renewable energy sources by reserve requirement calculation," in *Energy Conversion Congress and Exposition (ECCE), 2010 IEEE*, sept. 2010, pp. 666 –673.

[36] Peiyuan Chen, Kasper Klitgaard Berthelsen, Birgitte Bak-Jensen, and Zhe Chen, "Markov model of wind power time series using Bayesian inference of transition matrix," in *Industrial Electronics, 2009. IECON'09. 35th Annual Conference of IEEE*. IEEE, 2009, pp. 627–632.

[37] R.H. Lasseter and P. Paigi, "Microgrid: a conceptual solution," in *Power Electronics Specialists Conference, 2004. PESC 04. 2004 IEEE 35th Annual*, june 2004, vol. 6, pp. 4285 – 4290.

[38] A Leon-Garcia, *Probability and random processes for electrical engineering*, Addison-Wesley, 1994.

[39] NOAA, "Hourly weather forecast," `http://forecast.weather.gov/MapClick.php?lat=43.16870&lon=-77.6158&unit=0&lg=english&FcstType=graphical`.

[40] Peter Doyle, "Matlab probability demos," http://www.math.dartmouth.edu/~doyle/docs/17/matlab/matlabdemo.pdf.

[41] "Census data bulk download," http://census.ire.org/data/bulkdata.html.

[42] "Vehicles per capita by state," http://www1.eere.energy.gov/vehiclesandfuels/facts/2009_fotw573.html.

[43] Mark Wienkes and David Lefty, "Americas: Clean Energy: Energy Storage," Tech. Rep., The Goldman Sachs Group, Inc, July 2010.

[44] "Plug-in Electric Vehicles," Tech. Rep., Pike Research, September 2010.

[45] C.E. Sandy Thomas, "Transportation options in a carbon-constrained world: Hybrids, plug-in hybrids, biofuels, fuel cell electric vehicles, and battery electric vehicles," *International Journal of Hydrogen Energy*, vol. 34, no. 23, pp. 9279–9296, Dec. 2009.

[46] JD Graham, NM Messer, and D Hartmann, "Plug-in Electric Vehicles: A Practical Plan for Progress," Tech. Rep., Indiana University, Feb. 2011.

[47] "Illinois Travel Statistics," http://www.dot.state.il.us/adttravelstats.html.

[48] Maria Carmen Falvo and F Foiadelli, "Preliminary analysis for the design of an energy-efficient and environmental sustainable integrated mobility system," in *Power and Energy Society General Meeting, 2010 IEEE*. IEEE, 2010, pp. 1–7.

[49] Thomas Trabold, "Vehicle Power Requirement," Lecture notes, Sustainable Mobility Systems - 5001.700.04, November 2013.

[50] General Electric, "1.5 MW Wind Turbine Series," http://site.ge-energy.com/prod_serv/products/wind_turbines/en/downloads/GEA14954C15-MW-Broch.pdf.

[51] "Wind and solar hybrid systems: A complementary relationship," http://www.windenergy.com/community/blog/wind-and-solar-hybrid-systems...relationship.

[52] National Climate Data Center, "Wind - Average Speed," http://www.ncdc.noaa.gov/oa/climate/online/ccd/avgwind.html.

[53] Mack Grady, "Solar radiation data from professor mack grady, baylor university," http://web.ecs.baylor.edu/faculty/grady/Solar_data.html, January 2013.

[54] W House, "Blueprint for a Secure Energy Future," http://www.whitehouse.gov/sites/default/files/blueprint_secure_energy_future.pdf, Mar. 2011.

[55] U.S. Department of Energy, "Net Metering," http://apps3.eere.energy.gov/greenpower/markets/netmetering.shtml, May 2011.

Appendix A

Energy Supply Forecast Model Matrices

See the attached CD-ROM

Appendix B

Energy Demand Forecast Figures

Full resolution images available on CD-ROM

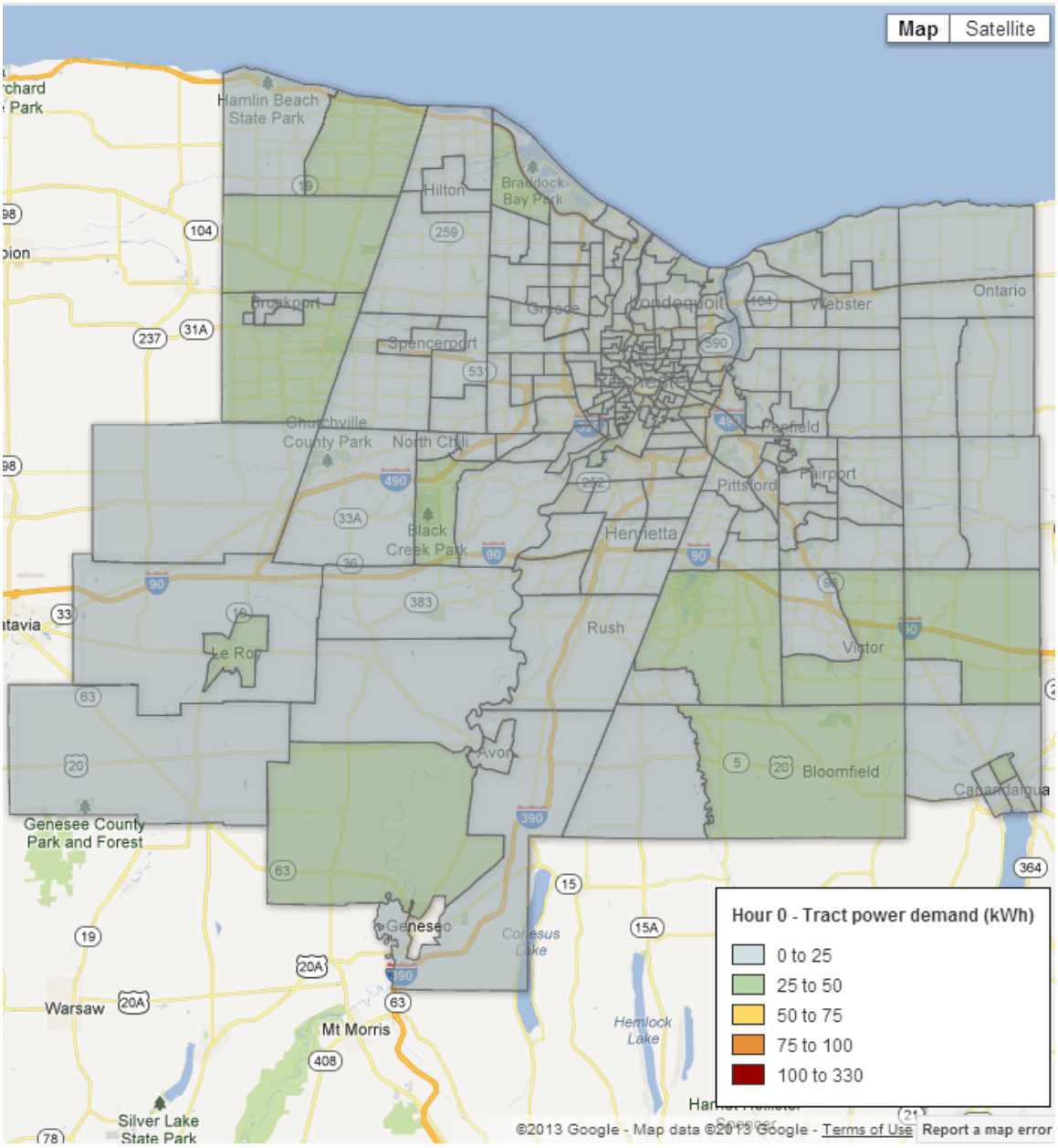
Map
Satellite
Hamlin Beach State Park
Braddock Bay Park
Hilton
Brockport
Spencerport
Greece
Rochester
Webster
Ontario
Churchville County Park
North Chili
Penfield
Pittsford
Fairport
Black Creek Park
Henrietta
Rush
Victor
Le Roy
Avon
Bloomfield
Canandaigua
Genesee County Park and Forest
Geneseo
Conesus Lake
Hemlock Lake
Warsaw
Mt Morris
Silver Lake State Park
Hour 0 - Tract power demand (kWh)
0 to 25
25 to 50
50 to 75
75 to 100
100 to 330
©2013 Google - Map data ©2013 Google - Terms of Use
Report a map error

12AM - 1AM

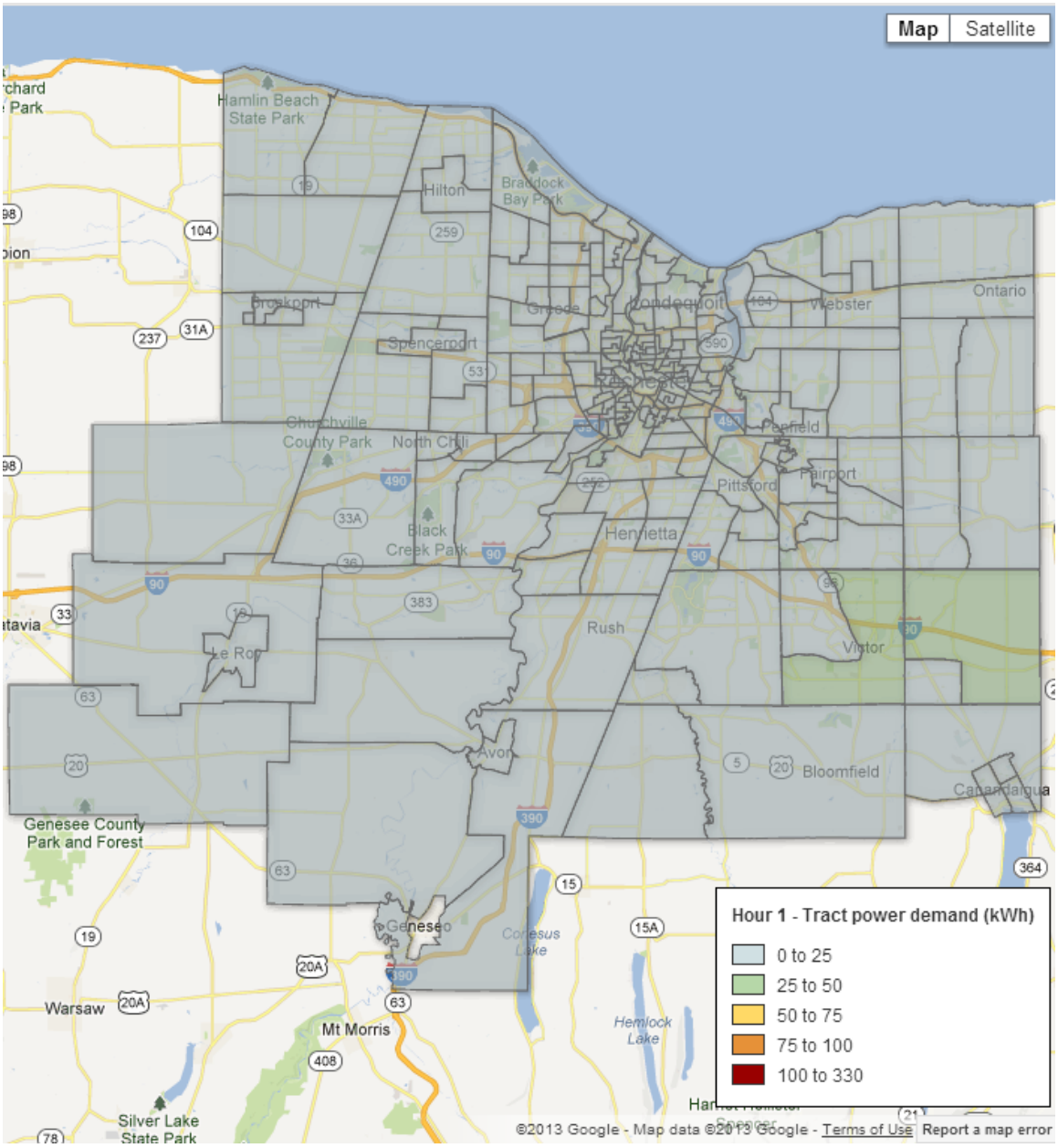
Map
Satellite
Hamlin Beach State Park
Braddock Bay Park
Hilton
Brockport
Spencerport
Greece
Rochester
Webster
Ontario
Churchville County Park
North Chili
Penfield
Pittsford
Fairport
Black Creek Park
Henrietta
Le Roy
Rush
Victor
Avon
Bloomfield
Canandaigua
Genesee County Park and Forest
Geneseo
Conesus Lake
Hemlock Lake
Warsaw
Mt Morris
Silver Lake State Park
Hour 1 - Tract power demand (kWh)
0 to 25
25 to 50
50 to 75
75 to 100
100 to 330
©2013 Google - Map data ©2013 Google - Terms of Use
Report a map error

1AM - 2AM

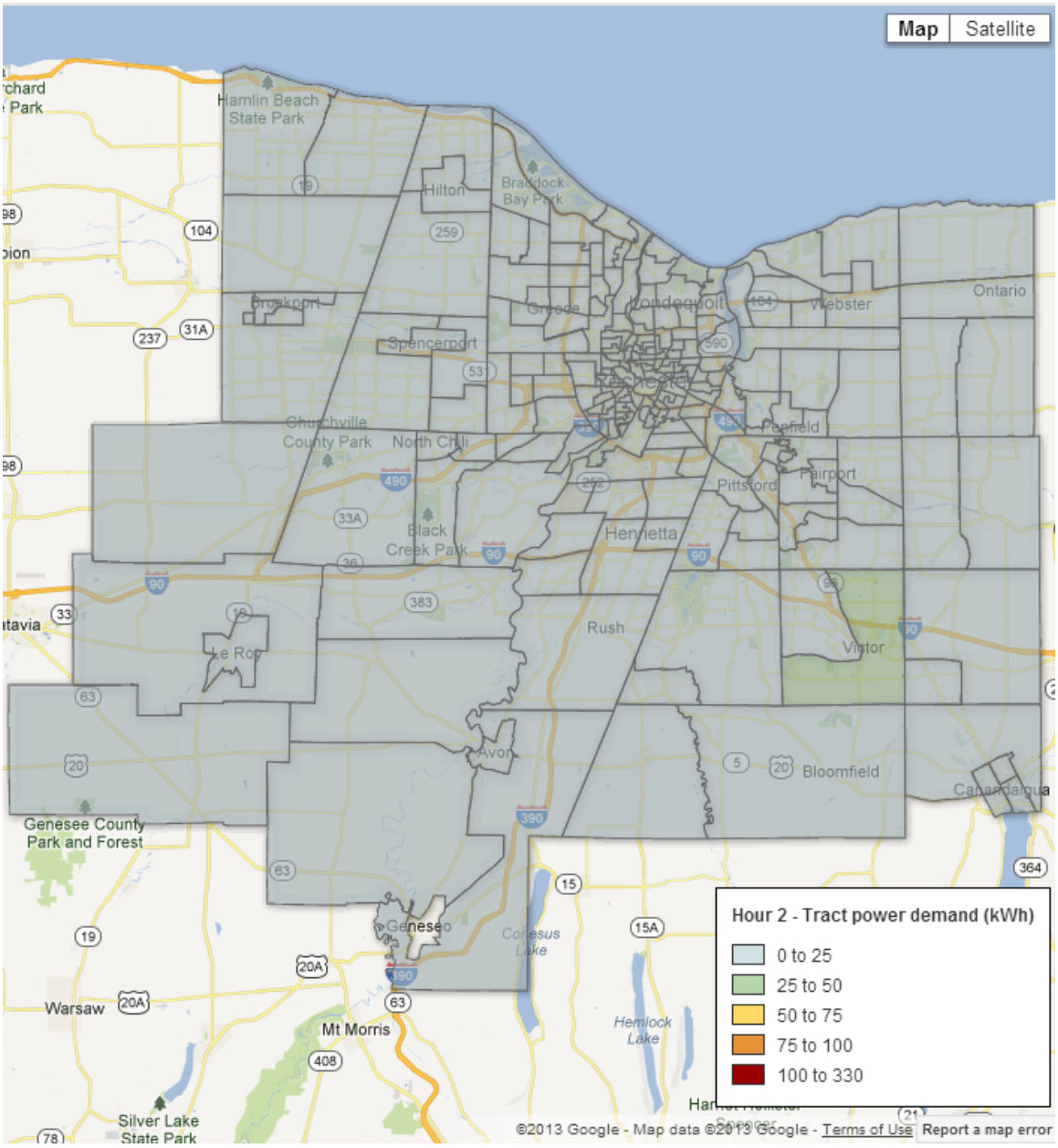
Map
Satellite
Hamlin Beach State Park
Braddock Bay Park
Hilton
Brockport
Spencerport
Greece
Rochester
Webster
Ontario
Churchville County Park
North Chili
Penfield
Pittsford
Fairport
Black Creek Park
Henrietta
Le Roy
Rush
Victor
Avon
Bloomfield
Canandaigua
Genesee County Park and Forest
Geneseo
Conesus Lake
Warsaw
Mt Morris
Hemlock Lake
Silver Lake State Park
Hour 2 - Tract power demand (kWh)
0 to 25
25 to 50
50 to 75
75 to 100
100 to 330
©2013 Google - Map data ©2013 Google - Terms of Use
Report a map error

2AM - 3AM

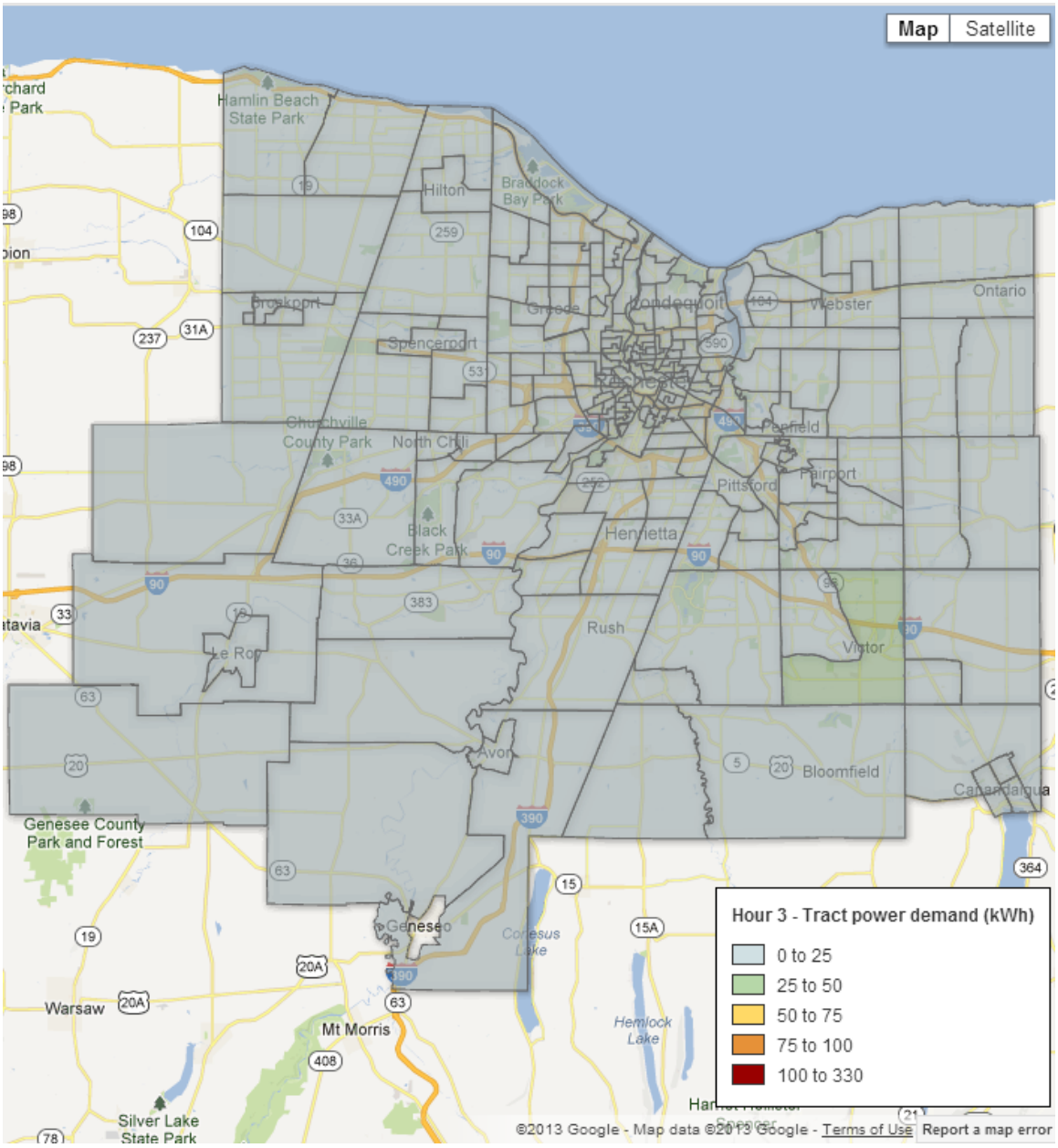
Map
Satellite
Hamlin Beach State Park
Braddock Bay Park
Hilton
Brockport
Spencerport
Greece
Rochester
Webster
Ontario
Churchville County Park
North Chili
Penfield
Pittsford
Fairport
Black Creek Park
Henrietta
Le Roy
Rush
Victor
Avon
Bloomfield
Canandaigua
Genesee County Park and Forest
Geneseo
Conesus Lake
Warsaw
Mt Morris
Hemlock Lake
Silver Lake State Park
Hour 3 - Tract power demand (kWh)
0 to 25
25 to 50
50 to 75
75 to 100
100 to 330
©2013 Google - Map data ©2013 Google - Terms of Use
Report a map error

3AM - 4AM

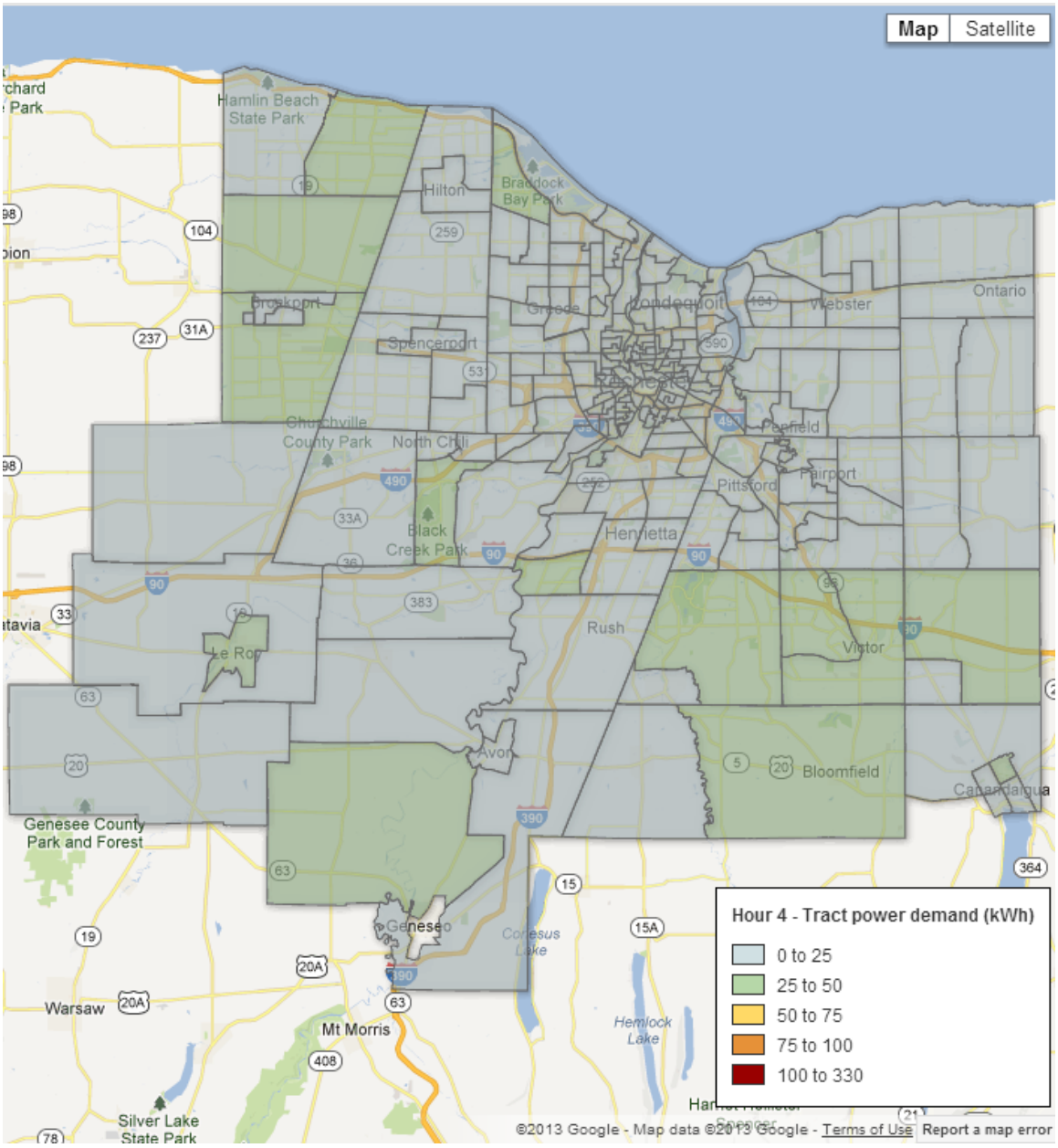
Map
Satellite
Hamlin Beach State Park
Braddock Bay Park
Hilton
Brockport
Spencerport
Greece
Rochester
Webster
Ontario
Churchville County Park
North Chili
Penfield
Pittsford
Fairport
Black Creek Park
Henrietta
Le Roy
Rush
Victor
Avon
Bloomfield
Canandaigua
Genesee County Park and Forest
Geneseo
Conesus Lake
Warsaw
Mt Morris
Hemlock Lake
Silver Lake State Park
Hour 4 - Tract power demand (kWh)
0 to 25
25 to 50
50 to 75
75 to 100
100 to 330
©2013 Google - Map data ©2013 Google - Terms of Use
Report a map error

4AM - 5AM

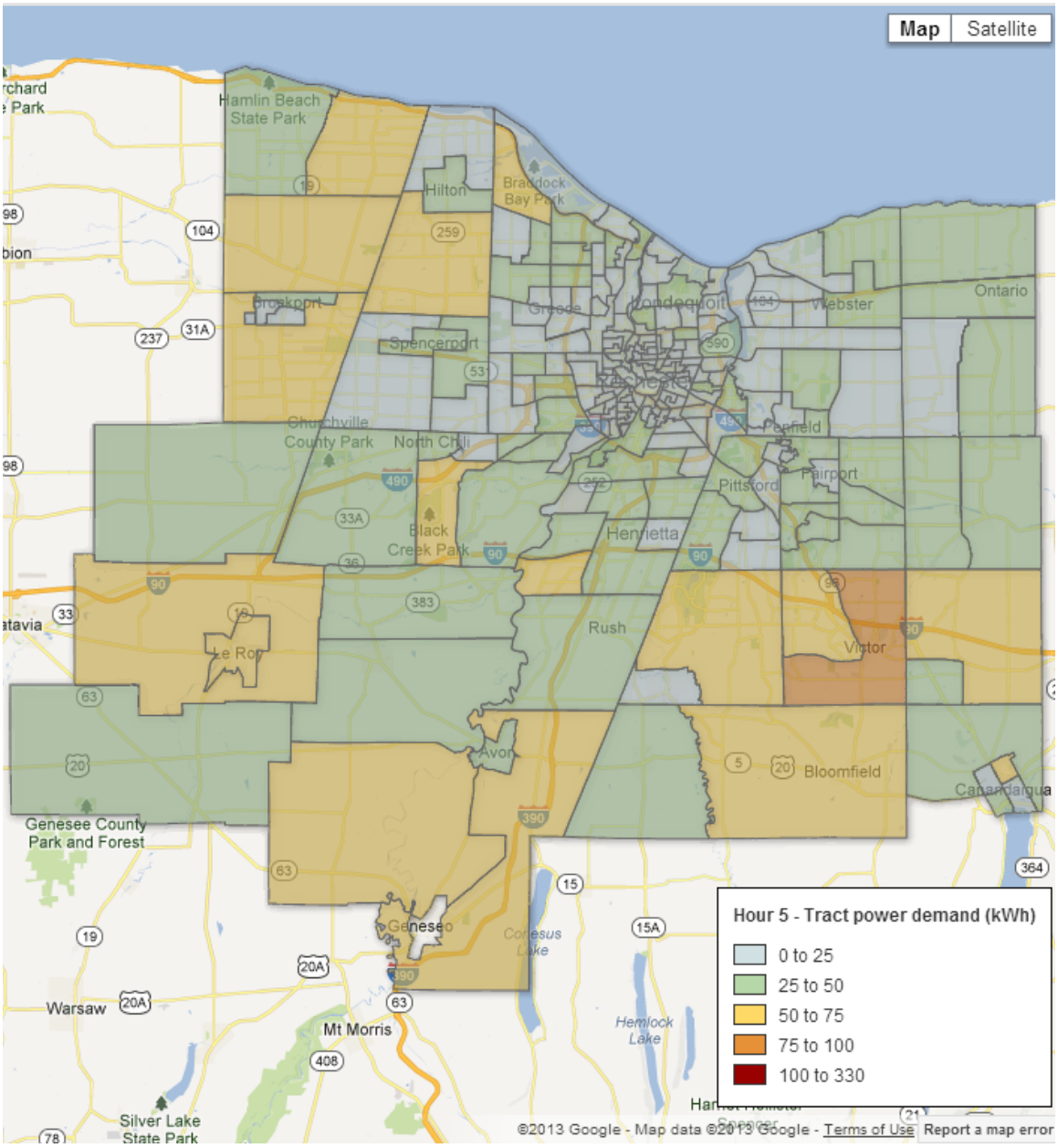
Map
Satellite
Hamlin Beach State Park
Hilton
Braddock Bay Park
Brockport
Spencerport
Greece
Rochester
Webster
Ontario
Churchville County Park
North Chili
Penfield
Pittsford
Fairport
Black Creek Park
Henrietta
Rush
Le Roy
Avon
Bloomfield
Canandaigua
Genesee County Park and Forest
Geneseo
Conesus Lake
Hemlock Lake
Warsaw
Mt Morris
Silver Lake State Park
Hour 5 - Tract power demand (kWh)
0 to 25
25 to 50
50 to 75
75 to 100
100 to 330
©2013 Google - Map data ©2013 Google - Terms of Use
Report a map error

5AM - 6AM

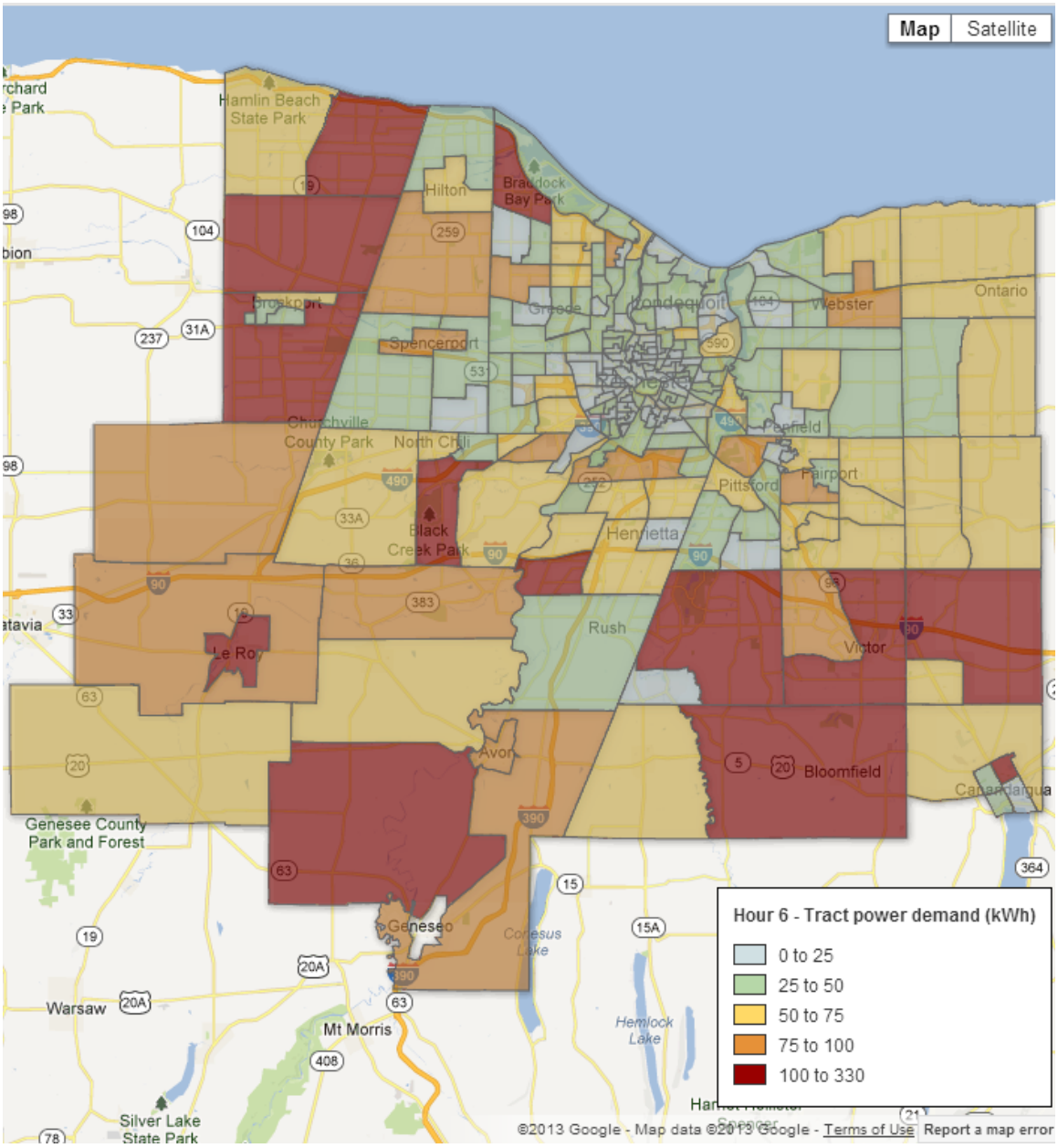
Map
Satellite
Hamlin Beach State Park
Braddock Bay Park
Hilton
Greece
Webster
Ontario
Spencerport
Churchville County Park
North Chili
Penfield
Pittsford
Fairport
Black Creek Park
Henrietta
Rush
Victor
Le Roy
Avon
Bloomfield
Canandaigua
Genesee County Park and Forest
Geneseo
Conesus Lake
Hemlock Lake
Warsaw
Mt Morris
Silver Lake State Park
Hour 6 - Tract power demand (kWh)
0 to 25
25 to 50
50 to 75
75 to 100
100 to 330
©2013 Google - Map data ©2013 Google - Terms of Use
Report a map error

6AM - 7AM

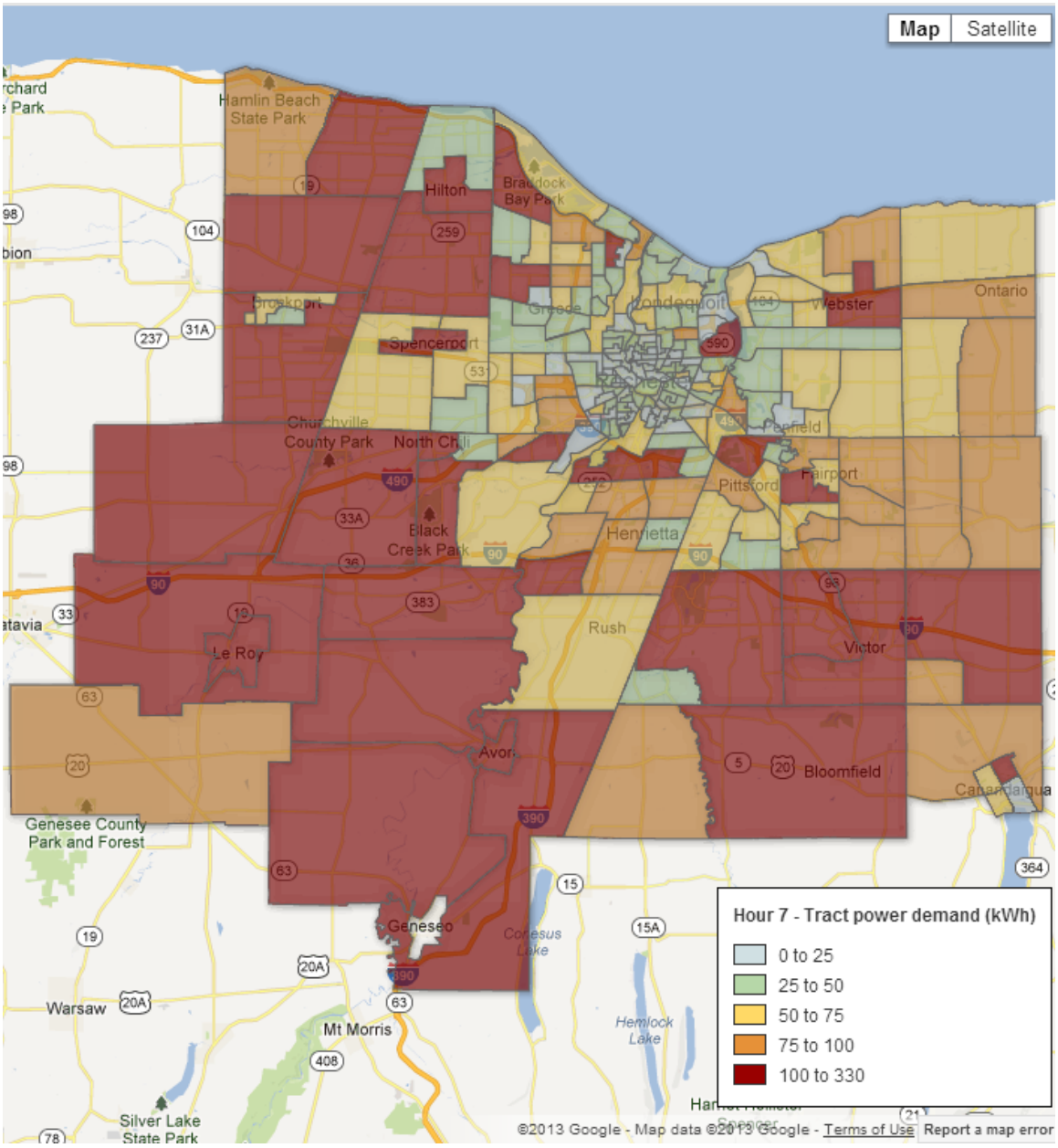
Map
Satellite
Hamlin Beach State Park
Hilton
Braddock Bay Park
Brockport
Greece
Spencerport
Rochester
Webster
Ontario
Churchville County Park
North Chili
Penfield
Pittsford
Fairport
Black Creek Park
Henrietta
Rush
Victor
Le Roy
Avon
Bloomfield
Canandaigua
Genesee County Park and Forest
Geneseo
Conesus Lake
Hemlock Lake
Warsaw
Mt Morris
Silver Lake State Park
Hour 7 - Tract power demand (kWh)
0 to 25
25 to 50
50 to 75
75 to 100
100 to 330
©2013 Google - Map data ©2013 Google - Terms of Use
Report a map error

7AM - 8AM

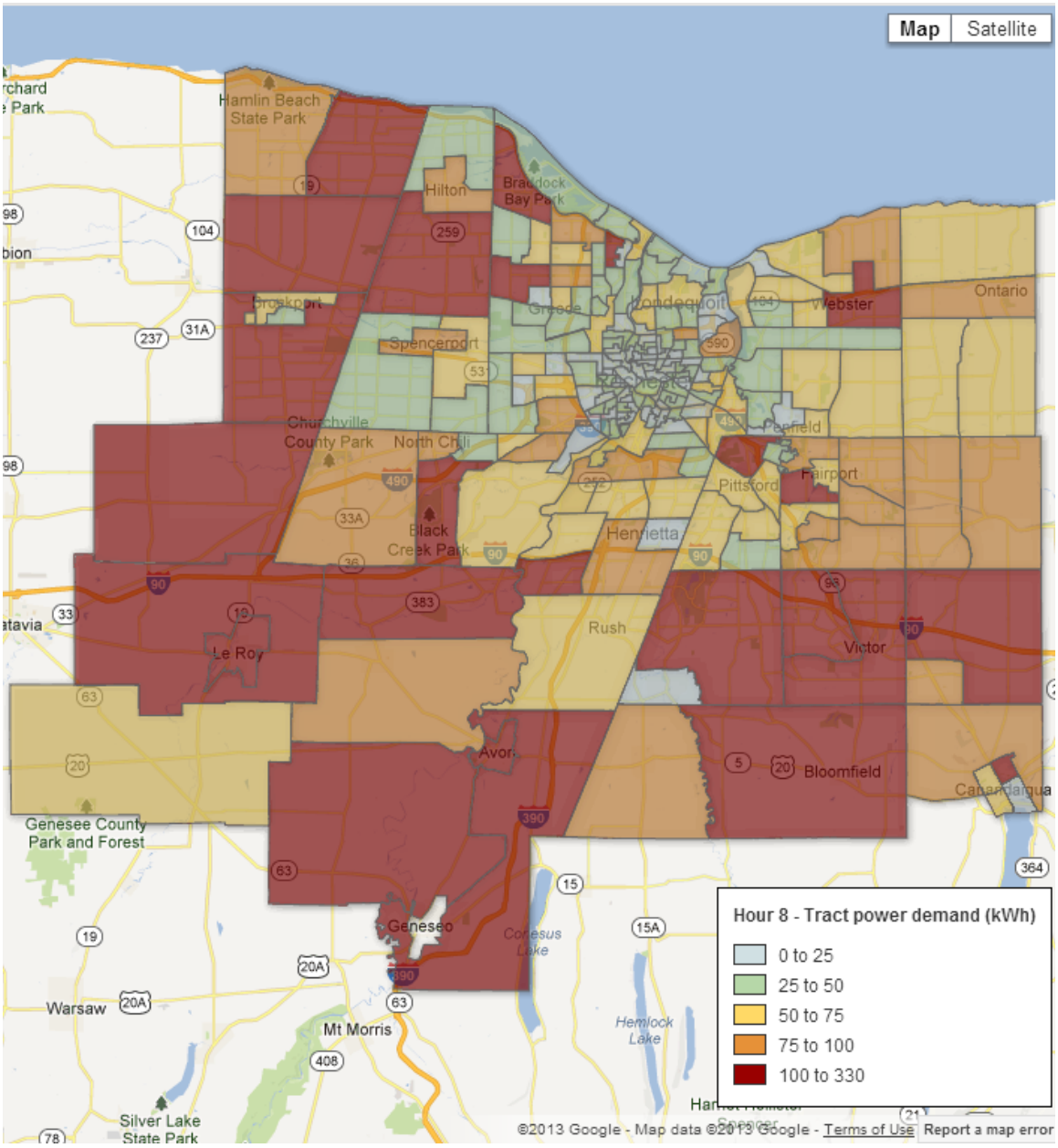
Map
Satellite
Hamlin Beach State Park
Hilton
Braddock Bay Park
Brockport
Greece
Spencerport
Rochester
Webster
Ontario
Churchville County Park
North Chili
Penfield
Pittsford
Fairport
Black Creek Park
Henrietta
Rush
Victor
Le Roy
Avon
Bloomfield
Canandaigua
Genesee County Park and Forest
Geneseo
Conesus Lake
Hemlock Lake
Warsaw
Mt Morris
Silver Lake State Park
Hour 8 - Tract power demand (kWh)
0 to 25
25 to 50
50 to 75
75 to 100
100 to 330
©2013 Google - Map data ©2013 Google - Terms of Use
Report a map error

8AM - 9AM

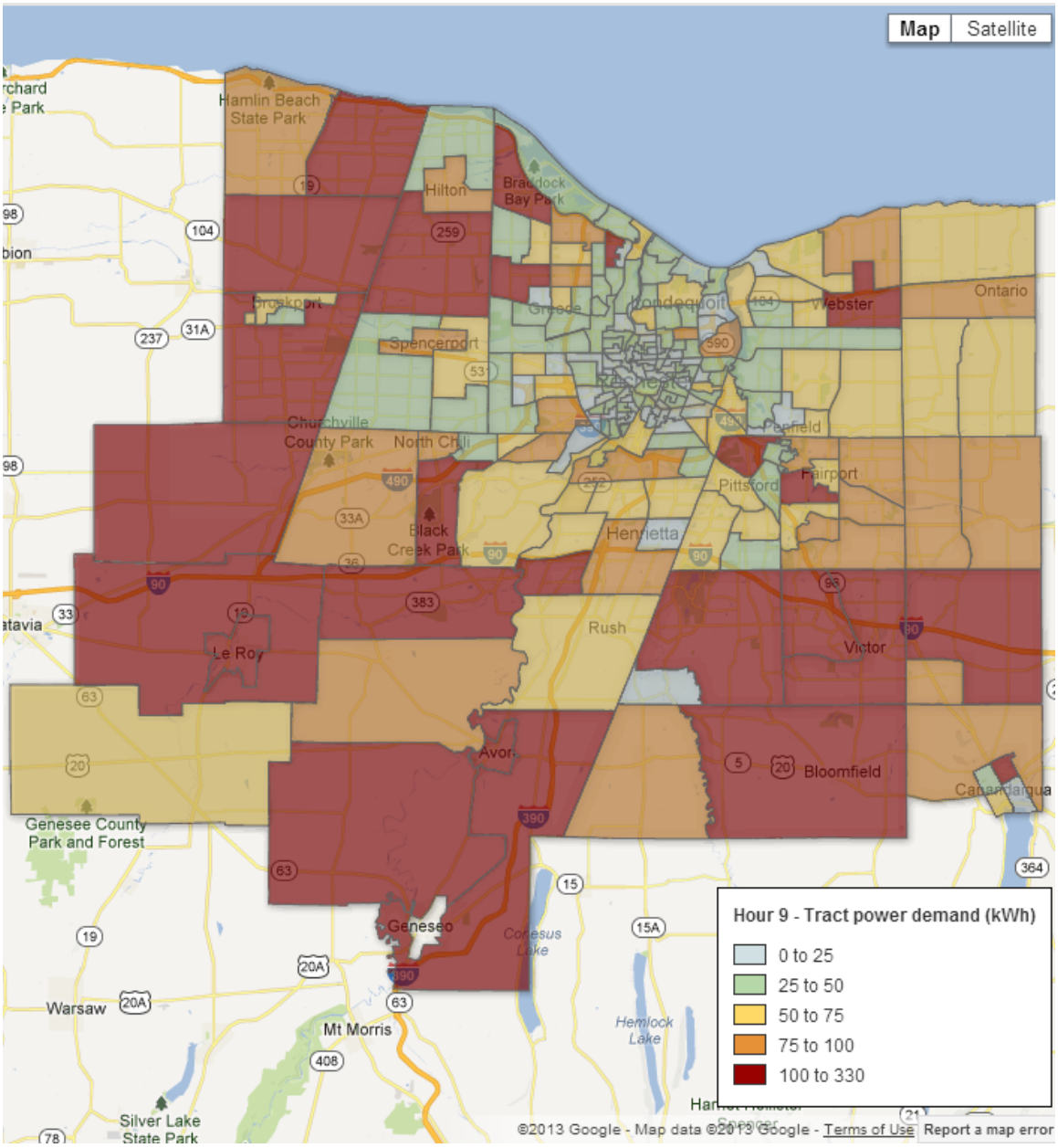
Map
Satellite
Hamlin Beach State Park
Hilton
Braddock Bay Park
Brockport
Greece
Spencerport
Rochester
Webster
Ontario
Churchville County Park
North Chili
Penfield
Pittsford
Fairport
Black Creek Park
Henrietta
Rush
Victor
Le Roy
Avon
Bloomfield
Canandaigua
Genesee County Park and Forest
Geneseo
Conesus Lake
Hemlock Lake
Warsaw
Mt Morris
Silver Lake State Park
Hour 9 - Tract power demand (kWh)
0 to 25
25 to 50
50 to 75
75 to 100
100 to 330
©2013 Google - Map data ©2013 Google - Terms of Use
Report a map error

9AM - 10AM

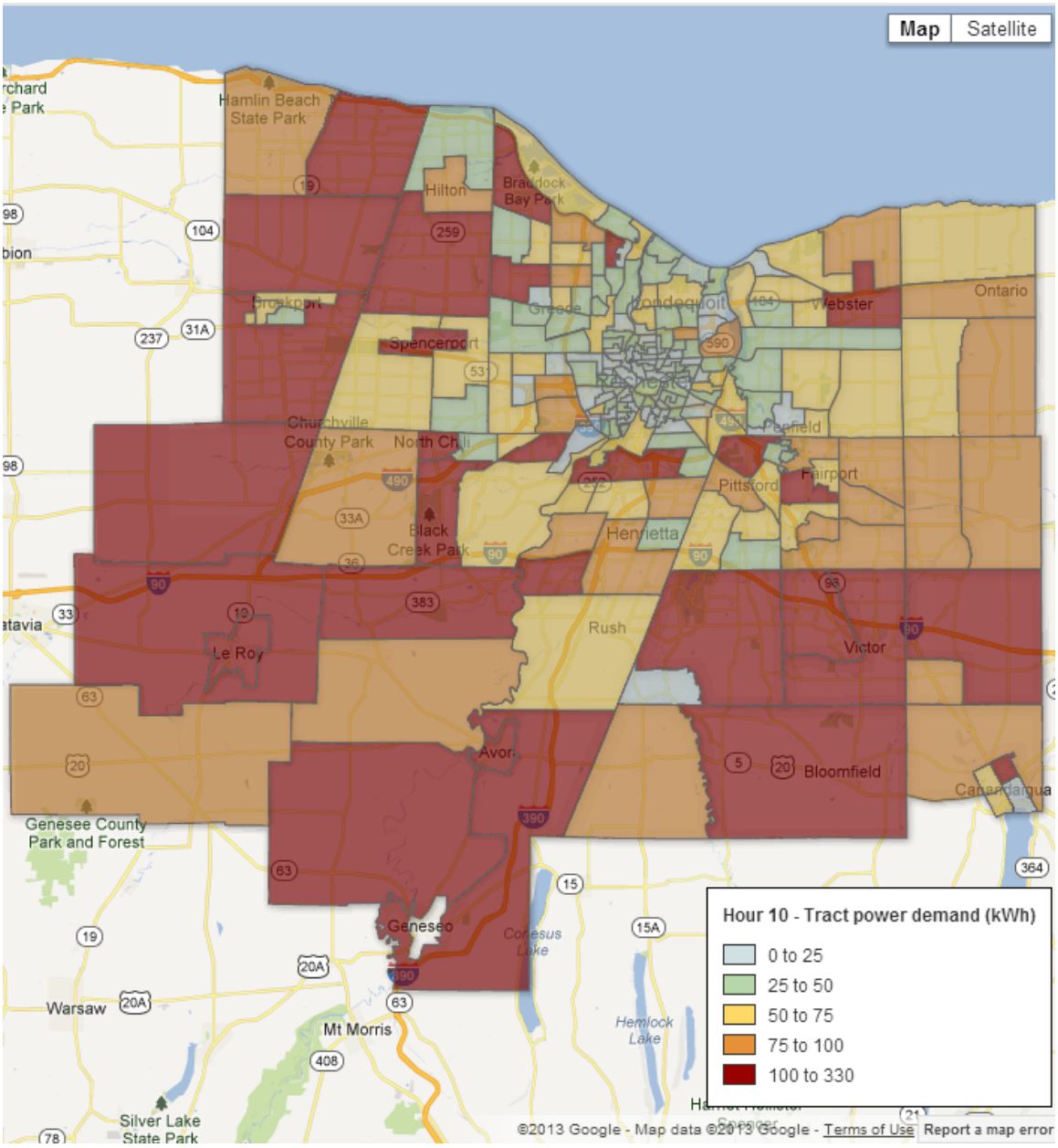
Map
Satellite
Hamlin Beach State Park
Hilton
Braddock Bay Park
Brockport
Greece
Spencerport
Rochester
Webster
Ontario
Churchville County Park
North Chili
Penfield
Pittsford
Fairport
Black Creek Park
Henrietta
Rush
Victor
Le Roy
Avon
Bloomfield
Canandaigua
Genesee County Park and Forest
Geneseo
Conesus Lake
Hemlock Lake
Warsaw
Mt Morris
Silver Lake State Park
Hour 10 - Tract power demand (kWh)
0 to 25
25 to 50
50 to 75
75 to 100
100 to 330
©2013 Google - Map data ©2013 Google - Terms of Use
Report a map error

10AM - 11AM

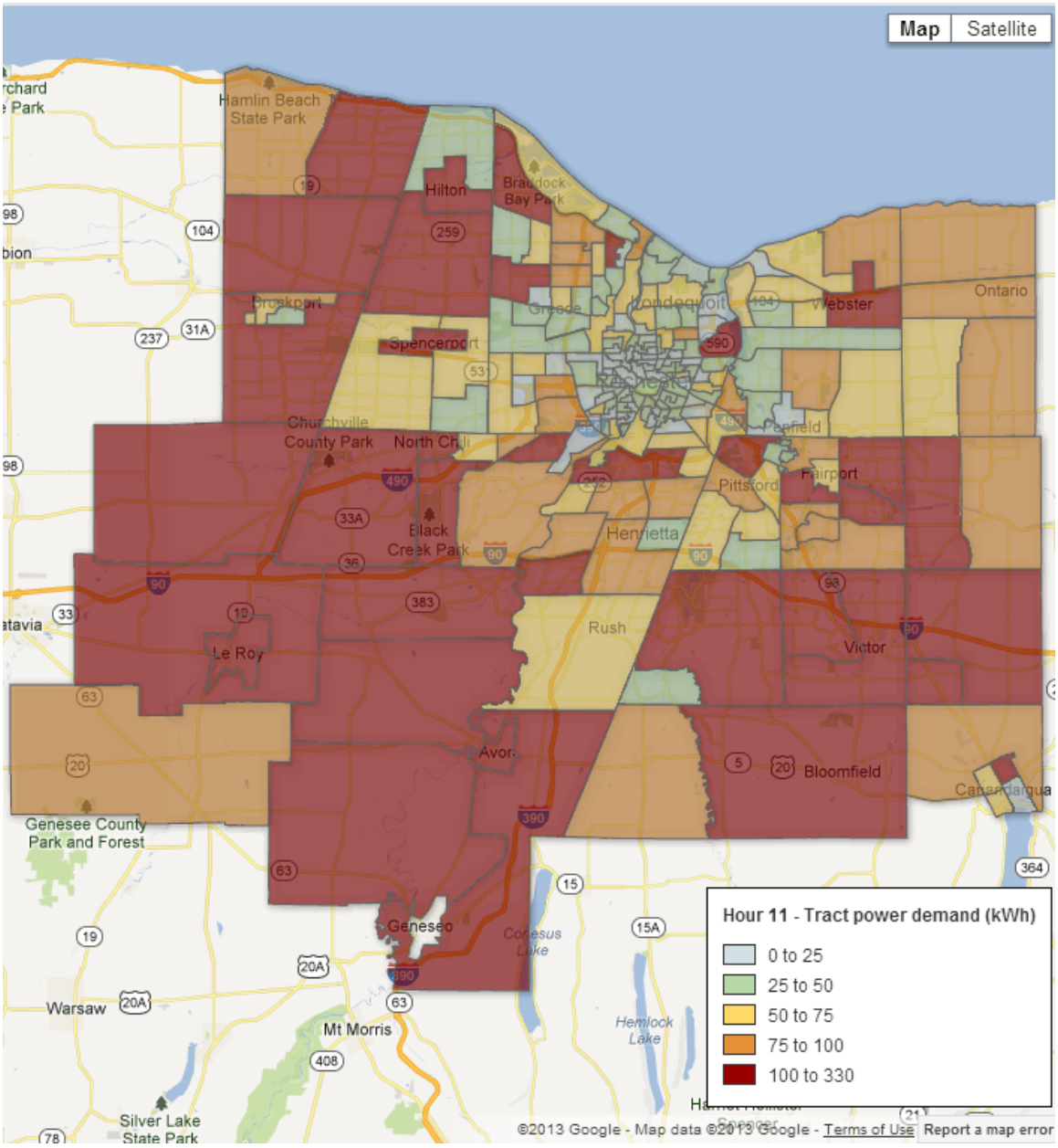
Map
Satellite
Hamlin Beach State Park
Hilton
Braddock Bay Park
Brockport
Greece
Spencerport
Rochester
Webster
Ontario
Churchville County Park
North Chili
Penfield
Pittsford
Fairport
Black Creek Park
Henrietta
Rush
Victor
Le Roy
Avon
Bloomfield
Canandaigua
Genesee County Park and Forest
Geneseo
Conesus Lake
Hemlock Lake
Warsaw
Mt Morris
Silver Lake State Park
Hour 11 - Tract power demand (kWh)
0 to 25
25 to 50
50 to 75
75 to 100
100 to 330
©2013 Google - Map data ©2013 Google - Terms of Use
Report a map error

11AM - 12PM

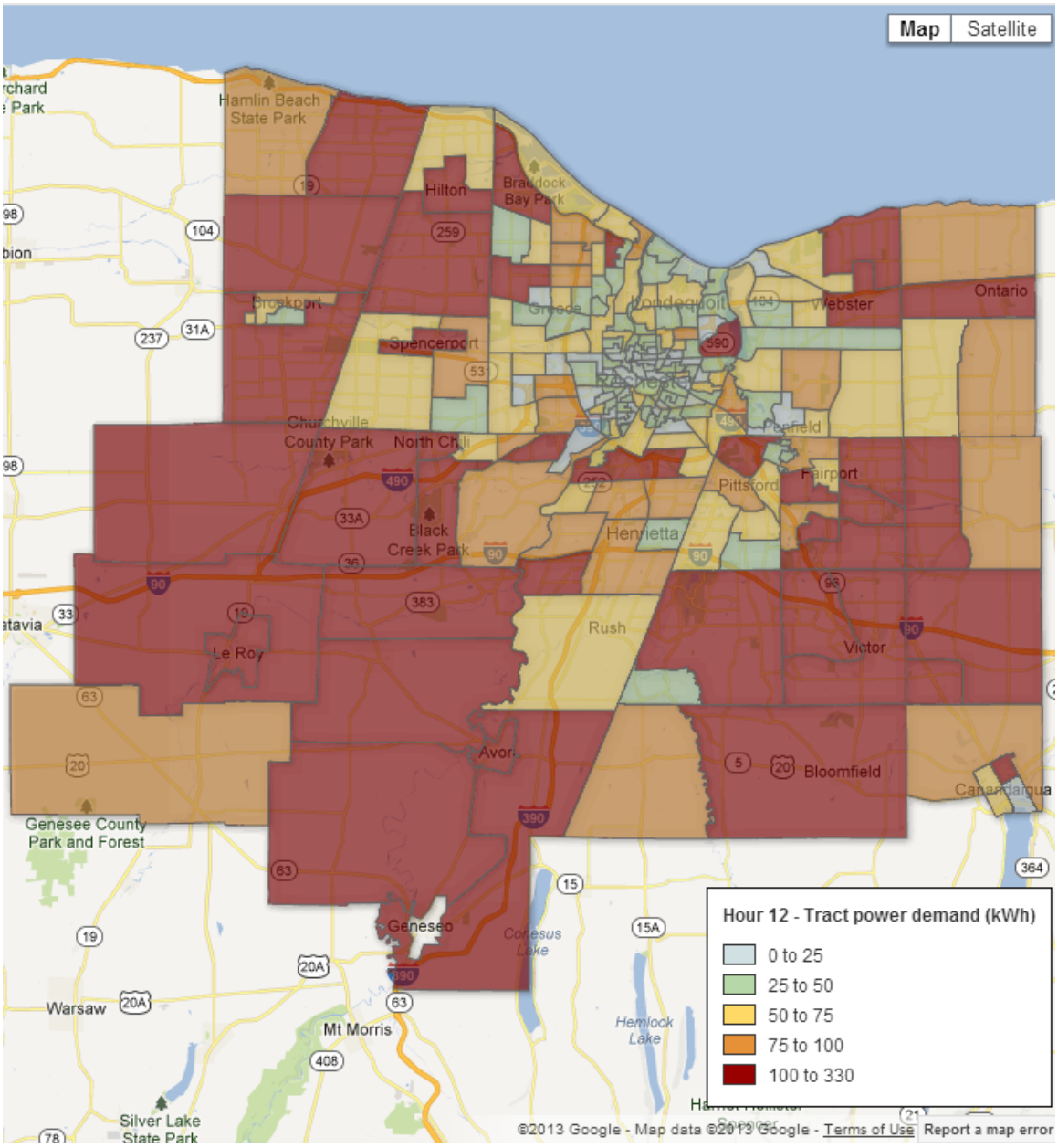
Map
Satellite
Hamlin Beach State Park
Hilton
Braddock Bay Park
Brockport
Spencerport
Greece
Rochester
Webster
Ontario
Churchville County Park
North Chili
Penfield
Pittsford
Fairport
Black Creek Park
Henrietta
Rush
Victor
Le Roy
Avon
Bloomfield
Canandaigua
Genesee County Park and Forest
Geneseo
Conesus Lake
Hemlock Lake
Warsaw
Mt Morris
Silver Lake State Park
Hour 12 - Tract power demand (kWh)
0 to 25
25 to 50
50 to 75
75 to 100
100 to 330
©2013 Google - Map data ©2013 Google - Terms of Use
Report a map error

12PM - 1PM

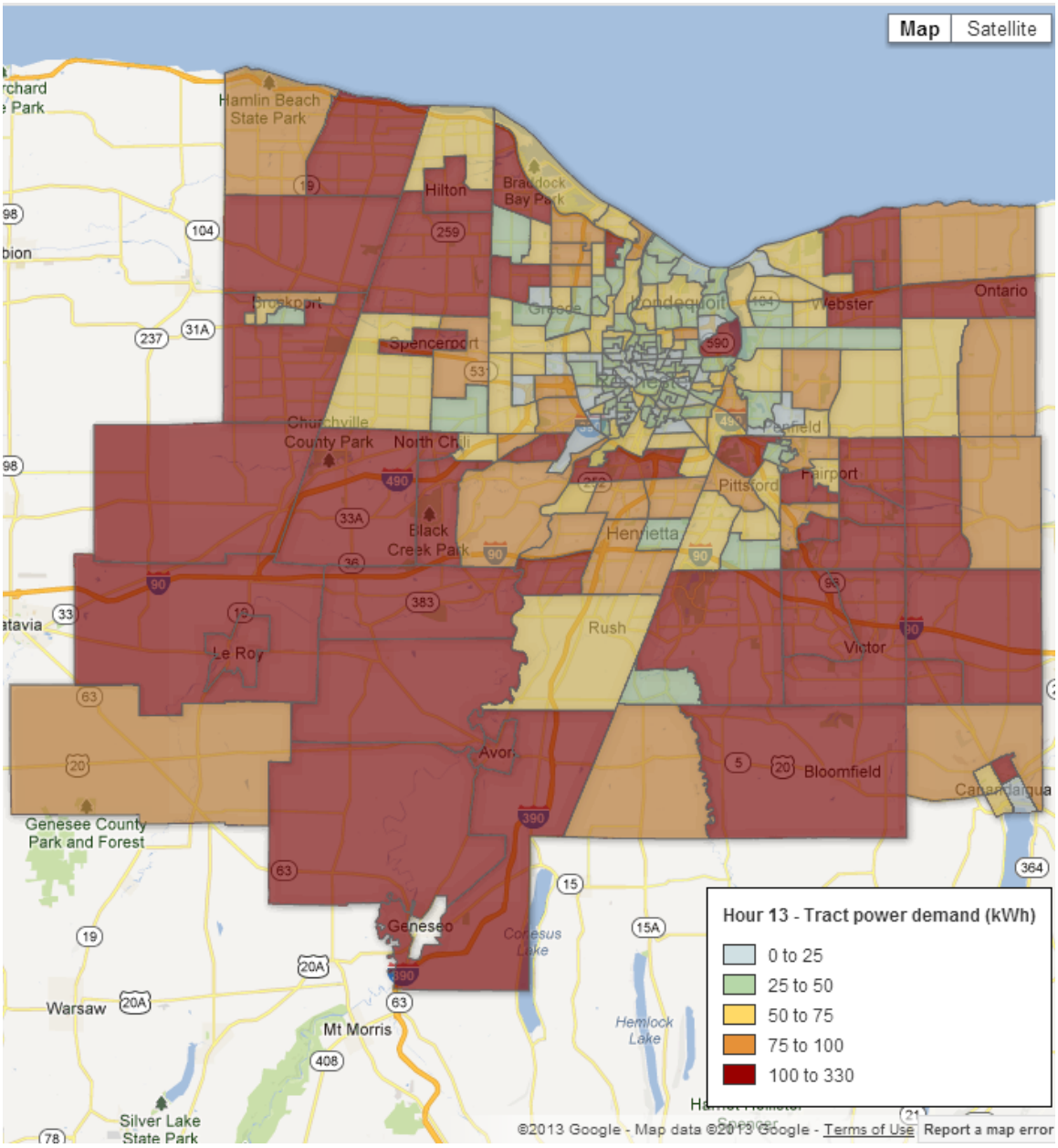
Map
Satellite
Hamlin Beach State Park
Hilton
Braddock Bay Park
Brockport
Spencerport
Greece
Rochester
Webster
Ontario
Churchville County Park
North Chili
Penfield
Pittsford
Fairport
Black Creek Park
Henrietta
Rush
Victor
Le Roy
Avon
Bloomfield
Canandaigua
Genesee County Park and Forest
Geneseo
Conesus Lake
Hemlock Lake
Warsaw
Mt Morris
Silver Lake State Park
Hour 13 - Tract power demand (kWh)
0 to 25
25 to 50
50 to 75
75 to 100
100 to 330
©2013 Google - Map data ©2013 Google - Terms of Use
Report a map error

1PM - 2PM

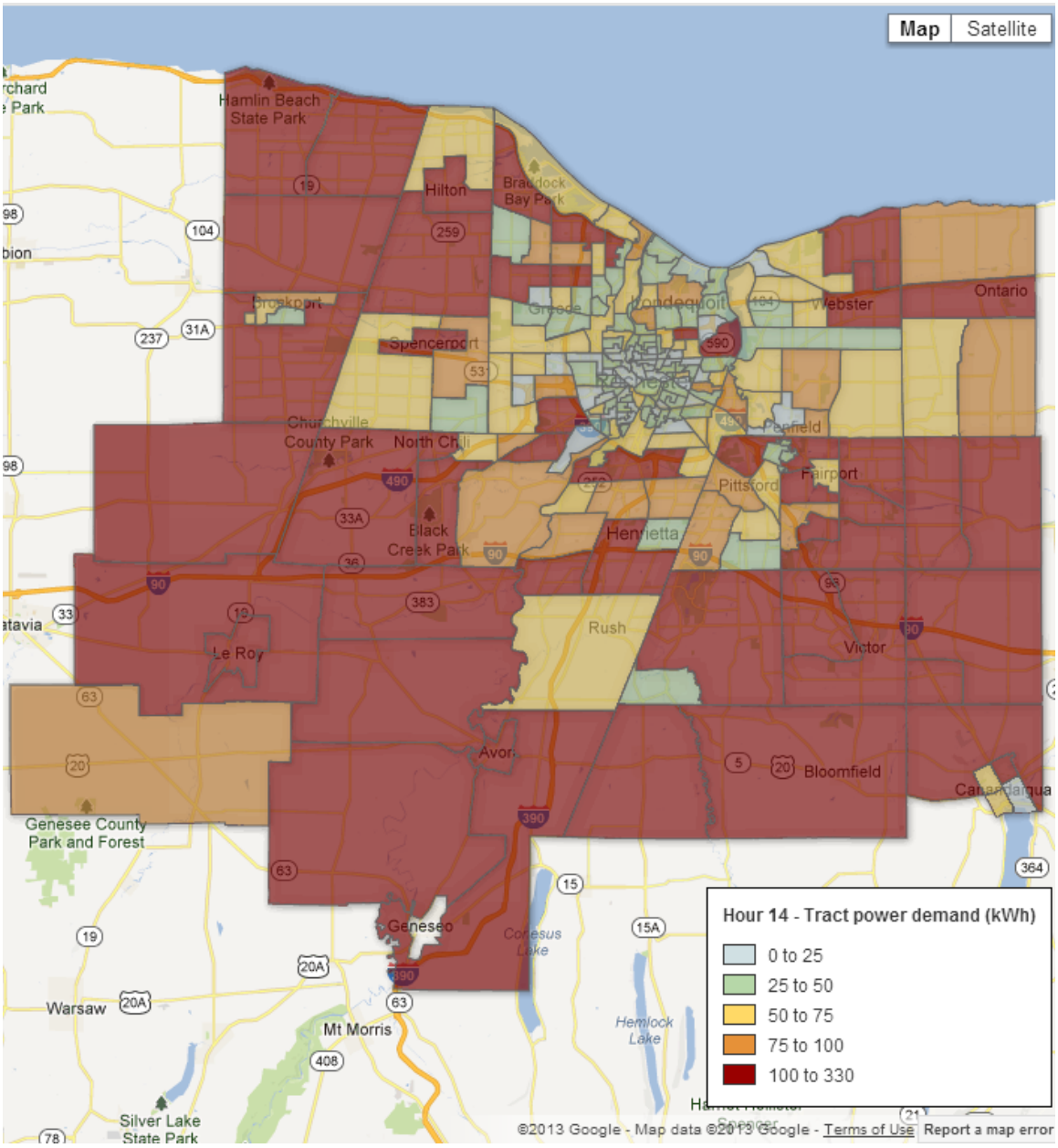
Map
Satellite
Hamlin Beach State Park
Hilton
Braddock Bay Park
Brockport
Spencerport
Greece
Rochester
Webster
Ontario
Churchville County Park
North Chili
Penfield
Pittsford
Fairport
Black Creek Park
Henrietta
Rush
Victor
Le Roy
Avon
Bloomfield
Canandaigua
Genesee County Park and Forest
Geneseo
Conesus Lake
Hemlock Lake
Warsaw
Mt Morris
Silver Lake State Park
Hour 14 - Tract power demand (kWh)
0 to 25
25 to 50
50 to 75
75 to 100
100 to 330
©2013 Google - Map data ©2013 Google - Terms of Use
Report a map error

2PM - 3PM

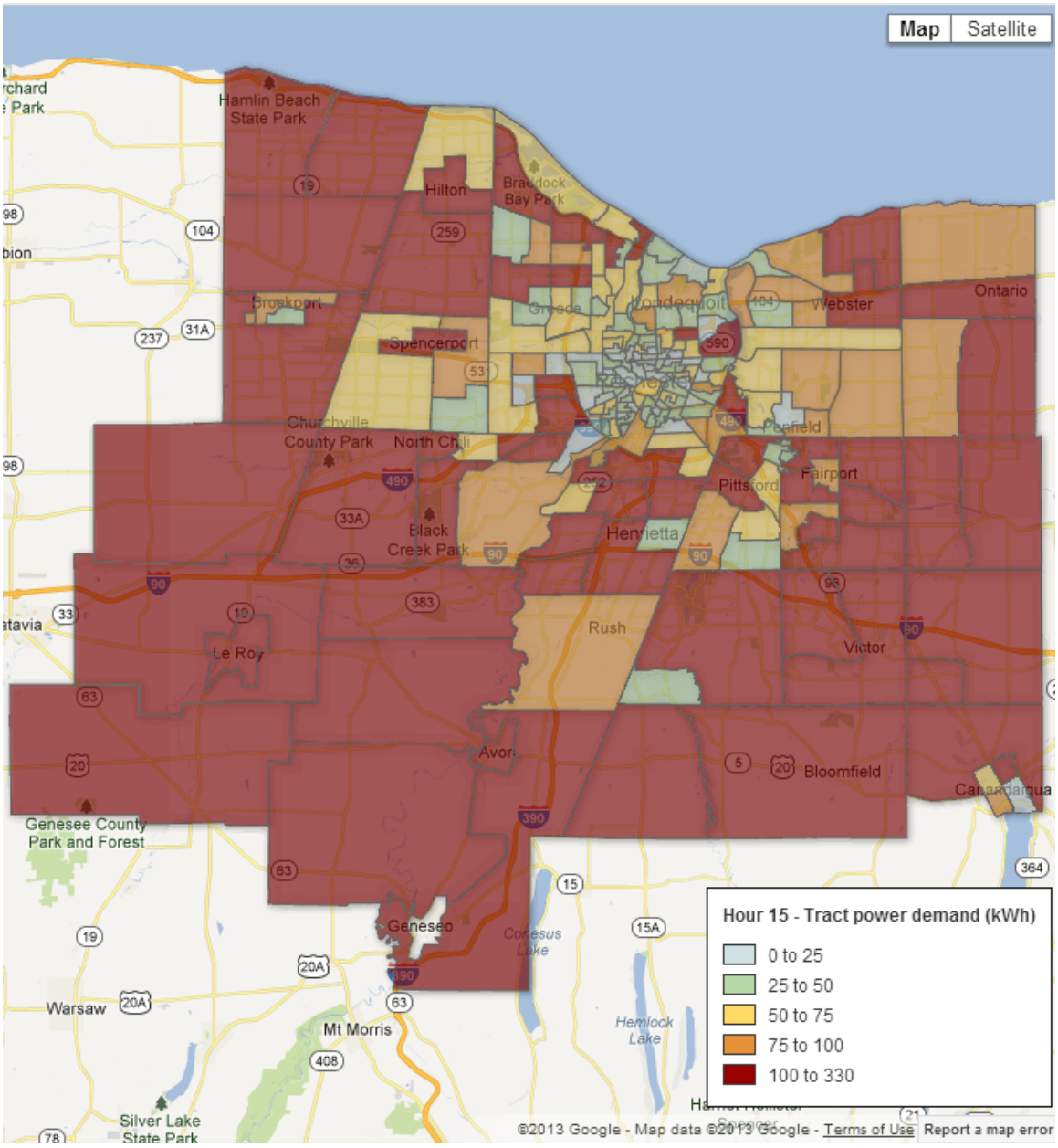
Map
Satellite
Hamlin Beach State Park
Hilton
Braddock Bay Park
Brockport
Spencerport
Churchville County Park
North Chili
Black Creek Park
Greece
Rochester
Webster
Ontario
Penfield
Pittsford
Fairport
Henrietta
Rush
Victor
Le Roy
Avon
Bloomfield
Canandaigua
Genesee County Park and Forest
Geneseo
Conesus Lake
Hemlock Lake
Warsaw
Mt Morris
Silver Lake State Park
Hour 15 - Tract power demand (kWh)
0 to 25
25 to 50
50 to 75
75 to 100
100 to 330
©2013 Google - Map data ©2013 Google - Terms of Use
Report a map error

3PM - 4PM

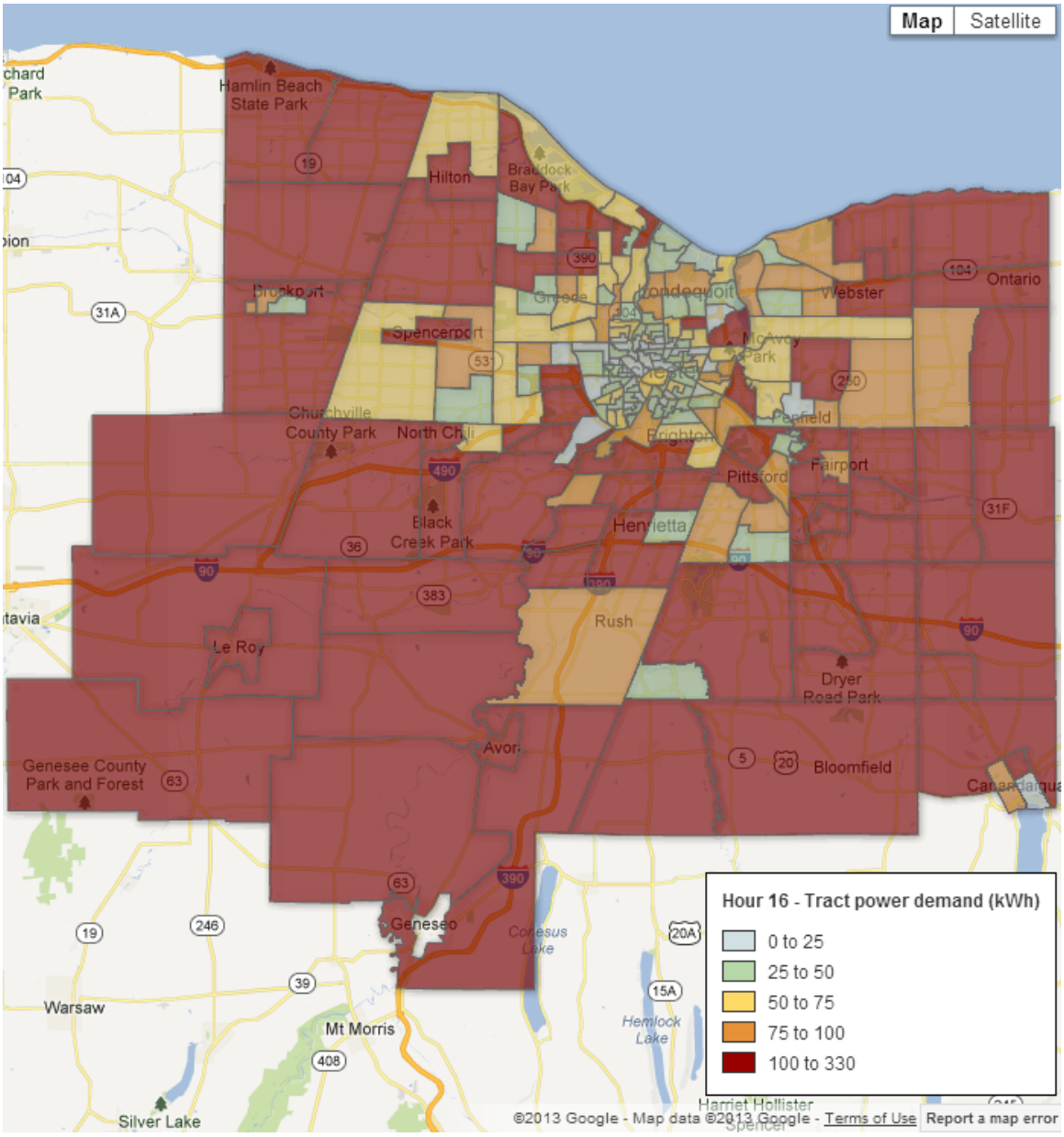
Map
Satellite
Hamlin Beach State Park
Hilton
Braddock Bay Park
Brockport
Spencerport
Greece
Rochester
Webster
Ontario
McAvoy Park
Perinton
Fairport
Pittsford
Brighton
Churchville County Park
North Chili
Black Creek Park
Henrietta
Rush
Le Roy
Dryer Road Park
Avon
Bloomfield
Genesee County Park and Forest
Geneseo
Conesus Lake
Hemlock Lake
Warsaw
Mt Morris
Silver Lake
Harriet Hollister
Hour 16 - Tract power demand (kWh)
0 to 25
25 to 50
50 to 75
75 to 100
100 to 330
©2013 Google - Map data ©2013 Google - Terms of Use
Report a map error

4PM - 5PM

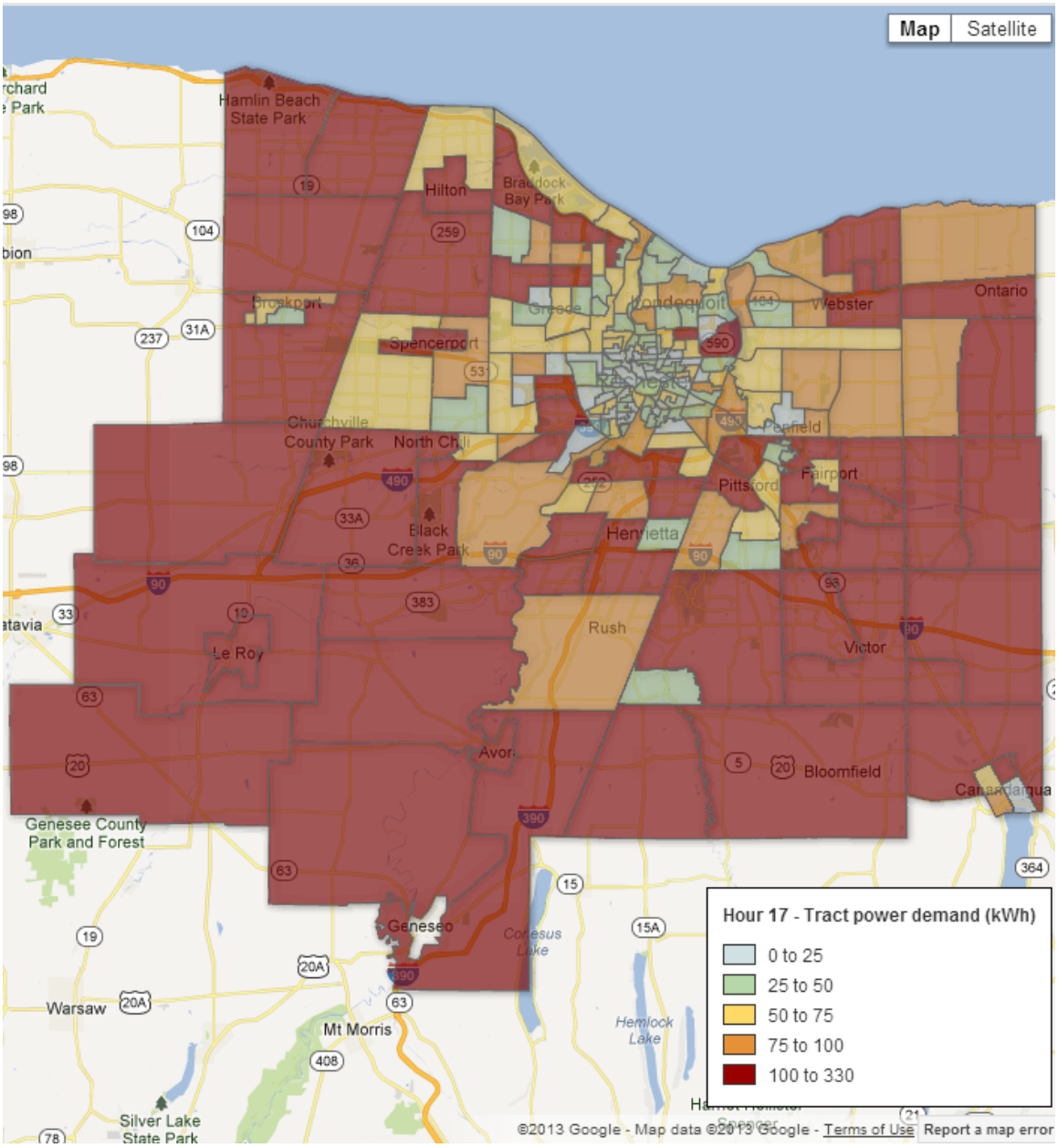
Map
Satellite
Hamlin Beach State Park
Hilton
Braddock Bay Park
Brockport
Spencerport
Churchville County Park
North Chili
Greece
Rochester
Webster
Ontario
Penfield
Pittsford
Fairport
Henrietta
Black Creek Park
Rush
Victor
Le Roy
Avon
Bloomfield
Canandaigua
Genesee County Park and Forest
Geneseo
Conesus Lake
Hemlock Lake
Warsaw
Mt Morris
Silver Lake State Park
Hour 17 - Tract power demand (kWh)
0 to 25
25 to 50
50 to 75
75 to 100
100 to 330
©2013 Google - Map data ©2013 Google - Terms of Use
Report a map error

5PM - 6PM

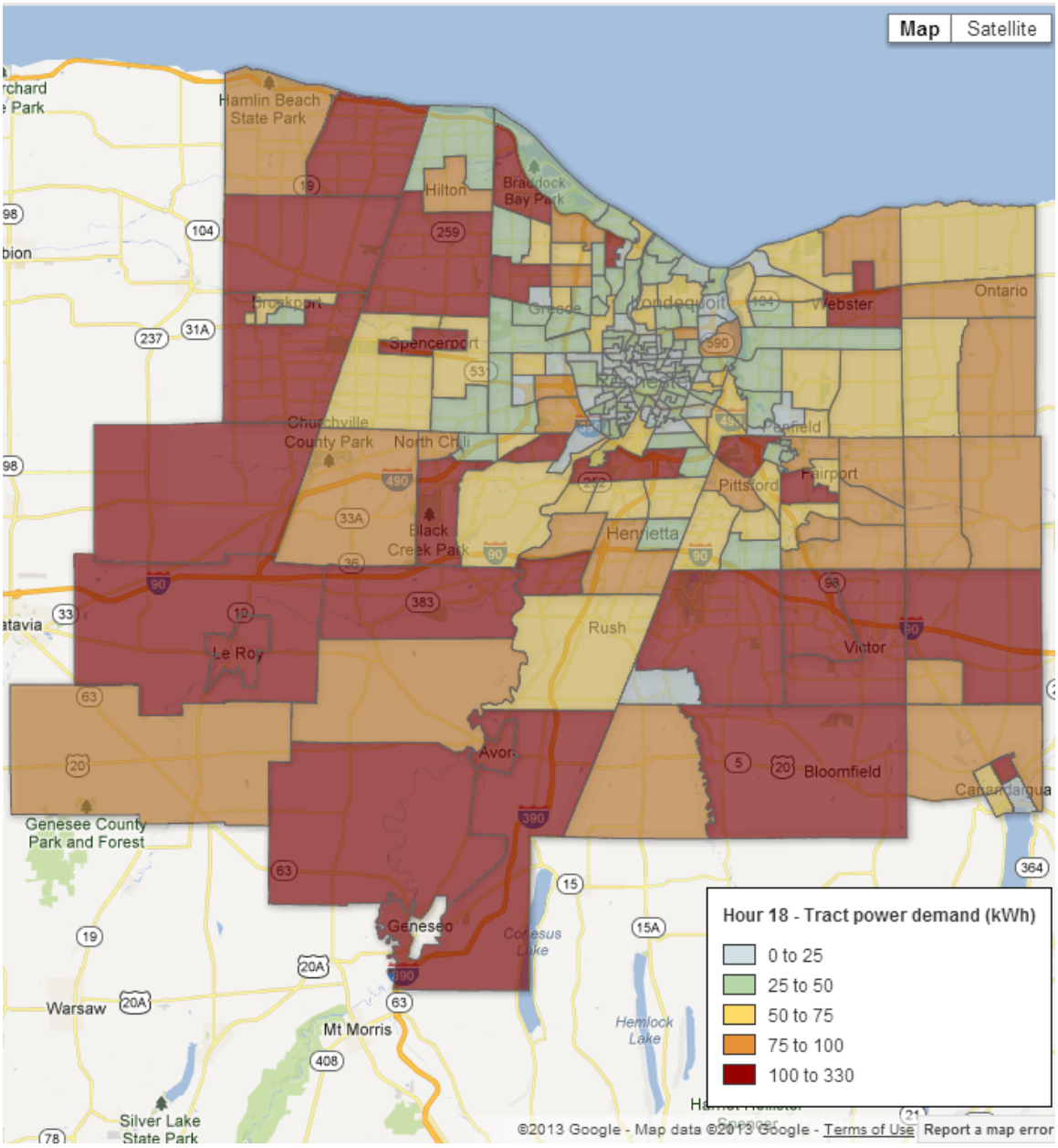
Map
Satellite
Hamlin Beach State Park
Hilton
Braddock Bay Park
Brockport
Greece
Spencerport
Rochester
Webster
Ontario
Churchville County Park
North Chili
Penfield
Pittsford
Fairport
Black Creek Park
Henrietta
Rush
Victor
Le Roy
Avon
Bloomfield
Canandaigua
Genesee County Park and Forest
Geneseo
Conesus Lake
Hemlock Lake
Warsaw
Mt Morris
Silver Lake State Park
Hour 18 - Tract power demand (kWh)
0 to 25
25 to 50
50 to 75
75 to 100
100 to 330
©2013 Google - Map data ©2013 Google - Terms of Use
Report a map error

6PM - 7PM

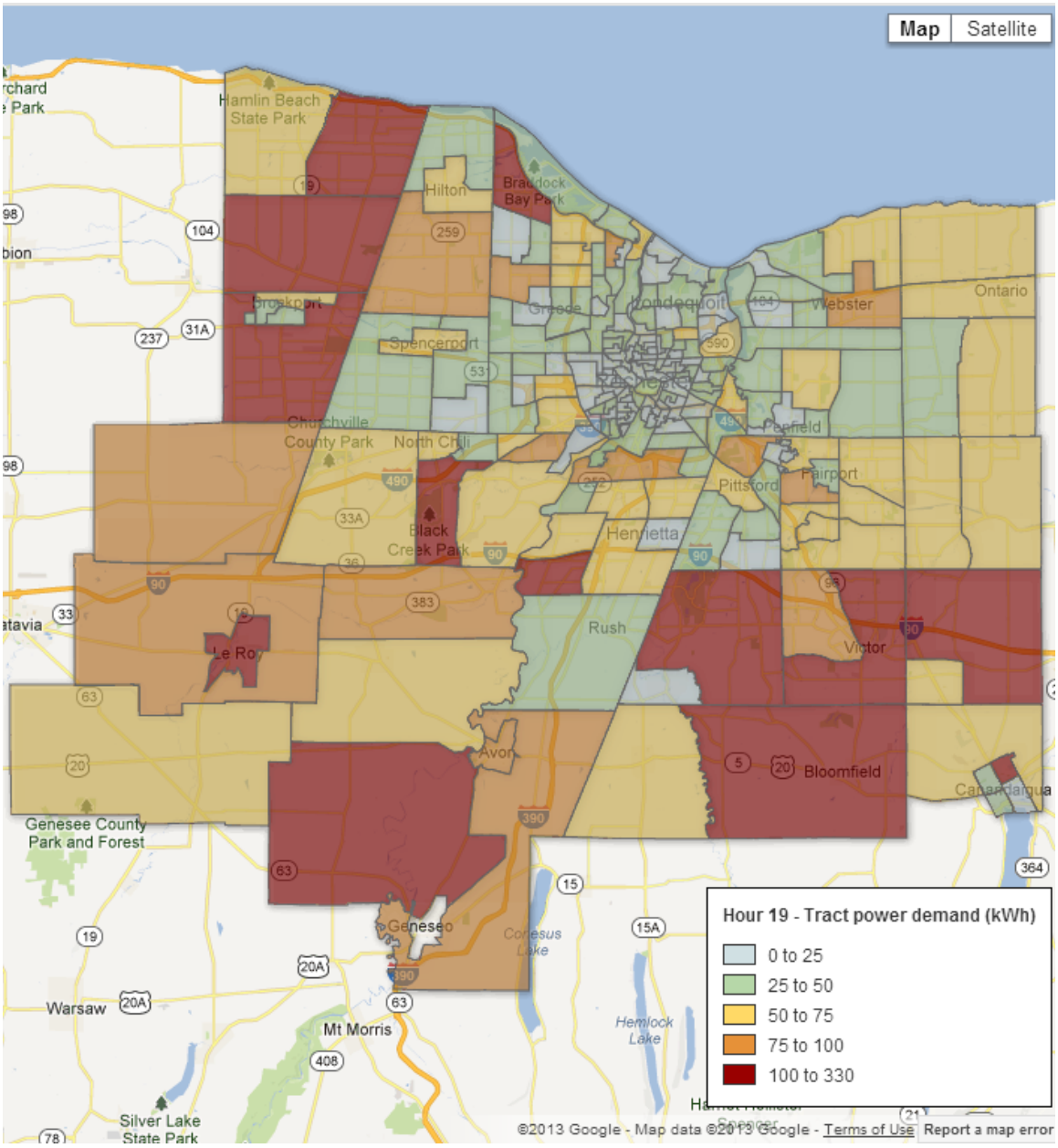
Map
Satellite
Hamlin Beach State Park
Hilton
Braddock Bay Park
Brockport
Greece
Spencerport
Webster
Ontario
Churchville County Park
North Chili
Penfield
Pittsford
Fairport
Black Creek Park
Henrietta
Rush
Victor
Le Roy
Avon
Bloomfield
Canandaigua
Genesee County Park and Forest
Geneseo
Conesus Lake
Hemlock Lake
Warsaw
Mt Morris
Silver Lake State Park
Hour 19 - Tract power demand (kWh)
0 to 25
25 to 50
50 to 75
75 to 100
100 to 330
©2013 Google - Map data ©2013 Google - Terms of Use
Report a map error

7PM - 8PM

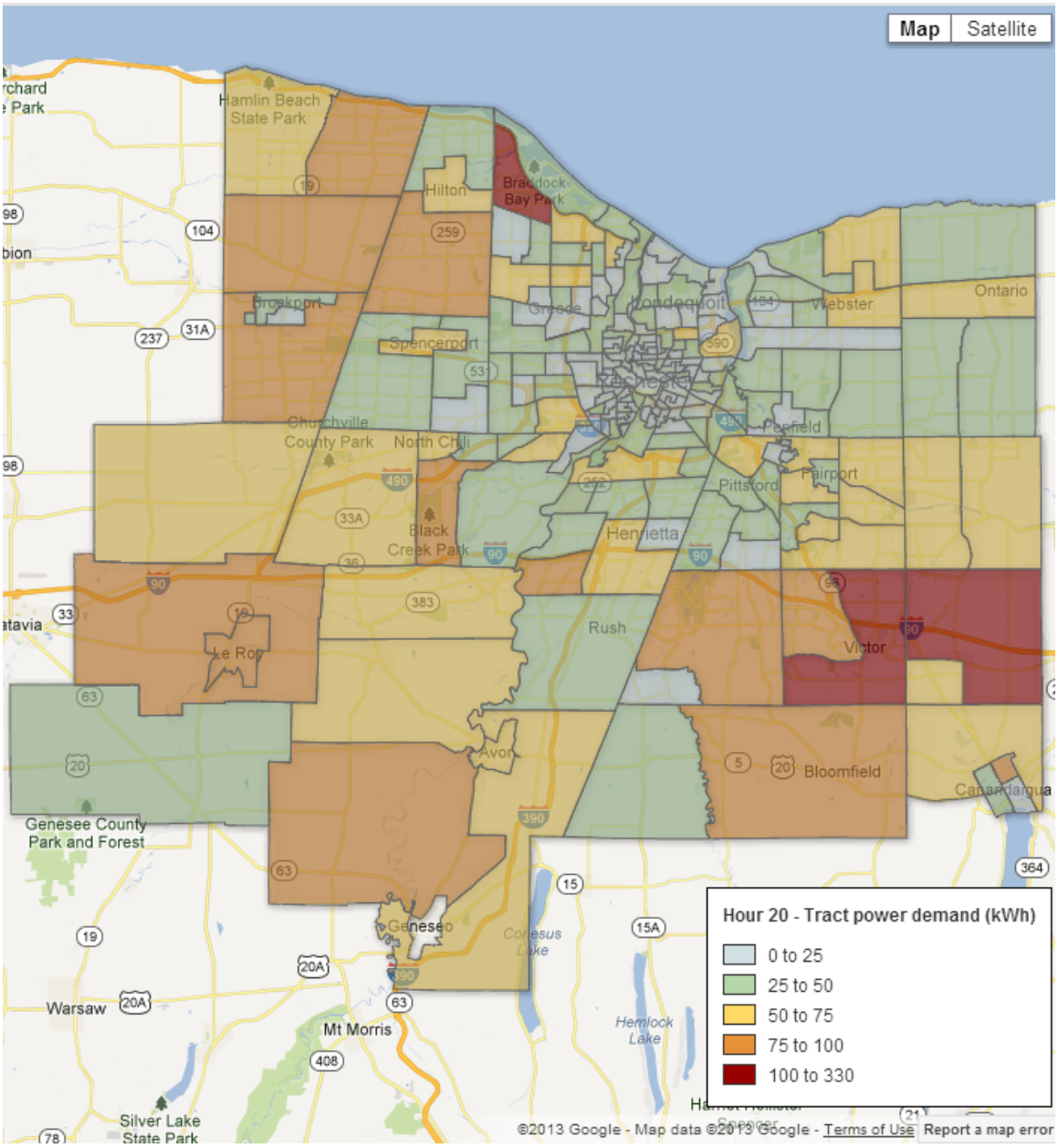
Map
Satellite
Hamlin Beach State Park
Braddock Bay Park
Hilton
Brockport
Greece
Rochester
Webster
Ontario
Spencerport
Churchville County Park
North Chili
Penfield
Pittsford
Fairport
Black Creek Park
Henrietta
Le Roy
Rush
Victor
Avon
Bloomfield
Canandaigua
Genesee County Park and Forest
Geneseo
Conesus Lake
Hemlock Lake
Warsaw
Mt Morris
Silver Lake State Park
Hour 20 - Tract power demand (kWh)
0 to 25
25 to 50
50 to 75
75 to 100
100 to 330
©2013 Google - Map data ©2013 Google - Terms of Use
Report a map error

8PM - 9PM

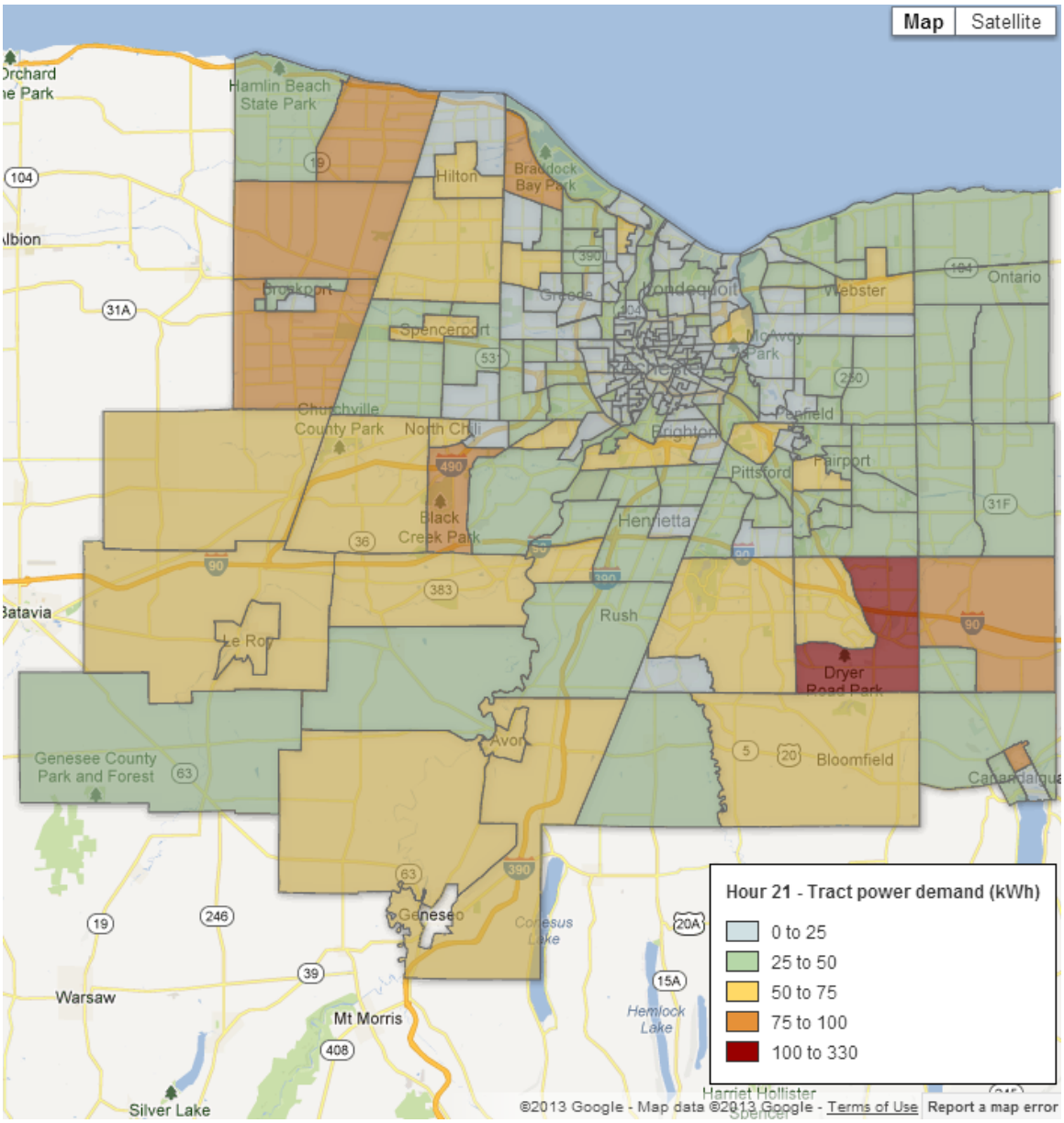
Map
Satellite
Hamlin Beach State Park
Braddock Bay Park
Hilton
Brockport
Spencerport
Churchville County Park
North Chili
Black Creek Park
Greece
Rochester
Irondequoit
Webster
Ontario
McAvoy Park
Penfield
Pittsford
Fairport
Henrietta
Rush
Dryer Road Park
Bloomfield
Avon
Genesee County Park and Forest
Geneseo
Warsaw
Mt Morris
Silver Lake
Hemlock Lake
Hour 21 - Tract power demand (kWh)
0 to 25
25 to 50
50 to 75
75 to 100
100 to 330
©2013 Google - Map data ©2013 Google - Terms of Use
Report a map error

9PM - 10PM

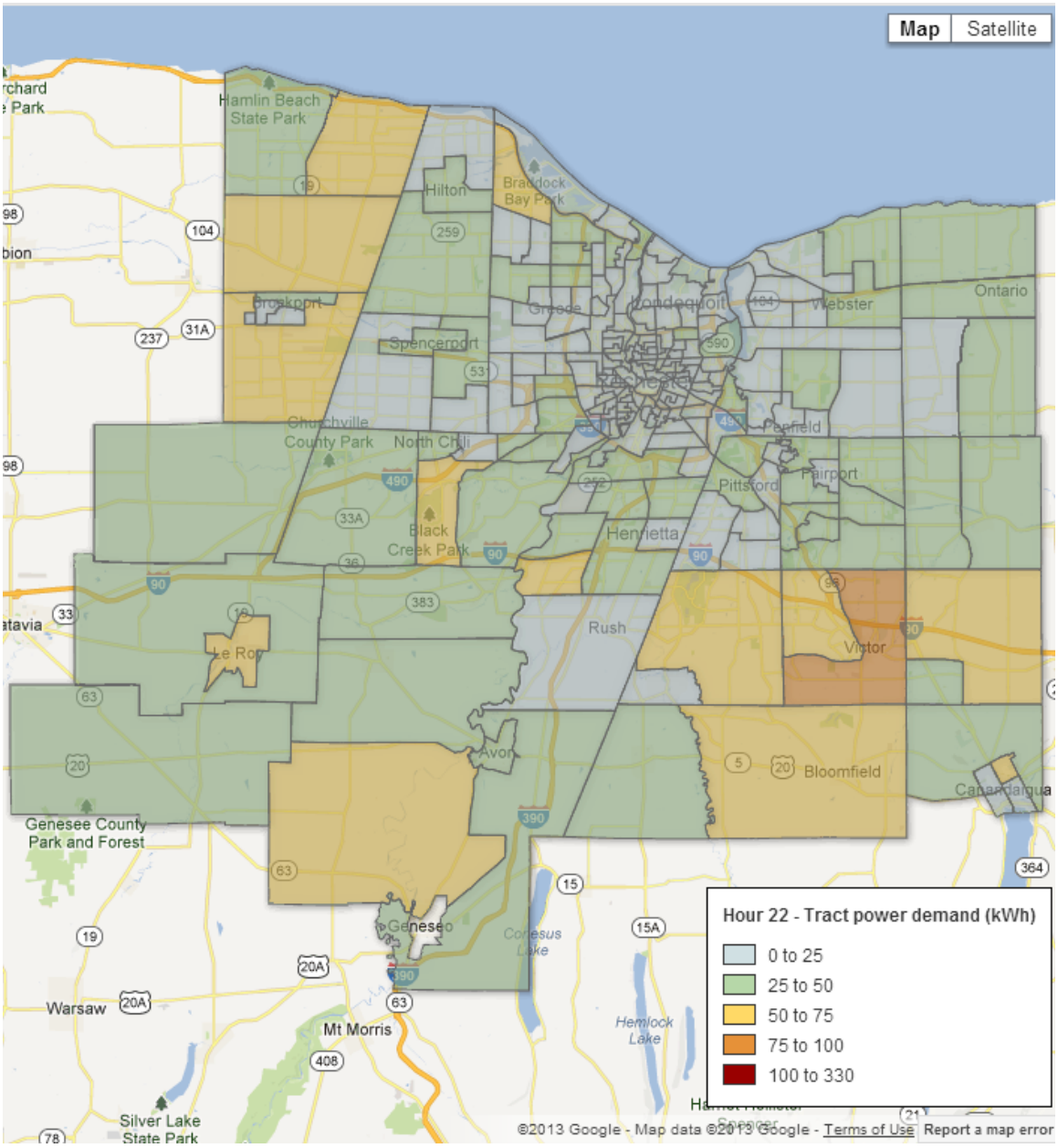
Map
Satellite
Hamlin Beach State Park
Hilton
Braddock Bay Park
Brockport
Spencerport
Greece
Rochester
Webster
Ontario
Churchville County Park
North Chili
Penfield
Pittsford
Fairport
Black Creek Park
Henrietta
Rush
Victor
Le Roy
Avon
Bloomfield
Canandaigua
Genesee County Park and Forest
Geneseo
Conesus Lake
Hemlock Lake
Warsaw
Mt Morris
Silver Lake State Park
Hour 22 - Tract power demand (kWh)
0 to 25
25 to 50
50 to 75
75 to 100
100 to 330
©2013 Google - Map data ©2013 Google - Terms of Use
Report a map error

10PM - 11PM

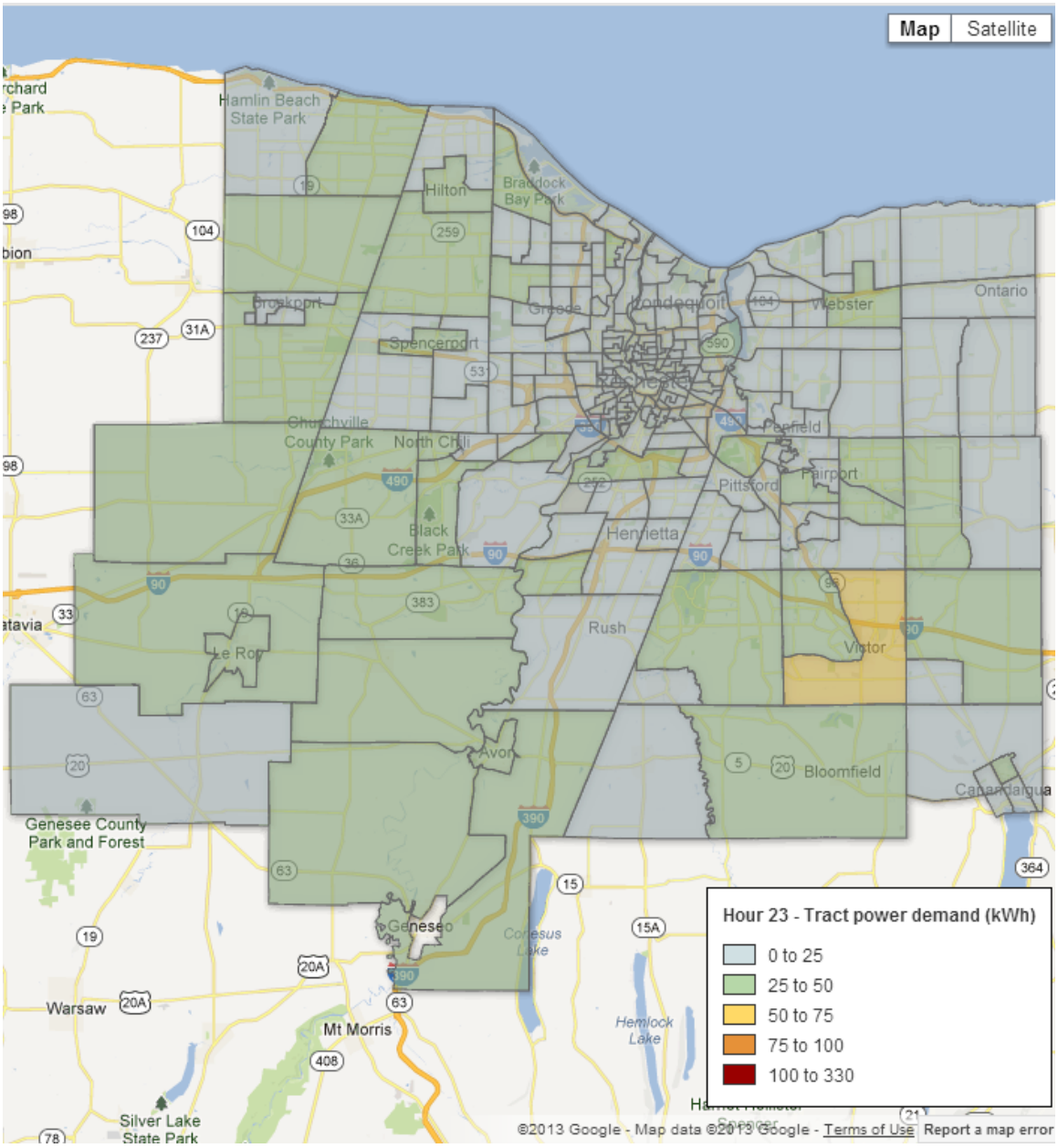
Map
Satellite
Hamlin Beach State Park
Braddock Bay Park
Hilton
Brockport
Spencerport
Greece
Rochester
Webster
Ontario
Penfield
Churchville County Park
North Chili
Pittsford
Fairport
Black Creek Park
Henrietta
Le Roy
Rush
Victor
Avon
Bloomfield
Canandaigua
Genesee County Park and Forest
Geneseo
Conesus Lake
Hemlock Lake
Warsaw
Mt Morris
Silver Lake State Park
Hour 23 - Tract power demand (kWh)
0 to 25
25 to 50
50 to 75
75 to 100
100 to 330
©2013 Google - Map data ©2013 Google - Terms of Use
Report a map error

11PM - 12AM

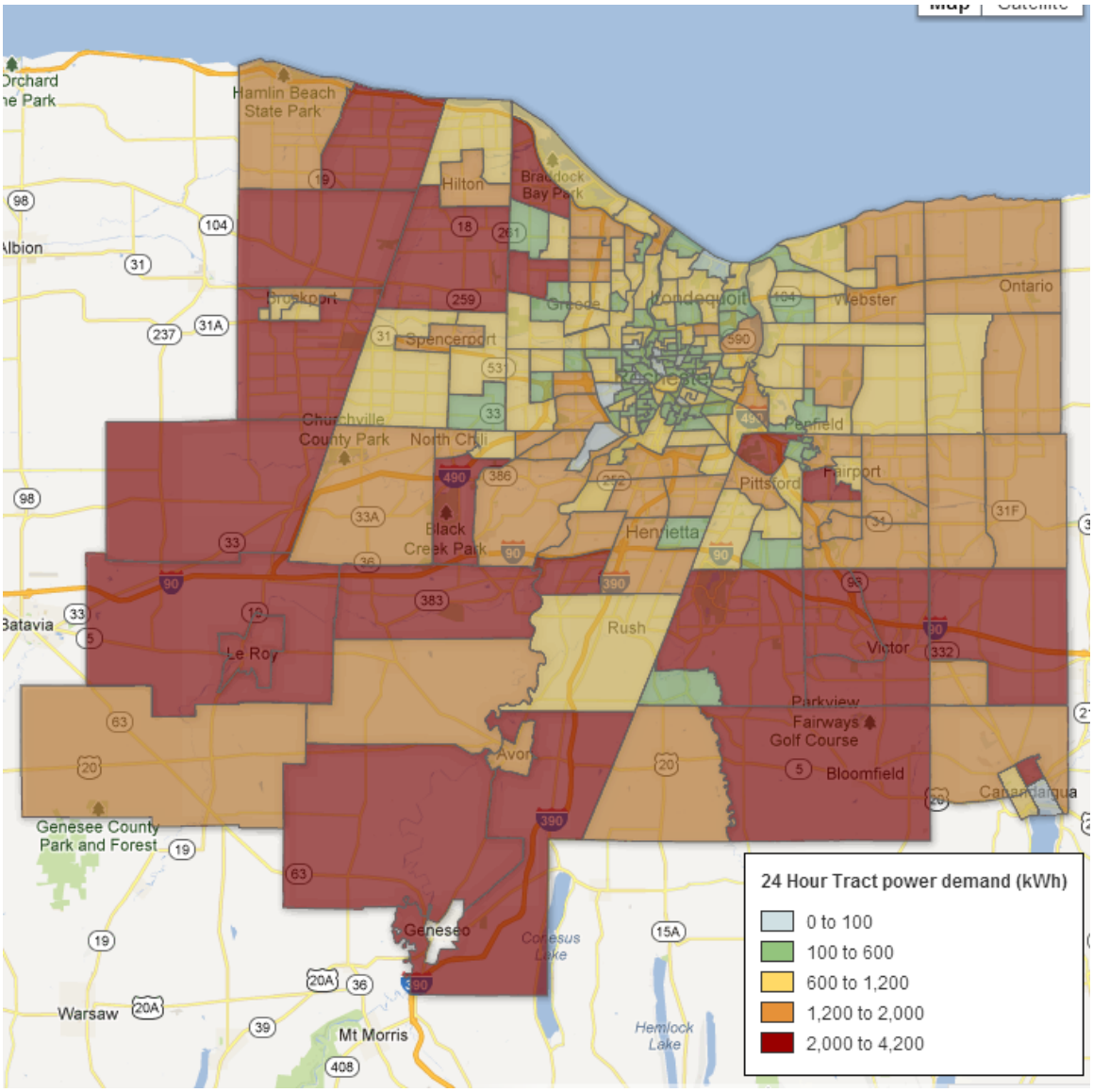

All Day Cumulative Demand

Appendix C

Code

See the attached CD-ROM